Demographic Divergence: The Legacy of the Opioid Epidemic

Carolina Arteaga* Victoria Barone† Stephen Claassen‡

May 28, 2026

Click here for the most recent version.

Abstract

We study how the opioid epidemic shaped local population growth in the United States. Exploiting variation in exposure to the epidemic—driven by Purdue Pharma's targeted marketing of OxyContin and proxied by 1996 cancer mortality rates—we find that commuting zones with greater exposure experienced lower population growth. By 2020, a one-standard-deviation increase in exposure reduced population growth among individuals aged 18 to 64 by 2.4 percentage points. Direct mortality from drug-induced deaths made only a limited contribution to these changes. Instead, population losses were primarily driven by migratory responses: exposure increased out-migration rates, especially among college-educated individuals. These responses are consistent with the opioid epidemic operating as a disamenity shock, deteriorating local quality of life. We also document a rise in fertility that, by 2020, partially offsets population losses. Our findings show that the opioid epidemic reshaped local demographic composition and contributed to the long-run divergence in population dynamics across U.S. commuting zones.

JEL No. I12, I18, I30, J13, R23.

*Department of Economics, University of Toronto and NBER (carolina.arteaga@utoronto.ca).
†Department of Economics, University of Notre Dame and NBER (mbarone2@nd.edu).
‡Department of Economics, University of Toronto (stephen.claassen@mail.utoronto.ca).

We thank Stephan Heblich, Kory Kroft, Ethan Lieber, Felipe Menares, Matthew Notowidigdo, Clementine Van Effenterre, Abbie Wozniak and conference and seminar participants at ASHEcon, CPEG, Northwestern Kellogg School of Management, University of Michigan, NBER Economics of Health, the New York Federal Reserve, Emory University, Purdue University, San Diego State University, the University of Toronto, Western Michigan University, Cornell Population Center (Brooks School of Public Policy), University of Wisconsin, Universidad de Chile, Queen's University, the 2026 Nebraska Labor Summit, University of Bologna and the 2026 European Meeting of the Urban Economics Association for their feedback.

I. Introduction

Regionally concentrated economic shocks have been one of the defining social and economic challenges of recent decades (Autor et al., 2025). A large body of research documents how globalization, automation, and the energy transition, among others, have created geographically uneven and long-lasting effects on local labor markets (Autor and Dorn, 2013; Acemoglu and Restrepo, 2020; Hansen et al., 2023). These shocks have not only depressed employment and earnings but have also had far-reaching consequences for health, family structure, and political polarization (Autor et al., 2019; Adda and Fawaz, 2020; Autor et al., 2020; Pierce and Schott, 2020; Rodrik, 2021; Choi et al., 2024; Finkelstein et al., 2026). During this period, the pace of income convergence across regions has slowed markedly (Ganong and Shoag, 2017), and widening economic disparities have been accompanied by demographic shifts (Autor et al., 2025).

Local population decline represents a growing challenge, with more than half of all U.S. counties losing population between the 2010 and 2020 censuses (Mackun et al., 2021). Population losses erode local tax bases, strain the provision of public goods, and generate fiscal pressures that are difficult to reverse, particularly in areas with fixed infrastructure and aging populations (Gyourko and Tracy, 1989; Suarez Serrato and Wingender, 2016; Glaeser and Gottlieb, 2009). Declining population can also trigger feedback effects, as falling housing demand, reduced local services, and deteriorating amenities further depress economic activity and accelerate out-migration (Glaeser and Gyourko, 2005). Understanding the determinants of local population decline is central to evaluating the long-run economic viability of places, and population dynamics are a key mechanism through which local economic shocks translate into persistent regional divergence (Blanchard et al., 1992).

In this paper, we examine a regionally concentrated shock of a different nature—the opioid epidemic—and study its effects on local population growth, internal migration, fertility, and mortality. The opioid epidemic stands as one of the most devastating and far-reaching public health crises in U.S. history, leading to rising mortality, widespread addiction, and economic and fiscal strain (Maclean et al., 2020; Cornaggia et al., 2022; Arteaga and Barone, 2026). To isolate the effects of the epidemic from broader demographic and socioeconomic trends, our identification strategy exploits Purdue Pharma's initial marketing strategy for OxyContin, uncovered through unsealed court records from litigation against the firm. These records reveal that Purdue initially targeted areas with high cancer pain incidence, with plans to expand to the larger non-cancer pain market within those same geographic areas. This strategy disproportionately exposed non-cancer patients in high-cancer areas to the opioid epidemic and its downstream consequences.

Following Arteaga and Barone (2026), we use 1996 cancer mortality—measured prior to the onset of OxyContin—as a proxy for local exposure. We treat this measure as a

source of quasi-exogenous variation in epidemic intensity. Since the opioid epidemic was a complex, multi-dimensional crisis with wide-ranging impacts, from prescription supply to reliance on public transfers, we focus on estimates from this measure of exposure in the reduced form. In this framework, 1996 cancer mortality serves as a predetermined shifter of how intensely communities were affected.[1]

Our results show that the opioid epidemic contributed to growing regional divergence across the United States. Areas more exposed to the epidemic experienced lower population growth 10 and 20 years after the onset of the crisis, especially among individuals aged 18 to 64 years old. We estimate that by 2010, a one–standard-deviation increase in exposure caused 1.3 percentage points lower working-age population growth; by 2020, this effect increased to 2.4 percentage points. This decline is equivalent to 40% of the 6% average local growth observed between 2000 and 2020. This persistent population decline was strongest among college-educated adults; by 2020, a one-standard-deviation increase in exposure decreased population growth rates by 3.8 p.p. among this group.

To understand the decline in population growth, we examine its demographic margins of adjustment: migration, fertility, and mortality. First, consistent with models predicting that migration is a primary channel of adjustment to local economic shocks (Blanchard et al., 1992), exposure to the epidemic induced significant migratory responses. A one–standard-deviation increase in exposure led to a 5.5% increase in out-migration rates by 2011, which persisted thereafter. These responses are present among adults with and without a college education, but are strongest for college-educated adults. Between 2006 and 2020, we estimate increases in out-migration probabilities that are at least twice as large as those for non–college-educated adults. In contrast, we do not find evidence of changes in in-migration rates.

To shed light on these migration patterns, we examine where movers from highly exposed areas relocate. On average, individuals leaving high-exposure locations moved to *better* areas—that is, to commuting zones with lower exposure to the epidemic. However, these moves did not represent a reorientation toward new destinations. Rather, migrants from highly exposed areas were more likely to move along established migration corridors. Thus, epidemic exposure operated as a *push* effect rather than generating new *pull* forces that redirected flows toward previously uncommon, less exposed destinations.

Beyond migration, shifts in fertility behavior provide another important demographic response to the opioid epidemic. We find that greater exposure led to higher fertility rates. By 2018, a one–standard deviation increase in exposure raised fertility rates by approximately 5.5%. This response is not driven by the compositional effects of out-migration: fertility rose within demographic groups, with increases at least twice as large

[1]For further reference, Arteaga and Barone (2026) estimate that areas with a one–standard-deviation higher cancer mortality rate in 1996 experienced an additional 0.97 opioid doses prescribed per capita by 2012—the year when prescription rates peaked—equivalent to 65% more than the baseline mean. By 2017, this translated into a 46% increase in drug-related mortality relative to its pre-epidemic average.

among women without a college education as among women with some college.

Mortality is a third and more direct channel through which the epidemic may have reduced population. Since 1999, more than 700,000 Americans have died from opioid overdoses (CDC, 2023*b*), and Arteaga and Barone (2026) estimate that exposure to the epidemic increased drug-related mortality rates by 46% per one standard deviation of exposure. We replicate these findings and document important differences by educational attainment. Specifically, all excess mortality from drug overdoses is concentrated among individuals without a college education.

We bring these findings together in a decomposition exercise, in which we use our regression estimates to compute the contribution of each demographic margin to changes in total population growth. We find that out-migration entirely drives the decline in population growth. Fertility responses have limited explanatory power for population changes up to 2010, but their importance grows over longer horizons and contributes to the widening divergence in family formation patterns by educational attainment (McLanahan, 2004; Lundberg and Pollak, 2014; Kearney, 2022). By 2020, population declines would have been approximately 40% larger in the absence of fertility responses. In contrast, mortality plays a negligible role in explaining changes in total population growth.[2]

Next, we investigate the mechanisms underlying these demographic changes—focusing on migration—through the lens of a spatial equilibrium model. We extend Borusyak et al. (2022) to include heterogeneous workers and model the opioid epidemic as a negative amenity shock that deteriorated local quality of life, yielding two main predictions. First, when college-educated workers have a higher willingness to pay for local amenities (Diamond, 2016) and are more responsive to differences in location attractiveness (e.g., Bound and Holzer, 2000), they exhibit a stronger migratory response to an amenity decline. Second, the amenity shock is capitalized into local housing markets: because workers exit and local output contracts, spatial equilibrium predicts that housing costs fall. The data confirm both predictions. The differential migration response by education, documented above, supports the first. Turning to the second, epidemic exposure is associated with a significant reduction in housing costs—by 2020, a one-standard-deviation increase in opioid exposure reduced house prices by 7.8% and rents by 2.5%.

Central to these results is the epidemic's impact on local quality of life, which deteriorated across several dimensions. Crime and local safety play a central role in the attractiveness of a place (Glaeser et al., 2001; Diamond, 2016), and the opioid epidemic severely disrupted both. Neighborhood conditions deteriorated markedly: 311 service requests and 911 emergency calls surged, drug-related EMS dispatches rose sharply, and emergency naloxone administrations became commonplace in public spaces.[3] Reflecting

[2]For reference, the median commuting zone recorded 21 and 38 drug poisoning deaths in 2010 and 2020, respectively. Thus, while we estimate large percent increases in drug-related mortality, the absolute magnitudes are small.

[3]In Boston, residents filed 4,654 needle-pickup requests through the 311 system in 2018 (Boston

this disorder, residents of communities with above-median opioid exposure are nearly twice as likely to report worrying daily about neighborhood safety (10.0% versus 5.1%; CES, 2016). These perceived risks are borne out in the data: we estimate that a one-standard-deviation increase in epidemic exposure leads to an increase in the crime rate of 2.9 per 1,000 people. Another manifestation is the rise in homelessness and high-poverty neighborhoods (Olvera et al., 2024; Kamada, 2026), reflecting severe hardship among individuals directly affected by addiction, health shocks, and economic instability.

Beyond amenities, we examine how exposure to the opioid epidemic affected labor markets as a further potential driver for the differential migration patterns. We find declines in local employment-to-population ratios among individuals without a college education, but no effects for college-educated workers, and we do not find evidence of changes in earnings for either group.[4] Thus, the out-migration of college-educated workers cannot be directly explained by standard labor-market incentives. The muted migration response of non-college workers, by contrast, is consistent with existing theory.[5]

Turning to fertility, we provide evidence that the epidemic reduced the cost of childbearing for women through two reinforcing channels. First, employment losses fell disproportionately on women, lowering the opportunity cost of childbearing—consistent with classic theories of fertility that emphasize opportunity costs as a driver of fertility choices (Becker, 1960, 1973). Second, the deterioration in local quality of life depressed housing costs, altering the affordability of family formation (Couillard, 2026). These mechanisms provide an economic rationale for the positive fertility response we document.

Our empirical analysis combines data from several sources. We use the Decennial Censuses, the American Community Survey (ACS) and Survey of Epidemiology and End Results (SEER) to construct local population counts and, jointly with IRS Statistics of Income (SOI) Tax Stats data, to measure migration behavior. We use data from the National Vital Statistics System (NVSS) to construct fertility outcomes, opioid-related and cancer mortality rates. To capture the economic impact of the epidemic, we rely on data from the Longitudinal Employer–Household Dynamics (LEHD) program, which provides detailed county-level information on employment and earnings. Finally, we use data on housing prices from the Federal Housing Finance Agency (FHFA) and data on crime from the FBI Uniform Crime Reporting System (UCRS), among other sources, to measure the quality of local life. Our analysis focuses on 585 commuting zones with

ODP, 2018); in New York City, drug-related incidents accounted for 7.2% of all EMS dispatches (NYC EMS, 2018); and nationwide, 36% of the 215,906 naloxone doses administered by emergency services in 2019 were delivered in public spaces (NEMSIS, 2019).

[4]The null earnings effect is consistent with our model, which predicts an ambiguous wage response to negative amenity shocks. If worker-types are complements, departing workers both raise wages through scarcity and lower them through reduced output; when these forces roughly offset, wages are unchanged.

[5]For example, if this group has a lower migration elasticity as suggested by Bound and Holzer (2000), or if its disproportionally compensated by housing prices declines as suggested by Notowidigdo (2020).

populations exceeding 25,000 in 1996, observed from 1980 to 2020.[6]

We provide several tests to support our empirical design and the robustness of our results. To assess whether there is a systematic relationship between cancer rates and our outcome variables, we perform an out-of-sample exercise using 1976 cancer mortality and replicate our empirical strategy for the pre-period. We find no evidence of a relationship between lagged cancer mortality and future population growth, out-migration, or fertility rates. We also construct placebo 1996 mortality rates from unrelated causes of death and replicate our main specification using these data. This exercise shows that our results are not driven by other health trends unrelated to the opioid epidemic, nor do they reflect underlying population health. We also account for geographic exposure to major economic shocks that could confound the relationship between opioid exposure and our outcomes. Specifically, we consider shocks such as increased competition from Chinese imports, the implementation of the North American Free Trade Agreement (NAFTA), the 2001 economic recession, and the Great Recession. Finally, our results are not sensitive to the exclusion of any single state or to changes in the minimum population restrictions.

This paper makes two contributions. First, we contribute to the literature on local economic shocks and demographic adjustment. Prior work has studied how trade shocks, robot adoption, the fracking boom, and recessions affect local labor markets and shape demographic outcomes (Autor and Dorn, 2013; Autor et al., 2019; Greenland et al., 2019; Yagan, 2019; Acemoglu and Restrepo, 2020; Adda and Fawaz, 2020; Finkelstein et al., 2026; Wilson, 2022). Yet even large negative shocks tend to generate surprisingly limited migration responses.[7] The opioid epidemic stands apart: exposure generated large and selective out-migration concentrated among college-educated adults. We interpret this pattern as reflecting the epidemic's disamenity-driven nature. Whereas many labor demand shocks studied to date have predominantly depressed employment among non-college individuals, a disamenity shock can disproportionately induce out-migration among the college-educated due to their stronger valuation of local amenities. We formalize this mechanism in a spatial equilibrium model extending Borusyak et al. (2022).

Second, this paper is the first to estimate the overall population effects of the opioid epidemic. We extend the research documenting the epidemic's consequences for mortality, addiction, disability claims, municipal finances, housing prices, children's outcomes, and political behavior (Park and Powell, 2021; Buckles et al., 2022; Cornaggia et al., 2022; Arteaga and Barone, 2026). Our findings reveal that the epidemic triggered profound demographic adjustments that ultimately reduced population growth in the communities most affected, and that will continue to shape their social and economic trajectories.

[6]These commuting zones account for over 97 percent of the total population in 1996.

[7]See Autor and Dorn (2013) for the China shock case. Borusyak et al. (2022) provides additional examples. Bassler et al. (2026) find that trade shocks show little employment and migration responses while employment shocks are associated with meaningful changes in employment and migration.

II. Background: The Unfolding of the Opioid Epidemic

The United States has experienced an unprecedented crisis related to the misuse of and addiction to opioids. Over the past three decades, the crisis has evolved from the misuse of prescription opioids to the growing prevalence and use of heroin and fentanyl, leaving a profound impact on the families and communities most directly affected. As of 2022, over 700,000 lives had been lost to opioid overdoses (CDC, 2023*b*). A sizeable body of research has studied the origins of the opioid crisis and the factors that shaped its evolution and propagation. This literature has established that the pharmaceutical industry and healthcare providers played a critical role in the origins of the crisis (Miloucheva, 2021; Alpert et al., 2022; Eichmeyer and Zhang, 2022; Finkelstein et al., 2025*a*; Arteaga and Barone, 2026). In particular, the aggressive and deceptive marketing of highly addictive opioids to physicians, together with financial incentives to expand prescribing and weak regulatory oversight, created the conditions that allowed the crisis to unfold.

The beginning of the opioid epidemic is traced to the introduction of OxyContin to the market in 1996 (Quinones, 2015). OxyContin is a prescription opioid manufactured by Purdue Pharma that changed the standard of practice for the treatment of noncancer and nonterminal pain. Prior to the mid-1990s, the use of opioids for pain management had focused on cancer and end-of-life pain treatment because of care providers' fears of the risk of severe addiction (Melzack, 1990). Soon after the introduction of OxyContin, reports of abuse and addiction started to be covered by the media. By 2001, West Virginia, Virginia, Ohio, and Kentucky were pursuing class-action lawsuits against Purdue Pharma and other pharmaceutical companies. During this time, United States Attorneys for Maine and Virginia, physicians, and community leaders raised concerns to the FDA and Congress about the level of OxyContin abuse (Meier, 2018). Nonetheless, the prescription of opioids continued to increase during the 2000s with limited restrictions. At their peak in 2012, opioid prescriptions numbered 81.3 prescriptions per 100 persons (CDC, 2020). The rate of substance use disorder grew by a factor of six between 1999 and 2009 (Paulozzi et al., 2011), and prescription opioid mortality grew by a factor of five (Maclean et al., 2020).

In response to the widespread misuse of prescription opioids and rising addiction, access to prescription opioids eventually tightened.[8] This, however, pushed many individuals toward a cheaper and far more dangerous substitute: heroin. As a result, heroin-related deaths, poisonings, emergency room visits, and treatment admissions rose sharply. Between 2010 and 2013 alone, heroin death rates quadrupled, with no corresponding reduction in the combined heroin–opioid mortality rate (Evans et al., 2019). From 2013 to this day, the epidemic has been characterized by surging deaths related to the use of synthetic opioids, particularly fentanyl. Fentanyl, an extremely potent syn-

[8]This include the introduction of prescription drugs monitoring programs (PDMPs), pill mill legislation and the reformulation of Oxycontin (Quinones, 2015).

thetic opioid, is more profitable to manufacture and distribute than heroin and has a higher risk of overdose. Indeed, fentanyl-related deaths account for almost the entire increase in drug overdose mortality between 2014 and 2021.

Mortality from opioids is only one of the many social costs associated with the opioid epidemic. In the U.S., an estimated 10.1 million people aged 12 or older misused opioids in the past year (SAMHSA, 2020). These figures are orders of magnitude larger than the number of opioid-related deaths, underscoring the extent to which the epidemic has disrupted individuals' health and economic opportunities and strained their communities. Consistent with this, the epidemic has increased disability rates and Supplemental Nutrition Assistance Program (SNAP) utilization (Powell et al., 2020; Savych et al., 2019; Arteaga and Barone, 2026), and has affected labor force participation and employment (Krueger, 2017; Ouimet et al., 2020). Between 2018 and 2021, 32% of Americans reported that drugs had been a problem in their family—a share that is remarkably similar across income, education, and urbanicity (Gallup, 2018–2021). When close friends are included, this share rises to 46% (Gramlich, 2017). In rural areas, opioid abuse was cited as the biggest problem facing communities (NPR et al., 2018). The intergenerational reach of the crisis is also substantial: an estimated 321,566 children lost a parent to drug overdose between 2011 and 2021 (Jones et al., 2024). Qualitative evidence further reveals how opioid misuse can reshape the social fabric of communities; for example, Roberson et al. (2020) document that many residents in affected areas express a desire or need to leave their communities to avoid the harms associated with widespread opioid misuse. Together, these disruptions to the social and economic fabric of communities set the stage for the demographic adjustments we examine in the remainder of the paper.

III. Data

We construct a commuting-zone (CZ) panel spanning four decades by combining administrative and survey sources that capture the main margins of demographic adjustment—mortality, migration, and fertility—along with local labor-market and amenity outcomes. This section summarizes the core inputs and the construction of key outcomes; additional variables and harmonization procedures are described in Appendix B..

Mortality. We use restricted-use Detailed Multiple Cause of Death (DMCD) files (1989–2018), which record the county of residence and cause-of-death information for all U.S. deaths. We compute the 1996 cancer mortality rate as our measure of exposure to the epidemic.[9] To study mortality outcomes during the epidemic, we construct drug-induced mortality rates by sex and education. Drug-induced deaths include poisonings and other drug-related conditions involving legal or illegal substances, including prescription opi-

[9]We define cancer deaths as malignant neoplasms (ICD-9 140–208; ICD-10 C00–C97) and in situ/benign/uncertain neoplasms (ICD-9 210–239; ICD-10 D00–D48).

oids, heroin, and synthetic opioids (e.g., fentanyl).[10] Figure 1 and Table 1 summarize the cross-CZ distribution of cancer mortality and the evolution of drug-induced mortality over time. The average CZ's cancer mortality rate was 2.5 deaths per 1,000 people. The 1996 standard deviation is 0.55 deaths per 1,000 people, which we use to standardize exposure throughout the paper.

Population counts. We use three data sources for population counts. First, the Survey of Epidemiology and End Results (SEER), which reports population at the county level and by age, race, sex, and Hispanic origin. We use these data to construct population counts for decennial census years and denominators for mortality rates, e.g., drug-induced mortality by sex. SEER does not provide population counts by educational attainment. For education-specific outcomes, we leverage data from the Census and the ACS. These data are at the county level and include the years 1980, 1990, and 2000 from Census and 2006 onward from the ACS. When using Census and ACS data to construct *denominators*, we linearly interpolate population counts. Panel (a) of Figure 1 presents the geographic distribution of local population growth between 2000 and 2020. Table 1 reports summary statistics for population growth rates overall, by age and by sex. From 1990 to 2000, the average commuting zone experienced population growth of 9.8 percentage points; from 2000 to 2020, growth slowed to 8.1 percentage points. This slowdown was pronounced for working-age adults (ages 18–64).

Migration. We collect data on county-to-county migration flows from the IRS Statistics of Income (SOI) Tax Stats. These data are based on the universe of Forms 1040 filed and processed by the IRS during a calendar year and are available for filing years 1990 through 2021. The dataset includes the number of personal exemptions claimed, which approximates the number of individuals in a given county. Migration flows are identified based on year-to-year address changes reported on individual income tax returns. These data capture migration patterns across all U.S. counties and include both inflows—the number of new residents moving into a county and their origin—and outflows—the number of residents leaving a county and their destination.[11] While these data cover most internal migration, they do not include demographic information. To examine

[10]We use a broad definition of drug-induced deaths. ICD-9: E850–E858, E950.0–E950.5, E962.0, E980.0–E980.5. ICD-10: X40–X44, X60–X64, X85, Y10–Y14, and T36–T39, T40–T50.

[11]The IRS suppresses small county-to-county migration flows to protect confidentiality. Because this censoring varies mechanically across regions, raw aggregation to CZs introduces differential missingness. To construct complete CZ-to-CZ migration flows for descriptive statistics, we rely on a gravity-based imputation procedure detailed in Appendix B.5.2. For all causal analyses, however, we estimate our specifications directly using the county-to-county flows due to known problems with imputing missing data based on covariates (e.g., Manski et al., 2021; Manski, 2025). Our county-level sample restricts to locations with 1996 populations over 20,000, accounting for 93% of the total population in our baseline analysis sample. Crucially, the share of suppressed flows is uncorrelated with local epidemic exposure. Finally, we validate our empirical findings using unsuppressed CZ-to-CZ migration data from the Census and ACS discussed next.

migration flows for specific subpopulations, we complement the IRS data with information from the Census and the ACS. Specifically, we construct the number of moves from each geographic area based on individuals' reported locations in the previous year and rely on person weights to generate representative estimates.[12,13] Figure 1(d) presents the geographic distribution of changes in local out-migration rates between 2018 and 1996. Table 1 reports out-migration rates overall and by education. Out-migration is higher among the college-educated (12.9% vs. 7.4% in 1995, five-year rates) and this gap persists through 2010 (one-year rates over 30% higher for the college group).

Fertility. We use the National Center for Health Statistics Natality and Linked Births files to construct CZ-level fertility rates. These data cover the universe of U.S. births and include county identifiers and maternal demographics (including age, marital status, and education). We define fertility rates as births to individuals in a given age group divided by the population of that age group.

Education groups. Throughout the paper, we disaggregate main outcomes by education to capture the heterogeneous impacts of and responses to the opioid epidemic across education groups. We define college-educated as any post-secondary education (some college, associate's, bachelor's, or graduate degree) and non-college as high school graduate or less.[14]

In sum, our main outcomes are available from 1980 to 2020, and our exposure measure is the 1996 cancer mortality rate. We use CZs as the unit of observation because they approximate local labor markets and capture the relevant economic geography. We restrict the sample to CZs with at least 25,000 residents, yielding a panel of 585 CZs covering 97% of the U.S. population.

IV. A Model of Amenity Shocks and Selective Migration

To guide our empirical analysis, we extend the spatial model of Borusyak et al. (2022) to include college- and non-college-educated workers. The model characterizes the equilibrium responses of local population, migration flows, wages, and rents to an amenity shock. It also delivers estimating equations for our population and migration regressions. We discuss the core components of the model below, additional details and derivations are presented in Appendix C..

[12]Unfortunately, the 1990 and 2000 Censuses ask about residence five years prior. Therefore, for Census years, we construct the number of moves based on this retrospective question.

[13]Informed by Foschi et al. (2023), we drop the four least populous states of the contiguous United States (South and North Dakota, Vermont, and Wyoming) from our analysis sample due to the volatile state population swings observed in the ACS data.

[14]This definition follows Cadena and Kovak (2016) who group together all workers with no college education, including those with and without a high school degree; evidence suggests these two groups are nearly perfect substitutes Card (2009).

IV.a Environment

Consider a small open economy with multiple sectors $n \in \mathcal{N}$ produced across locations $l \in \mathcal{L}$. Goods are differentiated by location of production, product markets are frictionless, and production uses labor as the only input. Output and labor markets are perfectly competitive. Each location is characterized by exogenous amenities A_l and an inelastic housing supply $\bar{H}_l$ which introduces a local congestion force in equilibrium.

IV.b Workers and Local Labor Supply

There are two types of workers indexed by $h \in \{c, nc\}$, representing college- and non-college-educated workers. They differ in valuation of local amenities, ζ^h; their sector-location-specific productivity, φ^h_{ln}; and their migration elasticity, θ^h. The exogenous initial distribution of type-h workers across locations is given by L_o^{0h}. Workers choose consumption, housing, and location of employment subject to migration frictions. Each worker supplies one unit of labor inelastically in their chosen location and earns wage rate w_l^h. Changes in employment are equivalent to changes in population. The indirect utility of individual i initially living in o of choosing destination l is:

$$V^h_{iol} = \underbrace{\zeta^h \ln A_l + \alpha \ln\left(\frac{w_l^h}{P}\right) + (1-\alpha)\ln\left(\frac{w_l^h \bar{H}_l}{W_l}\right) - \ln \tau_{ol}}_{\equiv \bar{V}^h_{ol}} + \frac{1}{\theta^h}\epsilon_{il} \ .$$

Here, P is the Cobb-Douglas exact price index, W_l is the local wage bill, and τ_{ol} is the bilateral migration cost with $\tau_{oo} = 1$. $\bar{V}^h_{ol}$ is the deterministic component of indirect utility. ϵ_{il} is an i.i.d. taste shock following the standard Gumbel distribution across individuals and locations. Under this assumption, the probability that a worker of type h chooses to migrate from o to l is:

$$\pi^h_{ol} = \frac{\exp(\theta^h \bar{V}^h_{ol})}{\sum_d \exp(\theta^h \bar{V}^h_{od})} \ .$$

θ^h governs how strongly workers respond to differences in location attractiveness captured by wages, amenities, and housing congestion. The resulting labor supply in location l is:

$$L^h_l = \sum_o \pi^h_{ol} L_o^{0h} \ .$$

IV.c Local Labor Demand

We model production with a CES aggregator over college and non-college labor.[15] Labor demand for workers of type h in location l is:

$$L_l^h = D_l^h (w_l^h)^{-\rho}, \quad \text{where} \quad D_l^h \equiv \sum_{n \in \mathcal{N}} b_{ln}^h (\varphi_{ln}^h)^{\rho-1} p_{ln}^{\rho-\sigma} P_n^{\sigma-1} \eta_n.$$

Here, b_{ln}^h captures the importance of worker type h in production, ρ is the elasticity of substitution between worker types, σ is the elasticity of substitution across varieties, and P_n is the sector-level CES price index. D_l^h is a composite demand term which incorporates the interdependence of local labor demand across worker types.

IV.d Equilibrium responses to a local amenity shock

We consider a small change in local amenities A_l across locations and how it affects local population, local prices, and migration flows. In equilibrium, amenity changes affect workers' location choices directly and indirectly through their effects on local wages and rents. Following Borusyak et al. (2022) we focus on a low-mobility approximation to the model, assuming that migration is limited enough that the influence of indirect connections between locations becomes negligible and population-induced price feedback is second-order. Let hats represent proportional changes relative to the no-change counterfactual, so $\hat{x} = \frac{dx}{x} = d \ln x$.

The equilibrium population response to a small change in local amenities ($\hat{A}_l$) across locations for worker type h is:

$$\hat{L}_l^h \approx \theta^h \zeta^h \left[(1 - \pi_{ll}^h) \hat{A}_l - \sum_{o \neq l} \gamma_{ol}^h \hat{A}_o \right], \tag{1}$$

where $\gamma_{ol}^h \equiv \pi_{ol}^h L_o^{0h} / L_l^h$ is the share of type-h residents living in l who came from o. From this condition we derive our first prediction: amenity shocks change populations for both worker types, with larger changes among college-workers:

$$\theta^c \zeta^c (1 - \pi_{ll}^c) > \theta^{nc} \zeta^{nc} (1 - \pi_{ll}^{nc}) \implies \left| \hat{L}^c \right| > \left| \hat{L}^{nc} \right|.$$

That is, suppose college workers place greater value on local amenities and are more responsive to differences in location attractiveness (i.e., higher $\theta^c \zeta^c$) and/or have higher baseline mobility (i.e., higher $(1 - \pi_{ll}^c)$), consistent with the evidence in Bound and Holzer (2000), Diamond (2016), and Molloy et al. (2011). Then a negative amenity shock leads to a larger local population decline for college workers than for non-college workers.

[15] The use of a CES aggregator over education groups follows a large literature, including Katz and Murphy (1992); Card and Lemieux (2001). Embedding that structure in the Armington (1969)-style labor-demand framework of Borusyak et al. (2022) follows Claassen (2025).

Moving to the price-related predictions, in equilibrium a negative amenity shock is capitalized into lower local rental prices as individuals' willingness to pay to live in the location declines—a result that mirrors the Rosen-Roback framework. In contrast, a negative amenity shock has an ambiguous effect on local wages, as two forces operate in opposite directions: it contracts local labor supply, pushing wages up via scarcity, while simultaneously shrinking the aggregate scale of production pulling wages down—under the empirically supported assumption that the elasticity of substitution between worker types (ρ) is smaller than across varieties (σ).[16]

Finally, to study the effects of an amenity shock on migration flows—i.e., the migratory responses of workers—we derive the proportional change in the migration probability π^h_{ol}:

$$\hat{\pi}^h_{ol} \approx \theta^h \zeta^h \left(\hat{A}_l - \hat{A}_o \right). \tag{2}$$

This expression shows that flows from o to l increase when amenities in the origin o decline relative to the destination l. The magnitude of the response is governed by $\theta^h \zeta^h$. Therefore, a relative decline in amenities in the origin location raises the out-migration probability, with larger responses among college workers.[17]

V. Empirical Strategy

We now use the spatial equilibrium model to guide our empirical exercises. Locations correspond to CZs exposed to opioid shocks of varying intensity. Given an exposure measure, local population adjustments follow from Equation (1) and migration flows between CZ pairs are governed by Equation (2). For other outcomes of interest, we adopt a reduced-form approach that relates the exposure measure to changes in these outcomes.

To measure exposure to opioid shocks, we exploit rich geographic differences in early opioid promotional efforts as an exogenous source of variation. Specifically, we use 1996 cancer mortality as a proxy for local exposure to the opioid epidemic following the approach in Arteaga and Barone (2026). The rationale behind this strategy is that the size of the cancer pain market in the mid-1990s was a key determinant of where pharmaceutical companies initially concentrated their marketing efforts for opioids. A large body of research—and multiple legal rulings—has established a strong link between these early

[16] There is empirical evidence that σ is meaningfully larger than ρ. For example, Broda and Weinstein (2006) and Feenstra et al. (2018) find $\sigma \approx 4$ (as noted by Borusyak et al. (2022)) while $\rho \approx 2$ (e.g. Katz and Murphy, 1992; Card and Lemieux, 2001).

[17] Equation 2 implies that bilateral migration responses are symmetric to origin and destination shock exposure, a standard property of location-choice models; see Claassen (2025) for a detailed discussion. Our empirical specification does not impose this restriction.

promotional campaigns and the subsequent unfolding of the opioid crisis. Appendix D. presents additional empirical evidence supporting this strategy.

Our empirical strategy interacts cancer mortality rates in 1996 with period dummies in a continuous-treatment event-study design, as follows:

$$\Delta\, y_{ct} = \sum_{\tau=\underline{t}}^{T} \phi_\tau\, CancerMR_{c,1996} \mathbf{1}(Period = \tau) + \mathbf{\Gamma'} X_{ct_0} + \delta_{st} + \upsilon_{ct}\ , \tag{3}$$

where c indexes the commuting zone, s the state, and t the period. t_0 corresponds to 1996—the year of OxyContin's launch—or the closest year with available data; e.g., 2000 when Census data are used. We define Δ as the long-change operator: for any random variable W_{ct}, $\Delta W_{ct} = W_{ct} - W_{ct_0}$.

The outcome of interest is given by y_{ct}. The cancer mortality rate in commuting zone c in 1996 ($CancerMR_{c,1996}$) is interacted with a full set of year fixed effects indexed by τ. In this specification, the coefficients for the pre-epidemic period test whether outcomes in higher and lower cancer mortality areas followed similar trends before 1996. In the result section, we present scaled estimates of the ϕ_τ coefficients; we multiply the estimated coefficient by the standard deviation of 1996 cancer mortality rates, which yields the change in the outcome associated with a one standard deviation increase in exposure.

X_{ct_0} is a vector of control variables that includes baseline demographic variables such as the share female, White, and age groups interacted with year dummies. When the outcome of interest is log population, this vector includes two additional controls. First, following the derivation of Equation 1, we control for shocks in connected locations weighted by migration flows at baseline.[18] Second, we control for the lagged population growth rate to account for the autoregressive structure of population growth (Greenland et al., 2019).[19]

This research design allows us to control for state-specific trends and state-level policy changes, by including state-times-year fixed effects δ_{st}, which were common during this period, as well as time invariant commuting zone characteristics. When estimated on a balanced panel, this specification is equivalent to a regression with the outcome in levels and the inclusion of commuting zone fixed effects. However, our panel is not perfectly balanced for some outcomes—e.g., fertility by marital status cannot be constructed for California after 2016. In such cases, the specification in Equation (3) is more efficient, and we adopt it as our baseline approach.

Identifying assumptions. Our causal effects of interest are average changes in out-

[18]Specifically, we control for $\sum_{l \neq c} \lambda_{cl}\ CancerMR_{l,1996}$, where λ_{cl} represents the share of migrants from location c to location l.

[19]To see this, consider that population changes could be modeled as an AR(1) process. That is, $\Delta \ln(pop_{c,t}) = \theta \Delta \ln(pop_{c,t-1}) + \mu_{ct}$. Not including the lagged population change when estimating the effects of exposure to the epidemic may mistakenly attribute effects of prior growth to this shock.

comes—e.g., population growth rates—resulting from a marginal increase in exposure to the opioid epidemic. Following the continuous-treatment difference-in-differences framework of Callaway et al. (2024) we target Average Causal Response (ACR) parameters and discuss the assumptions required for their causal interpretation.

First, no anticipation, which in our setting implies that exposure to the opioid epidemic must not affect outcomes prior to the unfolding of the epidemic (i.e., prior to 1996). Second, strong parallel trends: the average change in (potential) outcomes associated with experiencing any level of exposure must be the same for all CZs, regardless of the level of exposure they actually experienced. Put differently, this assumption requires the standard parallel trends assumption to hold across all dose groups.[20] These two assumptions are enough for causal interpretation of two-way fixed effect estimates. However, Callaway et al. (2024) and Goldsmith-Pinkham et al. (2020) caution that such estimates suffer from weighting issues inherent to ordinary least squares, which can complicate interpretation. To address weighting challenges, our third assumption is linearity: treatment effects must be linear across the distribution of exposure. This assumption restores a causal interpretation of two-way fixed effects estimates as ACRs.[21]

We follow Callaway et al. (2024) and Goldsmith-Pinkham et al. (2020) and assess the plausibility of our assumptions using several complementary strategies. First, we test the exogeneity of our cancer-based exposure measure by examining pre-trends within a parametric event-study framework. We complement this analysis with a series of placebo tests, out-of-sample exercises, and specifications that include additional controls for alternative local shocks (e.g., the China shock) and baseline commuting-zone characteristics such as industrial composition and poverty rates. These exercises provide evidence in support of strong parallel trends by showing that cancer mortality does not proxy for other confounding trends—that is, that high- and low-cancer areas would have trended similarly in the absence of the opioid epidemic. Finally, we assess strong parallel trends and linearity of treatment effects by estimating treatment effects semi-parametrically across the distribution of treatment exposure in pre- and post-periods using binned scatter methods following Cattaneo et al. (2024). Section IX. describes in detail the results of these exercises and provides support for the validity of our identification strategy.

[20] In our context, the standard parallel trends assumption would require that, absent exposure to the opioid epidemic, the *untreated potential outcomes* in high- and low-exposure CZs would have trended similarly.

[21] As this weighting issue is inherent to two-way fixed effects estimation, our assumption of linearity is one of convenience. Absent linearity in treatment effects (which we directly assess), Callaway et al. (2024) make clear that ACRs are identified non-parametrically solely under no anticipation and strong parallel trends.

VI. Population Decline and the Opioid Epidemic

In this section, we examine how exposure to the opioid epidemic translated into changes in local population growth. Panel (c) of Figure 1 plots population growth rates among adults aged 18 to 64 from 2000 to 2020 across CZs. The map shows that a large share of communities experienced population decline during this period, despite overall national population growth of 16.2% over the same period. Figure 2 further illustrates these dynamics by showing the evolution of log population aged 18 to 64 for commuting zones in the top and bottom quartiles of opioid exposure. Before the onset of the epidemic, population growth rates were similar across exposure levels. Shortly thereafter, however, growth slowed markedly in more exposed areas.

To estimate the effect of the opioid epidemic on local population growth, we employ only decadal U.S. Census data on CZ population counts to avoid using intercensal data imputations. We estimate Equation (3) with log population as the outcome. We first examine changes in log population between 1990 and 2000 to capture pre-epidemic differential trends across CZs. We then analyze changes between 2000 and 2010, and between 2000 and 2020. To capture long-term effects, we focus on 20-year changes in population, which helps avoid including shorter-run lags already influenced by the epidemic. Specifically, we define the outcome as the change in log population from 2000 to 2020, $\Delta \ln(pop_{c,2020})$, and control for the lagged 20-year change in population, $\Delta \ln(pop_{c,2000})$.

Table 2 reports the estimated effects of exposure to the opioid epidemic on local population growth. Each coefficient reflects the change in log population growth associated with a one–standard-deviation increase in 1996 cancer mortality, our measure of exposure. Prior to the onset of the epidemic, there were no systematic differences in population growth across exposure levels. Between 1990 and 2000, the estimated coefficients are small and statistically insignificant across all age groups, indicating that high- and low-exposure areas followed similar demographic trends before the diffusion of OxyContin.[22] In contrast, after 2000—when the epidemic began to unfold—population growth diverged sharply. Between 2000 and 2010, commuting zones with higher exposure experienced lower population growth, and this effect persists 20 years after. These declines are concentrated among individuals aged 18–64, whose population growth rate fell by 1.3 p.p. in the 2000–2010 period and by 2.4 p.p. between 2000 and 2020. Effects are of similar magnitude for women and men through 2010 (see columns (3) and (4) of Table 2). By 2020, the decline in population growth among men aged 18–64 (2.7 p.p.) exceeds that among women (2.3 p.p.) though this discrepancy is not statistically different (p-value =

[22]We also examine differential trends across the 1970–1980 and 1980–1990 periods using state-level Census data (Appendix Table A1). Census data spanning 1960 to 1980 are available only at the PUMA and county group level, which are less granular than CZs. We perform this analysis at the state level, rather than disaggregating these coarser geographic units into CZs. We find no evidence of differential trends in population growth rates as a function of epidemic exposure.

0.2735).[23]

Next, Table 3 examines how the effects of exposure to the opioid epidemic on population growth among those aged 18 to 64 varied by educational attainment in columns (1) and (2). Across educational groups, population growth did not differ by exposure level prior to the epidemic. Between 2000 and 2010, high-exposure areas experienced a 1.1 p.p. decline in population growth among the non-college group, and by 2020 this effect had roughly doubled to 2 p.p. Declines show a similar gradient but are more pronounced among individuals with a college education, by 2020 this group's growth was 3.8 p.p. lower per one standard deviation of cancer mortality. Differences among these groups are economically meaningful (about 0.9 and 1.8 points) and statistically significant 20 years into the epidemic.[24] Columns (3) to (6) present results by education and sex. Declines are evident for all groups and these are larger for the college population for both sexes.[25]

Overall, these results suggest that areas more exposed to the opioid epidemic experienced population losses concentrated among working-age and relatively more educated adults. These effects strengthen over time, reflecting the long-term consequences of the epidemic. To put these figures into context, our estimates for the first 10-year change imply impacts of similar magnitude to the increase in import competition following the granting of Permanent Normal Trade Relations to China, commonly referred to as the "China shock." Greenland et al. (2019) estimate that local labor markets more exposed to Chinese import competition experienced reduced population growth. They estimate that an interquartile-range increase in import competition exposure would have reduced local working-age population growth by approximately 1.5 percentage points between 2000 and 2010.[26]

VII. Margins of Adjustment: Deaths, Moves, and Births

In this section, we explore the drivers of population change. We begin by examining each margin of adjustment: migration responses to the epidemic, fertility, and the direct mortality channel. We then present a decomposition exercise that quantifies the contribution of each channel to changes in population growth.

[23] Appendix table A2 reports coefficients for additional age group cuts.

[24] The p-value associated to the test with null hypothesis $\phi^{college} - \phi^{no\ college} = 0$ is 0.1970 for the 10-year effect and 0.0575 for the 20-year effect.

[25] The analysis in Table 3 defines college education as a bachelor's degree or higher. Appendix table A3 complements this analysis defining no-college education as any secondary education. Results are similar for both definitions. Appendix B.4 provides details on the construction of population counts by education and its limitations.

[26] This change corresponds roughly to the difference between the observed normal trade relations (NTR) tariff rates and the potential non-NTR rates for the median CZ. Specifically, the interquartile range is approximately 0.059, and the median CZ faced an average potential increase of 0.053 prior to the granting of Permanent Normal Trade Relations to China.

VII.a Moves

Migration is often viewed as a primary margin of adjustment to local economic shocks (Blanchard et al., 1992). Prior work, however, has typically found limited migration responses even to large disruptions such as trade liberalization (e.g., Autor and Dorn, 2013; Borusyak et al., 2022). The opioid epidemic differs from these shocks in that it was simultaneously a public-health crisis and a source of social distress, with potentially far-reaching consequences for local labor markets and amenities. We therefore examine how local exposure to the opioid epidemic affected in- and out-migration patterns across communities.

To capture the bilateral nature of location choices, we analyze origin-destination migration flows between location pairs. This allows for migration to depend on both origin and destination shocks and characteristics (Borusyak et al., 2022). Following the derivation of Equation (2), our regression of interest for an annual cross-section of origin-destination pairs in year t is:[27]

$$\Delta\, y_{ol,t} = \phi_{o,t}\, Cancer_{o96} + \phi_{l,t}\, Cancer_{l96} + \alpha_{o,t}\, X_{o96} + \alpha_{l,t}\, X_{l96} + \delta_{so,t} + \delta_{sl,t} + \upsilon_{ol,t}\ . \qquad (4)$$

$y_{ol,t}$ is the log probability of migrating from origin o to destination l in year t, and $\Delta\, y_{ol,t}$ is the change in this variable between year t and the baseline year (t_0).[28] In results using our IRS data, locations correspond to counties; in results using Census and ACS data, they correspond to CZs. $Cancer_{o96}$ and $Cancer_{l96}$ measure exposure to the epidemic in the origin and destination, respectively. $\delta_{so,t}$ and $\delta_{sl,t}$ are origin and destination state fixed effects. X_{o96} and X_{l96} are origin and destination demographic controls measured at baseline. We cluster standard errors two-way at the origin and destination level.

$\phi_{o,t}$ and $\phi_{l,t}$ are the main coefficients of interest and can be interpreted as migration semi-elasticities with respect to epidemic exposure: all else constant, a unit increase in origin (destination) cancer mortality leads to a $\phi_{o,t}$ ($\phi_{l,t}$) percent change in the probability of out- (in-) migration by year t, relative to the baseline year. Multiplying these semi-elasticities by the baseline migration probabilities therefore yields the implied change in migration rates (i.e., percentage points) for a given change in exposure.

Figure 3 presents semiparametric estimates of $\phi_{o,t}$ and $\phi_{l,t}$ (Panels (a) and (b), respectively) from the IRS county-to-county migration data, expressed in percentage points by

[27] We use cross-sectional regressions for computational efficiency. Estimating Equation 4 over all cross-sections is numerically equivalent to a stacked "event-study style" panel regression, analogous to Equation 3.

[28] Consistent with, e.g., Borusyak et al. (2022); Moretti and Wilson (2017) (among others), we study proportional changes in migration rates thereby focusing on location pairs with non-zero flows in 1996. This has almost no bearing on the number of origin-destination moves in our sample: in our IRS migration data, 96.4% of the moves occur between counties with non-zero flows in 1996. Borusyak et al. (2022) show these estimates can be aggregated to reflect local population changes; we carry out such an aggregation in Section VII.d.

scaling the estimates by the average 1996 inter-county migration rate (6.2%). We follow Cattaneo et al. (2024) to construct binned scatter plots where we group the data into deciles of exposure and focus on changes in migration rates across deciles (i.e., the slope). For example, in panel (a) the x-axis corresponds to the average 1996 cancer mortality in the origin counties among county pairs in a given decile and the y-axis reports the average change in the out-migration rate relative to 1996. Consistent with an absence of pre-trends across the distribution, both Panels (a) and (b), show no relation between exposure and changes in migration rates in 1993. By 2009, a distinct positive slope emerges in Panel (a): increases in origin exposure lead to increased out-migration rates. This effect persists through 2019. In contrast, Panel (b) reveals no evidence of a relationship between destination exposure and in-migration rates in either of the post-epidemic periods.

Figure 4 presents parametric estimates of $\phi_{o,t}$ from Equation 4, reported in percentage-point terms. Panel (a) is the parametric counterpart to Figure 3(a) for the full set of years. Meaningful effects on out-migration begin in 2003, and by 2011 a one-standard-deviation increase in exposure to the epidemic raised out-migration by 0.4 percentage points (5.5%), with effects persisting thereafter. By contrast, exposure to the epidemic does not affect in-migration, as shown in Figure A2(a), the parametric counterpart to Figure 3(b).

Figure A2(b) and (c) present corresponding parametric estimates of $\phi_{o,t}$ and $\phi_{l,t}$ for inter-CZ migration using ACS and decennial Census data.[29] These estimates generally encompass the corresponding inter-county IRS estimates, which gives us confidence in using the ACS and Census data to study heterogeneity in out-migration responses across demographic groups.[30] Figures 4(b) and (c) report inter-CZ estimates by educational attainment (no college versus college) and nativity, respectively. Out-migration responses are concentrated among the college-educated: between 2006 and 2010, a one-standard-deviation increase in exposure raised out-migration by 0.97 percentage points among those with some college or more, compared with 0.4 percentage points among those without any college education. This gap reflects both larger semi-elasticities for the college-educated (12.7% versus 8.5%) and higher baseline migration rates (6.2% versus 3.8%). These differences narrow slightly over time but remain pronounced through 2020. Consistent with Cadena and Kovak (2016), out-migration responses are also substantially larger among the foreign-born population: foreign-born rates increased by 1.4 percentage points per one standard deviation increase in exposure, compared with 0.45 percentage

[29]Our inter-CZ migration analysis uses 5-year data from the 1990 and 2000 decennial censuses and 1-year data from the ACS. For comparability, we pool ACS data into multi-year windows (e.g., 2006–2010). Appendix Figure A1 presents the equivalent of Figure 3 using our ACS and Census data.

[30]That magnitudes are very slightly larger when using ACS and Census data is consistent with the under-representation of younger adults, who are at their most mobile stage of life (Bernard, 2017; Foster, 2017), in tax-filing data.

points among the native-born between 2006 and 2010. This gap cannot be reconciled by differences in educational composition, as foreign-born and native movers have similar college shares in the 2010 ACS. Figure 4(d) and Figure A2(d) show similar out-migration responses by sex and across the age distribution, respectively.

Where Do People Move? We characterize the destinations of these moves in terms of their exposure to the opioid epidemic using our county-to-county migration data. In this exercise, we construct a migration-weighted average of destination-exposure per origin. Weights ($w_{o,l}$) correspond to the share of movers from a given origin o who relocated to any destination $l \neq o$ ($m_{o,l}$):

$$\text{Avg. Dest. Cancer MR}_o = \sum_{l \neq o} w_{o,l} \, \text{Cancer MR}_l \quad \text{where} \quad w_{o,l} = \frac{m_{o,l}}{\sum_{l' \neq o} m_{o,l'}}$$

Figure 5 illustrates this relationship across deciles of origin exposure. For each decile of exposure, the squares plot the average exposure to the opioid epidemic in the origin county (x-axis) against that in the destination county (y-axis), based on 2009 migration patterns. For counties above the fifth decile of exposure, movers, on average, relocated to less exposed destinations, as indicated by the squares lying below the 45-degree line. However, average destination exposure does not fall by a full standard deviation relative to origin exposure until the ninth decile.

To assess whether destination choices were specific to the opioid epidemic, we compare the exposure of 2009 migration patterns to historical (pre-epidemic) migration patterns. Specifically, we examine whether migrants from high-exposure areas began moving to new destinations after the onset of the crisis or continued relocating to the same places as before. Using 1993 migration flows—when the epidemic had not yet emerged—represented by the hollow circles in Figure 5, we find that migrants in 2009 largely moved to the same destinations as they had historically. Thus, while greater exposure increased the frequency of moves, it did not alter where people moved.

We then assess whether these destination choices are consistent with social and informational constraints (Borusyak et al., 2022; Porcher, 2022). To examine whether individuals selected relatively less exposed destinations within their existing migration networks, we construct a placebo exercise that benchmarks the lowest possible destination exposure among the top five locations where migration flows had historically been established. In this *optimal* migration pattern, each origin's top five historical destinations, measured in 1993, are ranked by their exposure to the epidemic, and the lowest-exposure destination is identified as the "best" option. The hollow triangles in Figure 5 illustrate this comparison. The gap between the optimal and actual destinations indicates substantial unrealized scope to reduce exposure within existing migration networks: by the fourth

decile of origin exposure, migrants could have lowered destination exposure by roughly one standard deviation. Even within this historically defined choice set, migrants did not disproportionately select the least exposed destinations.

In summary, exposure to the opioid epidemic led individuals to move more frequently but not to new, less affected destinations. Although migrants from high-exposure areas generally ended up in less exposed locations in absolute terms, these movements primarily reflected historical migration patterns rather than a targeted response to the epidemic.[31]

VII.b Births

Fertility constitutes a second major margin through which the opioid epidemic may have altered local demographic trajectories. We begin by examining raw data trends, and plot the evolution of fertility rates in areas more exposed to the epidemic—those in the top quartile of 1996 cancer mortality—relative to areas with lower exposure, corresponding to the bottom quartile. Panel (a) of Figure A4 shows fertility rates over time for these two groups. Prior to the crisis, fertility rates in high- and low-exposure communities followed similar trends, albeit from different levels, with low-exposure areas exhibiting higher fertility. As the epidemic unfolded, however, fertility declined more sharply in low-exposure communities.

We turn next to the event-study estimation of Equation (3), and find that exposure to the opioid epidemic led to a substantial increase in fertility rates. Panel (a) of Figure 6 shows that a one standard deviation increase in exposure—proxied by local 1996 cancer mortality rates—led to an average increase of 3 births per 1000 women, or approximately a 5.5% increase in the overall fertility rate among women aged 15 to 44 by 2018, relative to its 1996 baseline. These effects start to be significant in 2005, and have steadily grown since then.

Did births increase in levels? Having established that the opioid epidemic raised fertility rates in more exposed areas, we next ask what underlies this increase: did births rise in levels, or did the female population decline faster than births? To decompose these two forces, we write the change in the fertility rate as:

$$\Delta\text{Fertility Rate}_{ct} = \underbrace{\frac{\text{births}_{ct}}{\text{fem pop}_{c,1996}} - \frac{\text{births}_{c,1996}}{\text{fem pop}_{c,1996}}}_{\text{Birth effect}} + \underbrace{\frac{\text{births}_{ct}}{\text{fem pop}_{ct}} - \frac{\text{births}_{ct}}{\text{fem pop}_{c,1996}}}_{\text{Population effect}}.$$

[31] Complementary to this result, we find no evidence that the composition of movers and stayers varies across the exposure distribution. Figure A3 presents the distributions of age, household size, income, and homeownership for movers and stayers in the 2010 ACS, comparing above- and below-median exposure areas. The distributions are nearly identical across exposure levels: movers are disproportionately young (under 30), single, concentrated in the bottom quartile of the *unconditional* income distribution, and less likely to be homeowners. These patterns are consistent with Molloy et al. (2011).

The birth effect captures how the fertility rate would have changed had the female population remained fixed at its 1996 level; the population effect captures the mechanical contribution of a shrinking denominator, holding births fixed. Figure A5 shows that births declined in more exposed areas, but by less than the female population. The fertility rate increase therefore does not reflect more births in levels.

Can differential out-migration explain the fertility increase? In light of our migration results, which show higher out-migration rates among adults with a college education, it is possible that the observed increase in fertility reflects mostly compositional changes. In particular, because women without a college degree have higher baseline fertility rates than college-educated women (Kearney, 2022), differential migration by education could mechanically raise aggregate fertility if lower-fertility, college-educated women are more likely to leave highly exposed areas. To assess this, we estimate fertility responses separately by education group. If the aggregate increase were driven purely by compositional change, we would expect fertility to rise only because the share of high-fertility (non-college) women increases, not because fertility rises within groups. Panel (b) of Figure 6, however, shows that fertility increases within both education groups. The effect is larger among women without a college degree, but fertility also rises among college-educated women. Beginning in 2005 and persisting through 2018, the increase among women without a college degree is at least twice as large as the corresponding increase among women with some college education.

To formally quantify the relative contribution of composition versus within-group changes, we perform an Oaxaca decomposition of the aggregate change in fertility.[32] We estimate that more than 95% of the observed increase is driven by within-group fertility changes; shifts in the educational composition of women account for a negligible share. Compositional explanations based on observable characteristics are therefore insufficient to account for the fertility increase, though we cannot rule out selection on unobservable fertility preferences.

Heterogeneity by marital status and age. We next explore heterogeneity across marital status and age. We find that fertility increases for both married and unmarried women, but the timing differs. Among unmarried women, the effect becomes statistically significant in 2005, whereas among married women it does not reach significance until 2011 (Panel (c) of Figure A4). When splitting the sample by age, we find that the increase in fertility is concentrated among women aged 25 to 29, with no statistically significant

[32] We decompose the change in the fertility rate (F_{ct}) in commuting zone c between year t and a baseline year t_0 as follows:

$$\Delta F_{ct} = \sum_g \Delta S^g_{ct} F^g_{ct_0} + \sum_g S^g_{ct_0} \Delta F^g_{ct} + \sum_g \Delta S^g_{ct} \Delta F^g_{ct},$$

where g indexes education groups (college and non-college). The first term captures changes in group shares evaluated at baseline fertility rates, the second term captures within-group fertility changes evaluated at baseline population shares, and the third term is an interaction term.

changes in other age groups (Panel (d) of Figure A4).

Overall, the evidence indicates that the opioid epidemic led to a relative increase in fertility in more exposed areas. This pattern emerges despite substantial out-migration and cannot be explained by shifts in the educational or marital composition of women. Instead, fertility rose within demographic groups, with especially pronounced effects among women without a college degree. These findings suggest that the epidemic changed fertility behavior broadly, rather than simply altering the population's composition. In Section VIII., we examine the mechanisms underlying these effects.

VII.c Deaths

The opioid epidemic has been characterized by record levels of drug-related mortality. Prior research documents large increases in excess deaths attributable to opioids. Mortality is therefore a natural contributor to the population decline we estimate. However, mortality effects are not unique to local health crises: studies examining exposure to import competition from China and Mexico also find increases in mortality (Adda and Fawaz, 2020; Pierce and Schott, 2020; Finkelstein et al., 2025*b*).

We find that areas more exposed to the marketing of prescription opioids experienced higher drug-induced mortality, primarily among men and non-college-educated adults. By 2018, a one-standard-deviation increase in exposure led to a 1.97 additional deaths per 100,000, corresponding to a 53% increase relative to the pre-epidemic average (see panel (a) of Figure 7). We also find similar effects across sexes, despite higher baseline mortality rates among men (see panel (b)).

Adults without a college degree consistently exhibit higher levels of drug-induced mortality. Panel (c) shows the evolution of this outcome for high- and low-cancer-mortality CZs by education. We estimate positive and statistically significant increases in mortality among individuals without a college degree, while effects for those with a college education are statistically indistinguishable from zero. By 2010, a one-standard-deviation increase in exposure led to a 4.7 increase in drug-induced mortality per 100,000 among this group, corresponding to 57% of the pre-epidemic mean. Table A5 reports coefficients grouped into three post-periods to facilitate comparisons across subgroups.

VII.d Decomposition Exercise

How much does each margin of adjustment contribute to the change in population growth? To answer this question, we compute the change in population growth implied by our estimated exposure effects along each margin of adjustment. For any year T, population growth attributable to the opioid epidemic can be expressed as a function of changes in net migration, excess births, and excess mortality induced by exposure. That is, starting from a baseline year, we compute the implied evolution of the population growth rate for

the average commuting zone as shown in the next equation:

$$\Delta\text{Pop. Growth}_T = \ln \prod_{t=2000}^{T} \Big(1 \underbrace{- \tilde{\phi}_t^{\text{out-mig}}}_{\text{Excess net-migration}} \underbrace{+ \phi_t^{\text{birth}}}_{\text{Excess births}} \underbrace{- \phi_t^{\text{DI mort}}}_{\text{Excess mortality}}\Big), \tag{5}$$

where we choose 2000 as the baseline year so that growth rates are directly comparable to our population estimates. Appendix E. describes further details of this exercise.

Figure 8 presents the results of the decomposition exercise. Each solid line corresponds to the change in population growth attributable to a given channel, holding the other channels fixed, while the shaded areas indicate the absolute contribution of each channel to cumulative population growth. This exercise yields three main insights. First, out-migration is the primary driver of population changes. During the first decade, the absolute contribution of out-migration—the light-blue shaded area—accounts for nearly all of the cumulative decline in population growth. By 2010, the population growth rate implied by the migration channel alone is only 0.09 p.p. smaller than the observed change.

Second, excess births induced by the epidemic partially offset the negative effects of out-migration over the longer run. By 2020, the gap between the migration-implied change in population growth and the observed change reaches 0.54 p.p., while the fertility channel alone implies an increase of 0.58 p.p. in the growth rate. Thus, changes in the crude birth rate play a meaningful role in shaping longer-run population dynamics. Finally, the mortality channel contributes relatively little to overall population adjustment. Although mortality effects accumulate over time, they are not quantitatively large enough to substantially alter population growth over the 20-year horizon we study. We estimate that the population growth rate would have been almost unaffected if the opioid epidemic had not operated through other channels.

VIII. Mechanisms

Our results show that exposure to the opioid epidemic reduced population growth through selective out-migration, while simultaneously increasing fertility in more exposed areas. Guided by models in which migration responds to local labor market shocks (Blanchard et al., 1992) and by economic theories of fertility that emphasize income and opportunity costs (Becker, 1960, 1973), we study whether changes in economic conditions played a role in explaining both sets of findings. Yet the selectivity of this migration response—concentrated among college workers—points to forces beyond the labor market. As the model (Section IV.) makes explicit, migration decisions depend not only on wages and employment opportunities but also on local amenities that shape the desirability of places. Shocks that affect crime, housing markets, public services, or overall quality of life can therefore influence both population flows and family decisions. Thus, after examining

the effects of the epidemic on labor market conditions, we turn to its impact on local amenities.

VIII.a Economic Effects

To estimate the impacts of the opioid epidemic on labor market outcomes we consider a more parsimonious specification that aggregates effects for time periods but still permits some heterogeneity. We define five time bins [1990-1995], 1996, [1997 - 2003], [2004-2010], and [2011 - 2018] indexed by g:

$$\Delta y_{ct} = \sum_{g \neq 1996} \phi_g \, CancerMR_{c,1996} \, D_g(t) + \sum_g \alpha_g X_{ct_0} D_g(t) + \delta_{st} + \nu_{ct} \tag{6}$$

where $D_g(t) = \mathbf{1}\{t \in g\}$ is the indicator for time bin g, and the excluded category is 1996 to ease comparison with the rest of the analysis. The remaining variables are defined as in Equation (3).

Because we document substantial population changes in more exposed areas, it is important to distinguish between changes in employment levels and mechanical changes driven by migration.[33] We therefore present estimates for both log employment (capturing employment growth) and the employment-to-population ratio (capturing net labor market attachment). Panels (a) and (d) of Figure 9 show no evidence of differential pre-trends in employment growth prior to 1996, a pattern that holds for women and men, and for adults with and without a college degree. Panels (b) and (e) similarly confirm the absence of pre-trends in the employment-to-population ratio.

Turning to post-1996 effects, we find that exposure to the epidemic reduces employment growth across both sexes and education groups, and these effects increase over time. Nonetheless, the effects on the employment-to-population ratio show that the persistent negative effects are concentrated among adults without college education. These results suggest that exposure to the opioid epidemic translated into net employment losses for this group. By 2018, we estimate a reduction in their employment-to-population ratio of 2.4 percentage points per one standard deviation increase in exposure. Whether these negative employment effects translate into positive or negative changes in fertility depends on their differential impacts by sex. In Figure A7 we show that among the non-college group, employment losses are larger for women than for men. This gender asymmetry matters: when women bear a disproportionate share of employment losses, the opportunity cost of having children falls, creating upward pressure on fertility.

[33] To see this, note that the change in the employment-to-population ratio can be decomposed as follows: $\frac{emp_t}{pop_t} - \frac{emp_0}{pop_0} = \frac{emp_t - emp_0}{pop_t} + \frac{emp_0}{pop_t} - \frac{emp_0}{pop_0}$, where the first term captures the net employment change relative to the initial population level and the last two terms reflect the effect of population change on the employment-to-population ratio.

Finally, we examine earnings to assess whether these employment effects were accompanied by wage adjustments. We find no detectable effects on average earnings for either women or men. Estimates by education group are less precise, but we cannot reject the null of no earnings impact. These null results are consistent with the theoretically ambiguous wage predictions of the model. Overall, the evidence points to employment—rather than wages—declining as the primary labor market channel through which the epidemic affected local economic conditions. Yet these labor market patterns cannot account for the selective out-migration we document, where college-educated adults show the largest departure rates. This pattern points to an additional mechanism beyond labor market conditions.

VIII.b Local Amenities

The epidemic's reach extended well beyond direct health consequences, disrupting community conditions through several channels. One central manifestation is the increase in homelessness and high-poverty neighborhoods (Olvera et al., 2024; Kamada, 2026), reflecting severe hardship among individuals directly affected by addiction, health shocks, and economic instability. Communities also experienced rising neighborhood disorder, reflected in elevated volumes of 311 service requests and 911 emergency calls—forms of strain shown to be negatively capitalized into housing prices (Kallberg and Shimizu, 2025). In Multnomah County, Oregon, drug-related incidents account for 5.7% of all medical 911 calls—over 5,700 responses in 2024 alone—alongside more than 2,200 nonfatal overdose ambulance responses in 2023. Comparable patterns appear in other cities: in Boston, residents filed 4,654 311 service requests for needle pickup in 2018; in New York City, drug-related incidents accounted for over 110,000 EMS dispatches in 2018; and nationwide in 2019, emergency medical services administered more than 215,000 doses of naloxone, 36% of them in public or outdoor spaces (NEMSIS, 2019). These patterns point to a substantial and persistent strain on public services and shared urban space.

These indicators are mirrored in subjective perceptions of safety. According to the Cooperative Election Study (CES), residents of communities with above-median opioid exposure are nearly twice as likely to report worrying daily about their safety in their neighborhoods (10% vs. 5.1%; CES, 2016). Areas more affected by the opioid epidemic also experienced a higher incidence of crime. Using data from the FBI Uniform Crime Reporting System (UCRS), we estimate that a one–standard deviation increase in epidemic exposure leads to an increase in the crime rate of 2.9 per 1,000 people (all crimes), driven primarily by property crimes (2.4 per 1,000 people; Figure 10).

The spatial equilibrium framework predicts that deteriorations of this kind are capitalized into local housing prices and rents, reflecting households' willingness to pay for local quality of life. To measure housing prices, we use the county-level Federal Housing

Finance Agency (FHFA) House Price Index (HPI), which tracks changes in single-family home values using a weighted repeat-sales methodology based on properties with multiple mortgage transactions. To measure rental markets, we use median contracted rents from the Decennial Census and the American Community Survey. Consistent with this prediction, we find that exposure to the opioid epidemic led to substantial declines in local housing values and rents. By 2020, a one–standard-deviation increase in exposure reduced house prices by 7.8%. Figure 10 presents these results. Rents also decline: the same increase in exposure predicts a 2.5% reduction in median rents by 2020 (Table 4).[34]

To summarize, the evidence suggests that the opioid epidemic reshaped both the economic returns to staying and the quality of local life in more exposed areas. Persistent employment losses—concentrated among less-educated adults—reduced labor market opportunities without generating compensating wage gains. At the same time, declining housing values, rising crime, increased neighborhood disorder, and worsening perceptions of safety lowered the desirability of affected communities. Consistent with the model's prediction, such amenity deteriorations generate a disproportionate incentive to leave among college workers, whose higher valuation of amenities and greater geographic mobility amplify their out-migration response (Bound and Holzer, 2000; Diamond, 2016; Molloy et al., 2011). For those who remain, weaker labor market prospects—particularly for women with limited attachment—may reduce the opportunity cost of childbearing, while housing market adjustments alter the affordability of family formation (Couillard, 2026). Moreover, rising crime and neighborhood instability can directly influence fertility decisions (Churchill et al., 2022). These channels jointly help explain why more exposed areas experienced selective out-migration alongside higher fertility among those who remained.

IX. Robustness Checks

In this section, we provide evidence in support of our identification strategy, explore alternative explanations for our findings and test the sensitivity of our results.

[34]The implied elasticity of house prices to crime obtained by dividing our HPI effect (−7.8%) by our crime effect (a roughly 10% increase off a national baseline) is on the upper end of the literature, which generally finds elasticities of −0.1 to −0.3 (Gibbons, 2004; Linden and Rockoff, 2008; Pope, 2008; Pope and Pope, 2012; Ihlanfeldt and Mayock, 2010; Bishop and Murphy, 2011). This HPI estimate captures the *full* amenity bundle generated by the epidemic—homelessness, wide spread drug addiction, neighborhood disorder, increased 911/311 calls, perceived safety, and crime—and is therefore not directly comparable to crime-only elasticities. A 7.8% capitalization is, however, well within the range observed for bundled amenity shocks of similar visibility—e.g., toxic-plant openings (−11%; Currie et al., 2015), shale-gas drilling near groundwater-dependent homes (up to −16%; Muehlenbachs et al., 2015), and pediatric leukemia risk (−15%; Davis, 2004).

IX.a Evidence on the Exogeneity Assumption and Exclusion Restriction

The validity of the identification strategy requires that, in the absence of prescription opioid marketing, areas with higher cancer mortality in 1996 would have followed the same trends in health and economic outcomes as areas with lower cancer mortality—all along the support of the 1996 cancer mortality distribution. To support this assumption, we present several exercises.[35]

Out-of-sample. This exercise tests whether lagged cancer mortality predicts future population growth, migration, and fertility prior to the onset of the opioid epidemic. In panel (a) of Figure 11 we show that 1976 cancer mortality does not predict population growth between 1990 and 2000, i.e., there is no relationship between cancer mortality rates and population growth in the next 20 years or so. Similarly, in panel (a) of Figures 12 and A9, we find that cancer 1976 is not predictive of out-migration probabilities or fertility rates before 1996—the estimated coefficients are statistically indistinguishable from zero, and there is no evidence of a pattern—providing evidence of a lack of mechanical relationship between cancer mortality and these outcomes.

Placebo. We further probe the validity of our design by estimating event-study regressions with placebo instruments—i.e., mid-1990s mortality from causes unrelated to cancer.[36] Finding a good placebo instrument is challenging given that the causes that underlie the incidence of cancer and of other conditions such as heart disease are not independent (Chiang, 1991; Honoré and Lleras-Muney, 2006). As a result, there is substantial overlap across underlying causes, and the correlation across measures is very high, especially among elderly age groups. With this caveat, in panels (b) and (c) of Figure 11 we present placebo instrument regressions for mortality from hypertension, which are less likely to be affected by the previous concern but still capture community-level health trends. We find no relationship between mortality from these causes and population growth. Panel (b) of Figures 12 and A9, present this exercise for migration and fertility rates, the event study graph shows no effects of placebo mortality on these outcomes.

These two exercises also provide evidence against an alternative explanation for our results: that higher mortality could mechanically reduce population. Nonetheless, exploiting alternative mortality measures–i.e., cancer mortality in 1976 and placebo mortality rates– we provide evidence of a lack of mechanical or direct relationship between higher mortality and lower population growth.

Additional covariates. We also expand the set of covariates to account for health behaviors, access to healthcare and economic factors and the correlation of these with cancer. To do so, we consider three additional models. First, we control for contempo-

[35] In this paper we focus on population growth, migration, and fertility as the main outcomes of analysis. Arteaga and Barone (2026) provide complementary evidence on the validity of this strategy and present results for these tests on a variety of mortality, economic, and political outcomes.

[36] These placebo instruments are also known as negative instruments (Danieli et al., 2023).

raneous cancer mortality rates to account for the association between cancer and other socio-economic outcomes. Second, we expand the set of controls in our baseline to include the share of smokers, the share of adults with overweight, the share of primary care physicians, and the infant mortality rate, all measured at the CZ level at baseline or the earliest available data point. Third, we expand the set of controls to account for economic covariates, these controls include the unemployment rate, the share of employment in the manufacturing sector, and the share of the population that has completed some college. Panels (b) and (c) of Figure 11 and panel (c) of Figures 12 and A9 show that our results are robust to the inclusion of these covariates.

IX.b Exposure to Economic Shocks

We account for geographic exposure to major economic shocks that could confound the relationship between opioid exposure and our outcomes. Contemporaneous with the unfolding of the opioid epidemic, the United States economy was affected by the formation of the NAFTA, rising import competition from China and two major recessions (2001 and 2007-09). These developments could confound population changes and influence relocation decisions. To address rising import competition from the NAFTA and from China joining the WTO, we control for exposure to the regional import competition measure from Choi et al. (2024) and Pierce and Schott (2020) respectively. Exposure to the 2001 and Great Recession is measured using changes in CZ-level unemployment around each downturn, as in Yagan (2019).[37] For each shock, we include a measure of local exposure interacted with year dummies to flexibly control for its varying geographic impact. Figure 11, Figure 12(d), and A9(d) present these estimates and provide evidence that our results are not capturing exposure to these other local shocks.

IX.c Continuous Exposure and Linearity

As discussed in Section V., in settings with continuous exposure, such as ours, linearity of treatment effects ensures a fully causal interpretation of two-way fixed effects estimates as ACRs (Goldsmith-Pinkham et al., 2020; Callaway et al., 2024). To assess the validity of this assumption, we begin by dividing the sample into 10 equally sized groups based on 1996 cancer mortality rates and plotting the outcomes of interest across the full support of the exposure variable. Appendix Figure A8 presents this exercise for the 20-years log population change and for fertility rates, the changes in the out- and in-migration probabilities are presented in Figure 3. These visualizations transparently illustrate the reduced-form relationships between baseline cancer mortality and our various outcomes. They show a linear relationship between population growth and migration flows with

[37] We follow the literature to construct these measures; Arteaga and Barone (2026) provides the details. Correlations with opioid exposure range from –0.04 to 0.18: NAFTA: –0.04, China shock: 0.18, 2001 recession: 0.05, Great Recession: 0.02.

1996 cancer mortality rates. This linearity suggests that the changes in the outcome variables are relatively constant across levels of exposure.

As an additional robustness check, we re-define our treatment variable as a binary indicator equal to one for CZs above the median of the 1996 cancer mortality distribution and zero otherwise. We estimate our results using this alternative definition and refer to these results as "binary treatment" in Figures 11, 12(e), and A9(e), for population, migration, and fertility respectively. Results are qualitatively and quantitatively similar to exploiting the continuous treatment, lending further credibility to our main findings. We further test for heterogeneity by estimating the effects of cancer exposure on samples that exclude CZs in either the top or bottom quintile of the cancer mortality distribution. As shown in Figure 11, Figure 12(e), and A9(e), our results are consistent with the full-sample estimates in both cases, offering evidence that non-linear treatment effects are not a major feature in our setting.

IX.d Alternative periods and samples

We leverage data from the Census and the ACS to construct population counts; however, population measures derived from these sources may be influenced by disruptions to data collection during the COVID-19 pandemic. To assess whether our results are affected by this limitation, we use population estimates for 2018 and re-estimate our long-term effects. We find that results based on the 18-year change in log population are both qualitatively and quantitatively similar to our main estimates (panels (b) and (c) of Figure 11).

In our main specification, we restrict the sample to CZs with more than 25,000 residents; these areas represent over 97% of the total population in 1996. We reproduce the analysis using alternative restrictions on CZ size—specifically, thresholds of more than 20,000 and more than 30,000 residents—and arrive at conclusions analogous to those from the main analysis (see the last two rows of panels (b) and (c) of Figure 11 for population results and Figure A9(f) for fertility rates). Similarly, our county-level migration sample consists of counties that contribute to our CZ analysis sample and have 1996 populations over 20,000, which includes 93% of our analysis sample population in 1996. We re-estimate our migration effects using alternative thresholds of 15,000 and 25,000 residents in 1996; Figure 12(f) shows the results are unchanged with these alternative sample definitions.

Finally, we assess whether our results are sensitive to the exclusion of any single state. Figure A10 shows the estimated effects on the 20-year population growth rate, out-migration rates in 2010, and fertility rates in 2018. The figure indicates that our results are not driven by any particular state, as the estimates remain similar to those obtained using the full sample.

IX.e Additional explanations: fertility

A potential direct channel linking the opioid epidemic to fertility operates through opioid use disorder (OUD). Drug use is associated with lower contraceptive use and higher rates of unintended pregnancy (Terplan et al., 2015). Consequently, exposure to the epidemic could, in principle, increase fertility if it led to reduced contraception. However, the magnitude of this channel is likely limited. In 2018, 0.9% of women aged 15–44 had an OUD NSDUH (2020), while births diagnosed with neonatal abstinence syndrome (NAS) accounted for 0.6% of all births (CDC, 2023*a*). Given that withdrawal symptoms develop in 55% to 94% of neonates exposed to opioids in utero (Hudak et al., 2012), a back-of-the-envelope calculation suggests that women with OUD have fertility rates approximately 88%, thus lower than the general population. An alternative mechanism could operate through changes in abortion rates or access to abortion services. Using data from the Myers Abortion Facility Database, we find no evidence of changes in abortion rates as a function of exposure to the epidemic (Figure A11). Moreover, we do not observe any differential effects between areas with high and low access to abortion services.

X. Discussion

This paper documents how the opioid epidemic reshaped fundamental demographic processes through changes in internal migration, fertility, and mortality. Using quasi-exogenous variation in local exposure to Purdue Pharma's marketing of OxyContin, we show that communities more exposed to the epidemic experienced lower population growth, driven primarily by increased out-migration among college-educated adults. Working in the opposite direction, the opioid epidemic induced substantial increases in fertility, concentrated among non-college educated mothers, which by the end of our period partially offset these population declines. Although mortality rises sharply in proportional terms relative to pre-epidemic levels, the absolute increase is modest, yielding only a minimal effect on population growth. Together, these shifts reveal how the epidemic contributed to growing regional demographic divergence within the United States.

A key implication of our findings is that the opioid epidemic differs from canonical local economic shocks—such as trade exposure, automation, or industrial decline—in an important respect: beyond disrupting labor-market opportunities, it eroded the amenity value of places. Communities most exposed to the crisis were characterized by rising addiction, homelessness, neighborhood disorder, and a strain on public services, reducing local quality of life. This deterioration in local amenities helps explain why the migration response we document is both sizable and selective.

This interpretation also points to an important distinction from the amenity-capitalization literature, which has mostly studied discrete and exogenous shocks to local

amenities.[38] By contrast, disamenities arising from the opioid epidemic were a direct outgrowth of the epidemic's own social spillovers. Our findings of selective out-migration and fertility suggest that local shocks combining market and non-market disruptions may be particularly persistent, and even self-reinforcing, when amenity formation is shaped by the composition of residents, especially the college-educated (Diamond, 2016). This underscores the importance of research on how local amenities form and evolve, and how policy can engage with these endogenous processes. Moreover, gains from policies targeting local disamenities may be limited or difficult to sustain if they do not address the underlying drivers.

[38]Examples include toxic-plant openings (Currie et al., 2015), shale-gas drilling (Muehlenbachs et al., 2015), wind-turbine installations (Quentel, 2026), or the disclosure of localized health risks (Davis, 2004).

References

Acemoglu, Daron, and Pascual Restrepo. 2020. "Robots and jobs: Evidence from US labor markets." *Journal of Political Economy*, 128(6): 2188–2244.

Adda, Jérôme, and Yarine Fawaz. 2020. "The health toll of import competition." *The Economic Journal*, 130(630): 1501–1540.

Alpert, Abby, William N Evans, Ethan M J Lieber, and David Powell. 2022. "Origins of the Opioid Crisis and its Enduring Impacts." *The Quarterly Journal of Economics*. qjab043.

Armington, Paul S. 1969. "A Theory of Demand for Products Distinguished by Place of Production (Une theorie de la demande de produits differencies d'apres leur origine) (Una teoria de la demanda de productos distinguiendolos segun el lugar de produccion)." *Staff Papers - International Monetary Fund*, 16(1): 159.

Arteaga, Carolina, and Victoria Barone. 2026. "Republican support and economic hardship: The enduring effects of the opioid epidemic." *The Quarterly Journal of Economics*, 141(1): 499–558.

Autor, David, David Dorn, Gordon Hanson, and Kaveh Majlesi. 2020. "Importing political polarization? The electoral consequences of rising trade exposure." *American Economic Review*, 110(10): 3139–3183.

Autor, David, David Dorn, Gordon H Hanson, Maggie R Jones, and Bradley Setzler. 2025. "Places versus people: the ins and outs of labor market adjustment to globalization." National Bureau of Economic Research.

Autor, David. H., and David Dorn. 2013. "The Growth of Low-Skill Service Jobs and the Polarization of the US Labor Market." *American Economic Review*, 103(5): 1553–97.

Autor, David H., David Dorn, and Gordon H. Hanson. 2019. "When Work Disappears: Manufacturing Decline and the Falling Marriage Market Value of Young Men." *American Economic Review: Insights*, 1(2): 161–178.

Bassler, Sean, Kevin Rinz, David Wasser, and Abigail Wozniak. 2026. "A Shock by Any Other Name? Reconsidering the Impacts of Local Demand Shocks."

Becker, Gary S. 1960. *An Economic Analysis of Fertility.* Columbia University Press.

Becker, Gary S. 1973. "A Theory of Marriage: Part I." *Journal of Political Economy*, 81(4): 813–846.

Bernard, Aude. 2017. "Cohort Measures of Internal Migration: Understanding Long-Term Trends." *Demography*, 54(6): 2201–2221.

Bishop, Kelly C., and Alvin D. Murphy. 2011. "Estimating the Willingness to Pay to Avoid Violent Crime: A Dynamic Approach." *American Economic Review: Papers and Proceedings*, 101(3): 625–629.

Blanchard, Olivier Jean, Lawrence F Katz, Robert E Hall, and Barry Eichengreen. 1992. "Regional evolutions." *Brookings papers on economic activity*, 1992(1): 1–75.

Borusyak, Kirill, Rafael Dix-Carneiro, and Brian Kovak. 2022. "Understanding migration responses to local shocks." *Available at SSRN 4086847*.

Boston ODP. 2018. "311 Service Requests (2018)." Accessed February 27, 2026.

Bound, John, and Harry J. Holzer. 2000. "Demand Shifts, Population Adjustments, and Labor Market Outcomes during the 1980s." *Journal of Labor Economics*, 18(1): 20–54.

Broda, C., and D. E. Weinstein. 2006. "Globalization and the Gains From Variety." *The Quarterly Journal of Economics*, 121(2): 541–585.

Buckles, Kasey, William N Evans, and Ethan MJ Lieber. 2022. "The drug crisis and the living arrangements of children." *Journal of Health Economics*, 102723.

Cadena, Brian C., and Brian K. Kovak. 2016. "Immigrants Equilibrate Local Labor Markets: Evidence from the Great Recession." *American Economic Journal: Applied Economics*, 8(1): 257–290.

Callaway, Brantly, Andrew Goodman-Bacon, and Pedro HC Sant'Anna. 2024. "Difference-in-differences with a continuous treatment." National Bureau of Economic Research.

Card, D., and T. Lemieux. 2001. "Can Falling Supply Explain the Rising Return to College for Younger Men? A Cohort-Based Analysis." *The Quarterly Journal of Economics*, 116(2): 705–746.

Card, David. 2009. "Immigration and Inequality." *American Economic Review*, 99(2): 1–21.

Cattaneo, Matias D., Richard K. Crump, Max H. Farrell, and Yingjie Feng. 2024. "On Binscatter." *American Economic Review*, 114(5): 1488–1514.

CDC. 2020. "U.S. Opioid Dispensing Rate Maps."

CDC. 2023*a*. "Opioid Use During Pregnancy." Accessed: 2025-08-01.

CDC, National Center for Health Statistics. 2023*b*. "Drug Overdose Death Rates."

CES. 2016. "Cooperative Election Study, 2016: University of Maryland Team Module." Team module designed by the University of Maryland; survey administered by YouGov.

Chiang, Chin Long. 1991. "Competing risks in mortality analysis." *Annual review of public health*, 12(1): 281–307.

Choi, Jiwon, Ilyana Kuziemko, Ebonya Washington, and Gavin Wright. 2024. "Local Economic and Political Effects of Trade Deals: Evidence from NAFTA." *American Economic Review*.

Churchill, Sefa Awaworyi, Russell Smyth, Trong-Anh Trinh, and Siew Ling Yew. 2022. "Local crime and fertility." *Journal of Economic Behavior & Organization*, 200: 312–331.

Claassen, Stephen. 2025. "Consideration Sets and Migration Responses to Local Shocks."

Cornaggia, Kimberly, John Hund, Giang Nguyen, and Zihan Ye. 2022. "Opioid crisis effects on municipal finance." *The Review of Financial Studies*, 35(4): 2019–2066.

Couillard, Benjamin K. 2026. "Build, Baby, Build: How Housing Shapes Fertility." *Working Paper*. Working paper.

Currie, Janet, Lucas Davis, Michael Greenstone, and Reed Walker. 2015. "Environmental Health Risks and Housing Values: Evidence from 1,600 Toxic Plant Openings and Closings." *American Economic Review*, 105(2): 678–709.

Danieli, Oren, Daniel Nevo, Itai Walk, Bar Weinstein, and Dan Zeltzer. 2023. "Negative controls for instrumental variable designs." *arXiv preprint arXiv:2312.15624*.

Davis, Lucas W. 2004. "The Effect of Health Risk on Housing Values: Evidence from a Cancer Cluster." *American Economic Review*, 94(5): 1693–1704.

Diamond, Rebecca. 2016. "The determinants and welfare implications of US workers' diverging location choices by skill: 1980–2000." *American economic review*, 106(3): 479–524.

Eichmeyer, Sarah, and Jonathan Zhang. 2022. "Pathways into opioid dependence: Evidence from practice variation in emergency departments." *American Economic Journal: Applied Economics*, 14(4): 271–300.

Evans, William N., Ethan M.J. Lieber, and Patrick Power. 2019. "How the Reformulation of OxyContin Ignited the Heroin Epidemic." *Review of Economics and Statistics*, 101(1): 1–15.

Feenstra, Robert C., Philip Luck, Maurice Obstfeld, and Katheryn N. Russ. 2018. "In Search of the Armington Elasticity." *The Review of Economics and Statistics*, 100(1): 135–150.

Finkelstein, Amy, Matthew Gentzkow, and Dean Li. 2025*a*. "What drives risky prescription opioid use? Evidence from migration." *The quarterly journal of economics*, 140(4): 3133–3189.

Finkelstein, Amy, Matthew J. Notowidigdo, and Steven Shi. 2026. "Trading Goods for Lives: NAFTA's Mortality Impacts and Implications." Working paper.

Finkelstein, Amy, Matthew J Notowidigdo, Frank Schilbach, and Jonathan Zhang. 2025*b*. "Lives Versus Livelihoods: The Impact of the Great Recession on Mortality and Welfare." *The Quarterly Journal of Economics*, qjaf023.

Foschi, Andrea, Christopher L House, Christian Proebsting, and Linda L Tesar. 2023. "Labor Mobility and Unemployment over the Business Cycle." Vol. 113, 590–596, American Economic Association 2014 Broadway, Suite 305, Nashville, TN 37203.

Foster, Thomas B. 2017. "Decomposing American immobility: Compositional and rate components of interstate, intrastate, and intracounty migration and mobility decline." *Demographic Research*, 37: 1515–1548.

Gallup. 2018–2021. "Gallup Poll Social Series: Crime." *https://news.gallup.com/poll/1603/crime.aspx*, Accessed: 2025-11-26.

Ganong, Peter, and Daniel Shoag. 2017. "Why has regional income convergence in the US declined?" *Journal of Urban Economics*, 102: 76–90.

Gibbons, Steve. 2004. "The Costs of Urban Property Crime." *The Economic Journal*, 114(499): F441–F463.

Glaeser, Edward L, and Joseph Gyourko. 2005. "Urban decline and durable housing." *Journal of political economy*, 113(2): 345–375.

Glaeser, Edward L, and Joshua D Gottlieb. 2009. "The wealth of cities: Agglomeration economies and spatial equilibrium in the United States." *Journal of economic literature*, 47(4): 983–1028.

Glaeser, Edward L, Jed Kolko, and Albert Saiz. 2001. "Consumer city." *Journal of economic geography*, 1(1): 27–50.

Goldsmith-Pinkham, Paul, Isaac Sorkin, and Henry Swift. 2020. "Bartik Instruments: What, When, Why, and How." *American Economic Review*, 110(8): 2586–2624.

Gramlich, John. 2017. "Nearly half of Americans have a family member or close friend who's been addicted to drugs." *https://www.pewresearch.org/short-reads/2017/10/26/nearly-half-of-americans-have-a-family-member-or-close-friend-whos-been-addicted-to-drugs/*, Accessed: 2025-11-26.

Greenland, Andrew, John Lopresti, and Peter McHenry. 2019. "Import competition and internal migration." *Review of Economics and Statistics*, 101(1): 44–59.

Gyourko, Joseph, and Joseph Tracy. 1989. "The importance of local fiscal conditions in analyzing local labor markets." *Journal of Political economy*, 97(5): 1208–1231.

Hansen, Benjamin, Timothy Moore, and William Olney. 2023. "Importing the Opioid Crisis? International Trade and Drug Overdoses." *Working Paper*.

Honoré, Bo E, and Adriana Lleras-Muney. 2006. "Bounds in Competing Risks models and The War on Cancer." *Econometrica*, 74(6): 1675–1698.

Hudak, Mark L., Rosemarie C. Tan, Committee on Drugs, Committee on Fetus, and Newborn. 2012. "Neonatal Drug Withdrawal." *Pediatrics*, 129(2): e540–e560.

Ihlanfeldt, Keith, and Tom Mayock. 2010. "Panel Data Estimates of the Effects of Different Types of Crime on Housing Prices." *Regional Science and Urban Economics*, 40(2–3): 161–172.

Jones, Christopher M, Kun Zhang, Beth Han, Gery P Guy, Jan Losby, Emily B Einstein, Miriam Delphin-Rittmon, Nora D Volkow, and Wilson M Compton. 2024. "Estimated number of children who lost a parent to drug overdose in the US from 2011 to 2021." *JAMA psychiatry*, 81(8): 789–796.

Kallberg, Jarl G, and Yoshiki Shimizu. 2025. "Crime Measures and Housing Prices: an Analysis Using Quantile Regression and Spatial Autocorrelation." *The Journal of Real Estate Finance and Economics*, 1–53.

Kamada, Takuma. 2026. "Regulating Opioids, Creating Poverty: How the OxyContin Reformulation Shapes Neighborhood Disadvantage." Working paper.

Katz, L. F., and K. M. Murphy. 1992. "Changes in Relative Wages, 1963-1987: Supply and Demand Factors." *The Quarterly Journal of Economics*, 107(1): 35–78.

Kearney, Melissa Schettini. 2022. "The "college gap" in marriage and children's family structure." National Bureau of Economic Research.

Krueger, Alan B. 2017. "Where Have All the Workers Gone? An Inquiry into the Decline of the U.S. Labor Force Participation Rate." *Brookings Papers on Economic Activity*, 2017(2): 1.

Linden, Leigh, and Jonah E. Rockoff. 2008. "Estimates of the Impact of Crime Risk on Property Values from Megan's Laws." *American Economic Review*, 98(3): 1103–1127.

Lundberg, Shelly, and Robert A Pollak. 2014. "Cohabitation and the uneven retreat from marriage in the United States, 1950–2010." *Human capital in history: The American record*, 241–272.

Mackun, Paul, Joshua Comenetz, and Lindsay Spell. 2021. "More than half of US counties were smaller in 2020 than in 2010." *Washington DC: US Census Bureau.*

Maclean, Catherine, Justine Mallatt, Christopher J. Ruhm, and Kosali Ilayperuma Simon. 2020. "Review of Economic Studies on the Opioid Crisis." NBER Working Paper No. 28067.

Manski, Charles F. 2025. "Inference with Imputed Data: The Allure of Making Stuff Up." *Journal of Labor Economics*, 43(S1): S333–S350.

Manski, Charles F, Michael Gmeiner, and Anat Tamburc. 2021. "Misguided Use of Observed Covariates to Impute Missing Covariates in Conditional Prediction: A Shrinkage Problem."

McLanahan, Sara. 2004. "Diverging destinies: How children are faring under the second demographic transition." *Demography*, 41(4): 607–627.

Meier, Barry. 2018. *Pain Killer: An Empire of Deceit and the Origin of America's Opioid Epidemic.* Random House.

Melzack, Ronald. 1990. "The tragedy of Needless Pain." *Scientific American*, 262(2): 27–33.

Miloucheva, Boriana. 2021. "Pharmaceutical Promotion, Physician Response, and Opioid Abuse: Identifying the Role of Physicians in the Opioid Crisis." Working Paper.

Molloy, Raven, Christopher L Smith, and Abigail Wozniak. 2011. "Internal migration in the United States." *Journal of Economic perspectives*, 25(3): 173–196.

Moretti, Enrico, and Daniel J. Wilson. 2017. "The Effect of State Taxes on the Geographical Location of Top Earners: Evidence from Star Scientists." *American Economic Review*, 107(7): 1858–1903.

Muehlenbachs, Lucija, Elisheba Spiller, and Christopher Timmins. 2015. "The Housing Market Impacts of Shale Gas Development." *American Economic Review*, 105(12): 3633–3659.

NEMSIS. 2019. "2019 Public-Release Research Dataset." *https://nemsis.org*, U.S. Department of Transportation, National Highway Traffic Safety Administration.

Notowidigdo, Matthew J. 2020. "The incidence of local labor demand shocks." *Journal of Labor Economics*, 38(3): 687–725.

NPR, Robert Wood Johnson Foundation, and Harvard T.H. Chan School of Public Health. 2018. "Life in Rural America." *https://www.rwjf.org/en/insights/our-research/2018/10/life-in-rural-america.html*, Accessed: 2025-11-26.

NSDUH. 2020. "National Survey on Drug Use and Health, 2018." *https://www.datafiles.samhsa.gov/dataset/nsduh-2018-ds0001*, Accessed: 2025-08-01.

NYC EMS. 2018. "EMS Incident Dispatch Data (2018)." Accessed: February 27, 2026.

Olvera, Johabed G, Felipe Lozano-Rojas, Julio A Ramos Pastrana, and Sumedha Gupta. 2024. "Opioids prescribing restrictions and homelessness: Evidence from hydrocodone rescheduling." *Journal of Housing Economics*, 66: 102010.

Ouimet, Paige, Elena Simintzi, and Kailei Ye. 2020. "The impact of the opioid crisis on firm value and investment." *Available at SSRN 3338083*.

OxyContin Launch Plan. September 1995. Purdue Pharma.

OxyContin Team Meeting. April 1994. Purdue Pharma.

OxyContin Team Meeting. March 1995. Purdue Pharma.

Park, Sujeong, and David Powell. 2021. "Is the Rise in Illicit Opioids Affecting Labor Supply and Disability Claiming Rates?" *Journal of Health Economics*, 76: 102430.

Paulozzi, Leonard J, Edwin M Kilbourne, and Hema A Desai. 2011. "Prescription drug monitoring programs and death rates from drug overdose." *Pain medicine*, 12(5): 747–754.

Pierce, Justin R, and Peter K Schott. 2020. "Trade Liberalization and Mortality: Evidence from US Counties." *American Economic Review: Insights*, 2(1): 47–64.

Pope, Devin G., and Jaren C. Pope. 2012. "Crime and Property Values: Evidence from the 1990s Crime Drop." *Regional Science and Urban Economics*, 42(1–2): 177–188.

Pope, Jaren C. 2008. "Fear of Crime and Housing Prices: Household Reactions to Sex Offender Registries." *Journal of Urban Economics*, 64(3): 601–614.

Porcher, Charly. 2022. "Migration with Costly Information."

Powell, David, Rosalie Liccardo Pacula, and Erin Taylor. 2020. "How Increasing Medical Access to Opioids Contributes to the Opioid Epidemic: Evidence From Medicare Part D." *Journal of Health Economics*, 71: 102286.

Quentel, Milan. 2026. "Renewable Energy Infrastructure, Welfare, and Redistribution." Working paper.

Quinones, Sam. 2015. *Dreamland: The true tale of America's opiate epidemic.* Bloomsbury Publishing USA.

Roback, Jennifer. 1982. "Wages, Rents, and the Quality of Life." *Journal of Political Economy*, 90(6): 1257–1278.

Roberson, Patricia NE, Gina Cortez, Laura Hunt Trull, and Kathrine Lenger. 2020. "In their own words: how opioids have impacted the lives of "everyday" people living in Appalachia." *Journal of Appalachian Health*, 2(4): 26.

Rodrik, Dani. 2021. "Why does globalization fuel populism? Economics, culture, and the rise of right-wing populism." *Annual Review of Economics*, 13: 133–170.

Rosen, Sherwin. 1979. "Wage-based indexes of urban quality of life." *Current issues in urban economics*, 74–104.

SAMHSA. 2020. "Key Substance Use and Mental Health Indicators in the United States: Results from the 2019 National Survey on Drug Use and Health."

Savych, Bogdan, David Neumark, and Randall Lea. 2019. "Do Opioids Help Injured Workers Recover and Get Back to Work? The Impact of Opioid Prescriptions on Duration of Temporary Disability." *Industrial Relations: A Journal of Economy and Society*, 58(4): 549–590.

Suarez Serrato, Juan Carlos, and Philippe Wingender. 2016. "Estimating local fiscal multipliers." National Bureau of Economic Research.

Terplan, Mishka, Dennis J Hand, Melissa Hutchinson, Elizabeth Salisbury-Afshar, and Sarah H Heil. 2015. "Contraceptive Use and Method Choice Among Women with Opioid and Other Substance Use Disorders: A Systematic Review." *Preventive medicine*, 80: 23–31.

Wilson, Riley. 2022. "Moving to economic opportunity: the migration response to the fracking boom." *Journal of Human Resources*, 57(3): 918–955.

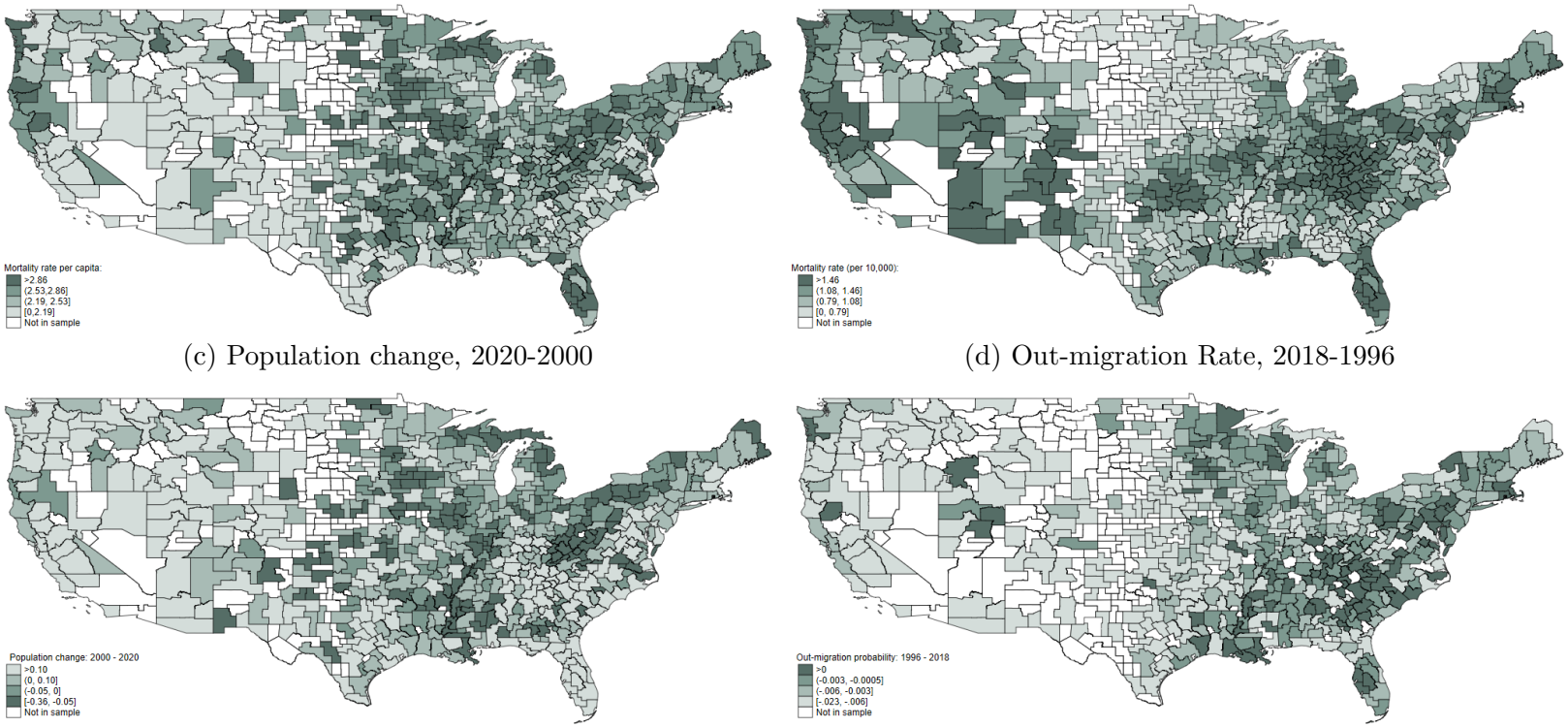
Yagan, Danny. 2019. "Employment Hysteresis from the Great Recession." *Journal of Political Economy*, 127(5): 2505–2558.

XI. Figures

Figure 1: Geographic Variation

(a) Cancer Mortality Rate, 1996

(b) Drug-Induced Mortality per 10,000, 2018-1996

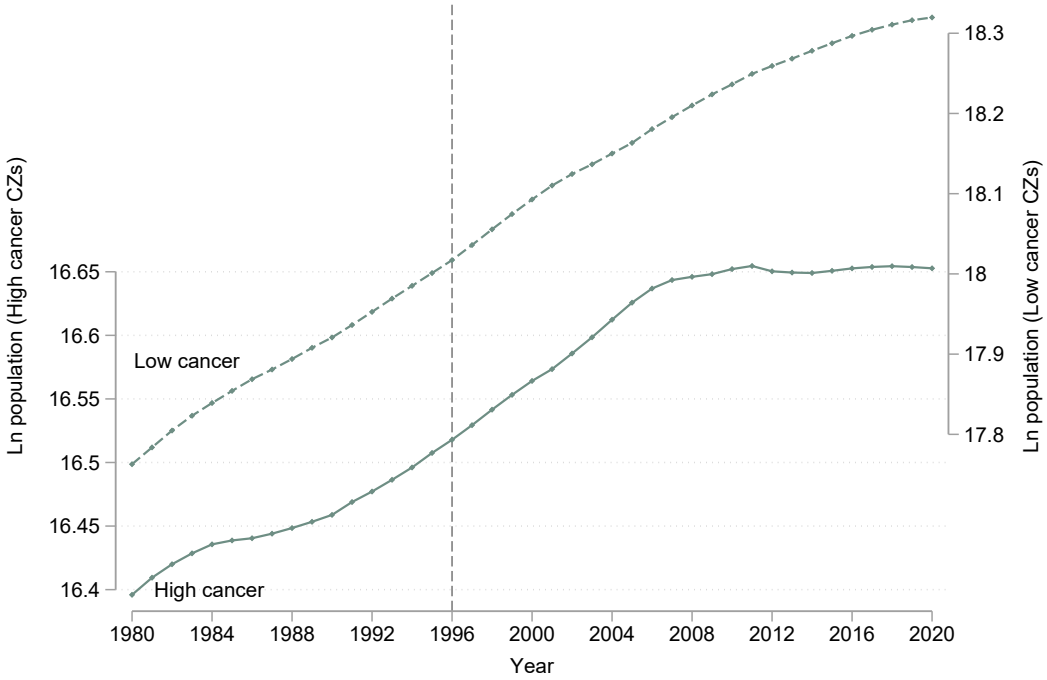


(c) Population change, 2020-2000

(d) Out-migration Rate, 2018-1996

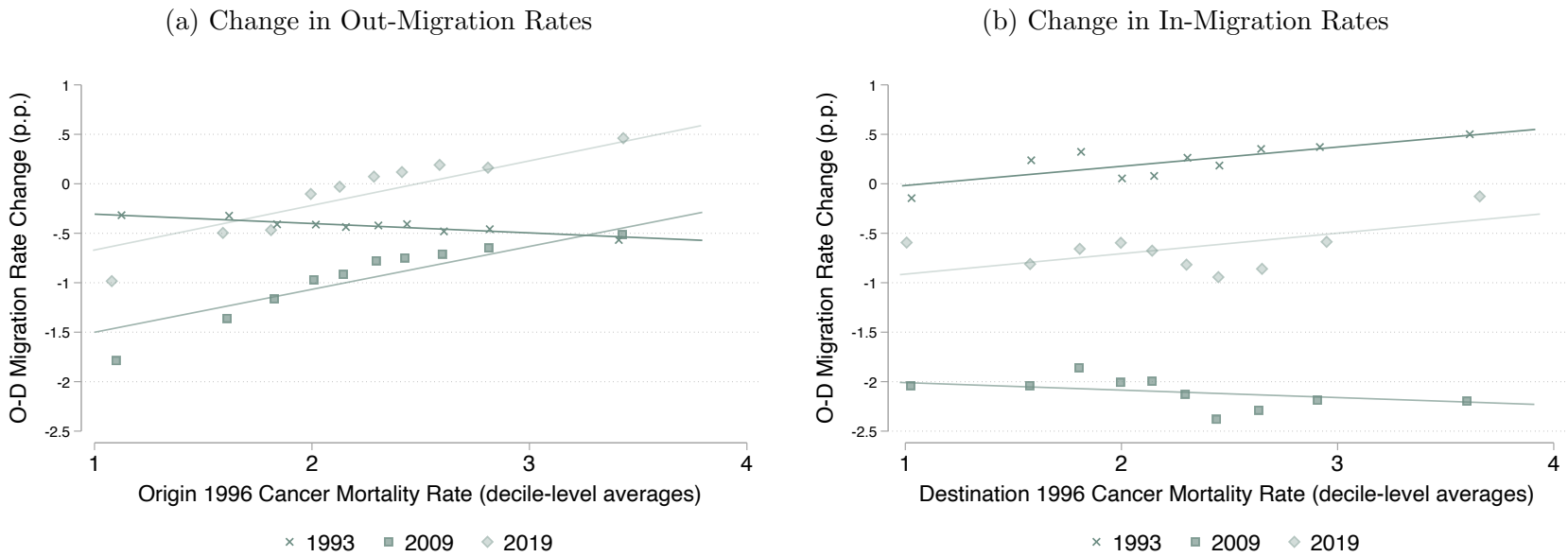
Notes: Panel (a) of this figure shows the geographic distribution of the cancer mortality rate (per 1,000) in 1996, our measure of exposure to the opioid epidemic. Panel (b) shows the geographic distribution of drug-induced mortality (per 10,000) between 1996 and 2018. Panel (c) shows the change in the log of population aged 18 to 64 years old between the decennial years 2020 and 2000. Panel (d) shows the change in out migration probabilities from 1996 to 2018. The break points correspond to the quartiles of the variable's distribution. In the bottom panels, we use zero as a break point to ease interpretation of population decline (panel c) and net-out migration (panel d). The sample is restricted to areas with more than 25,000 residents in 1996; these account for more than 97% of the total population in 1996. Commuting zones not included in the sample are white in the figure. We use geocoded National Vital Statistics System data to construct death counts; see Section III. for the ICD codes used. This figure is referenced in Sections III. and VI.

Figure 2: Evolution of Local Working Age Populations (ages 18-64) in High- vs. Low-Exposure Commuting Zones



Notes: This figure shows the evolution of log population aged 18 to 64 years in CZs in the bottom (dashed lines) and top (solid lines) quartiles of cancer mortality before the launch of OxyContin. This comparison is based on dichotomous high-versus-low categorization of CZs, and the outcome is weighted by population. The series for high-cancer-mortality CZs are plotted on the left vertical axis, while those for low-cancer-mortality CZs are shown on the right. This figure is referenced in Section VI.

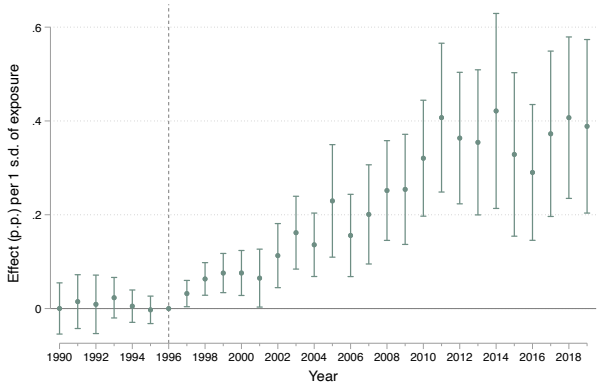
Figure 3: Changes in Out- and In-Migration Rates as a Function of Exposure to the Epidemic



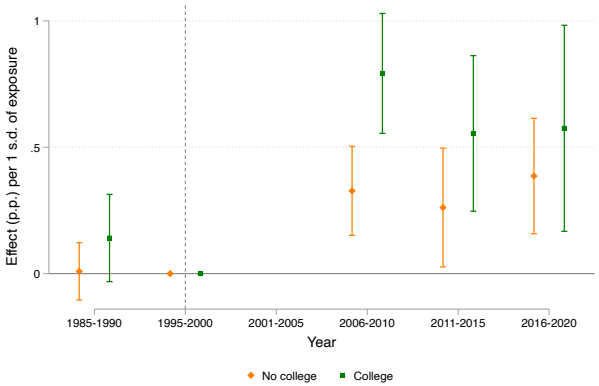
Notes: This figure presents binned scatter plots of percentage point changes in origin-by-destination migration rates, relative to 1996, along the distribution of 1996 cancer mortality rates in origin counties (panel a) and destination counties (panel b). The x-axis corresponds to the average 1996 cancer mortality in the origin (destination) counties among county pairs within a given decile of the exposure distribution. We follow the method of Cattaneo et al. (2024) to absorb origin and destination state fixed effects and control for destination (panel a) and origin (panel b) 1996 cancer mortality. We focus on changes in migration rates across deciles (i.e., slopes). The change in proportional migration rates across bins can be interpreted as semi-parametric estimates of $\phi_{o,t}$ and $\phi_{l,t}$ from Equation 4, multiplied by the average inter-county migration rate in 1996 (6.2%). This figure uses IRS migration data which covers inter-county internal migration for the overall population and provides year-to-year moves. This figure is referenced in Section VII.a.

Figure 4: Effects of Exposure to the Opioid Epidemic on Out-Migration

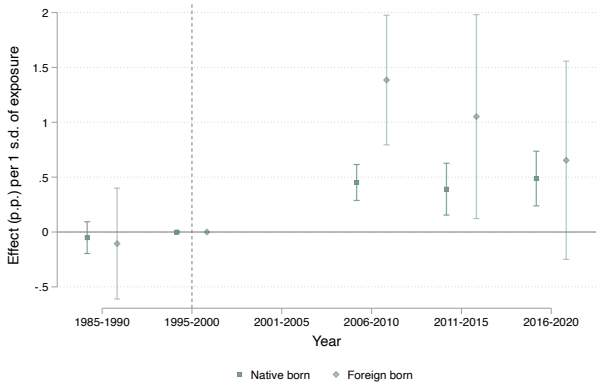
(a) Overall (IRS)



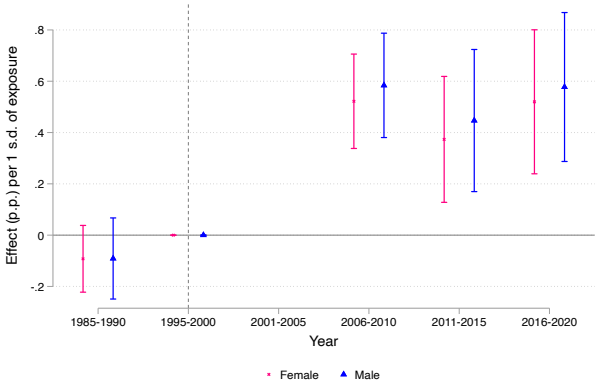
(b) By education (Census and ACS)



(c) By nativity (Census and ACS)

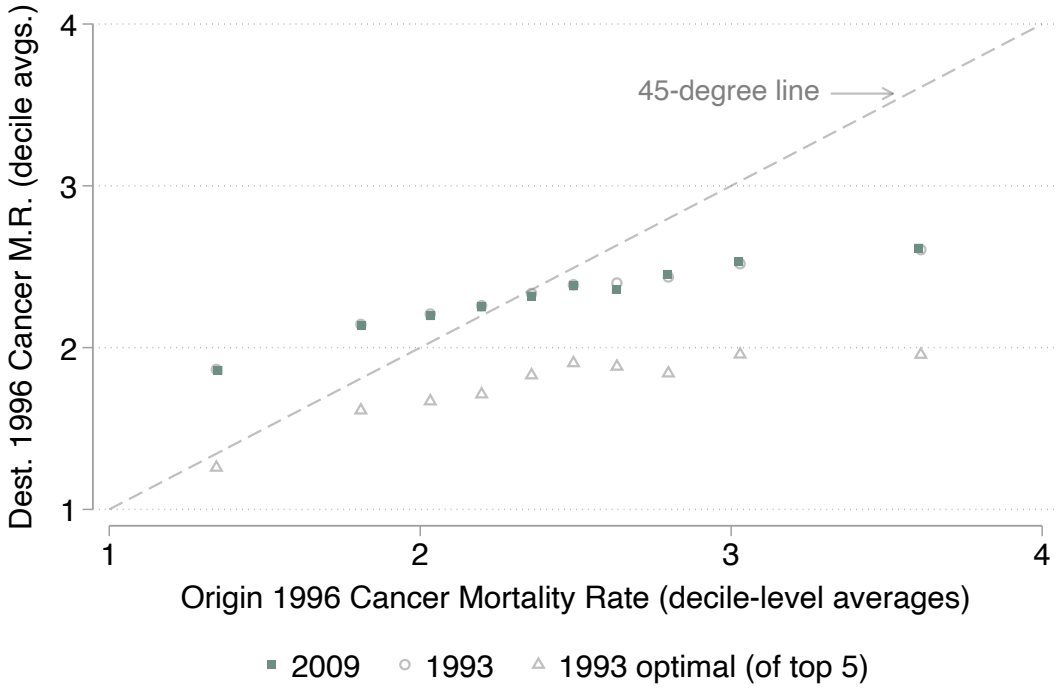


(d) By sex (Census and ACS)



Notes: This figure shows the effects of exposure to the opioid epidemic on out-migration rates. Panel (a) uses IRS annual inter-county flows for the full population. Panels (b)–(d) use Census/ACS data to construct inter-CZ migration by education, nativity and sex. The 1990/2000 Censuses report five-year moves, while the ACS (2006+) reports one-year moves; we pool ACS data into five-year windows for comparability. For panel (b), we restrict to individuals aged 19+ based on our definition of college-educated, as those with any education beyond high school. The plotted coefficients are $\phi_{o,t}$ from Equation 4, scaled by baseline migration probabilities and by the standard deviation of 1996 cancer mortality, so effects are interpretable as percentage-point changes in migration per one-standard-deviation increase in exposure. Standard errors are two-way clustered by origin and destination. This figure is referenced in Section VII.a.

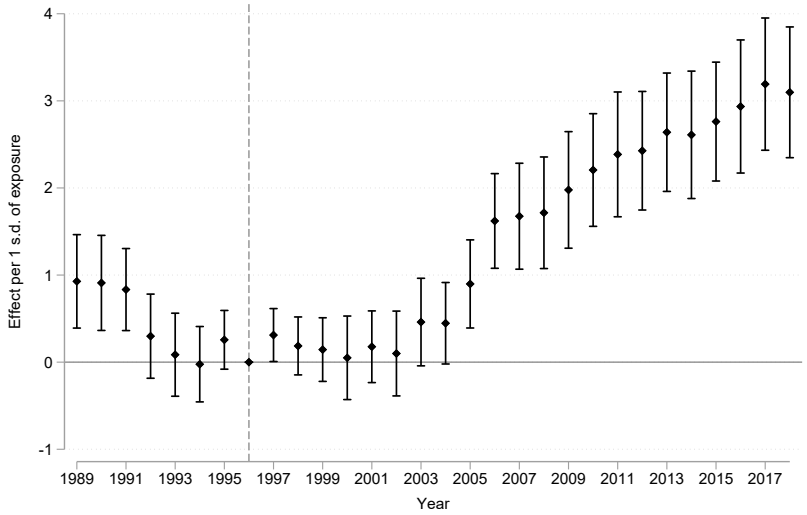
Figure 5: Where do People Move? (IRS data)



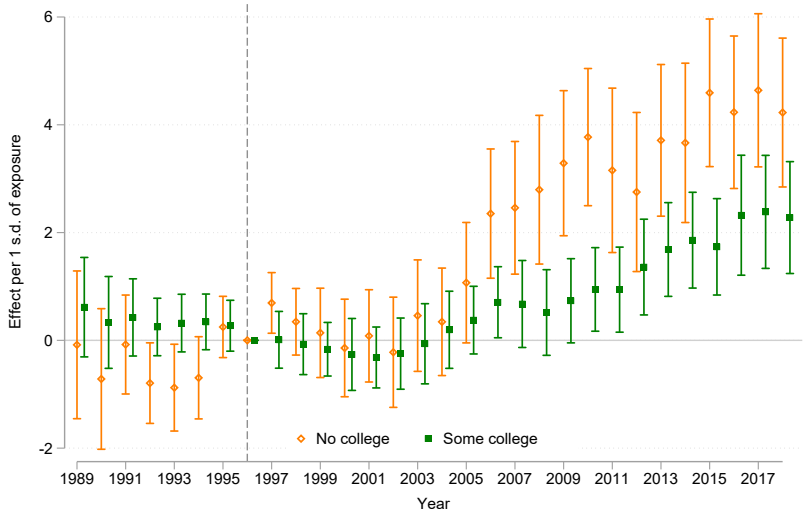
Notes: This figure plots, by decile of origin exposure (x-axis), the average migration-weighted destination exposure (y-axis). For 2009 (solid, teal squares) and 1993 (hollow, grey circles) we construct weights based on migration patterns in those years. 1993 optimal (hollow, grey triangles) shows a counterfactual in which each origin's movers choose the lowest-exposure county among its five most common 1993 destinations. A slope of negative one corresponds to migrants in the most exposed areas relocating to the least exposed areas, on average. We find a slope of 0.26 (s.e. 0.01). Destination exposure falls below origin exposure only above the 50th percentile, and declines by one standard deviation only above the 90th percentile. Data are IRS county-to-county flows. This figure is referenced in Section VII.a.

Figure 6: Effects of Exposure to the Opioid Epidemic on Fertility

(a) Total Fertility



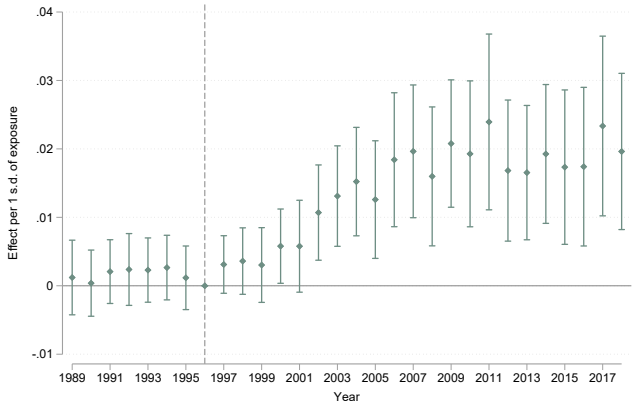
(b) By Education



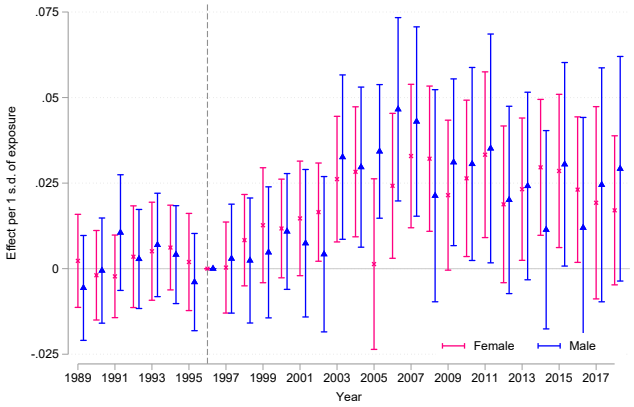
Notes: Total fertility is defined as the ratio of births to women aged 15 to 44 to the female population in this age group, per 1,000 women. Panel (a) presents estimates of the effects of opioid epidemic exposure on total fertility rates. Panel (b) presents these estimates by education. These are estimates of the ϕ_τ coefficients in Equation (3) multiplied by the standard deviation of the 1996 cancer mortality rate. These estimates exploit continuous variation in cancer mortality in 1996 and control for baseline characteristics and state-by-year fixed effects. Standard errors are clustered at the commuting zone-level. This figure is referenced in Section VII.b.

Figure 7: Exposure to the Opioid Epidemic and Drug Induced Mortality

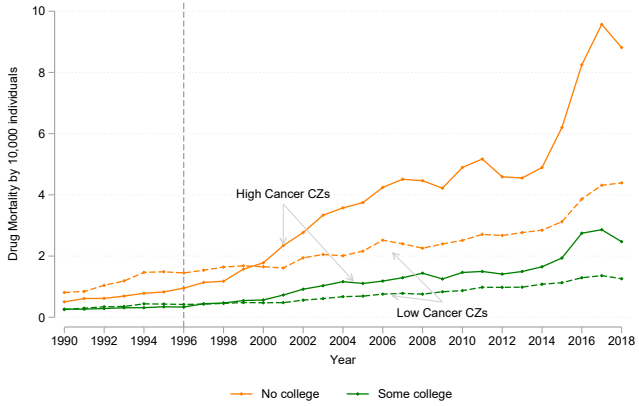
(a) Full population



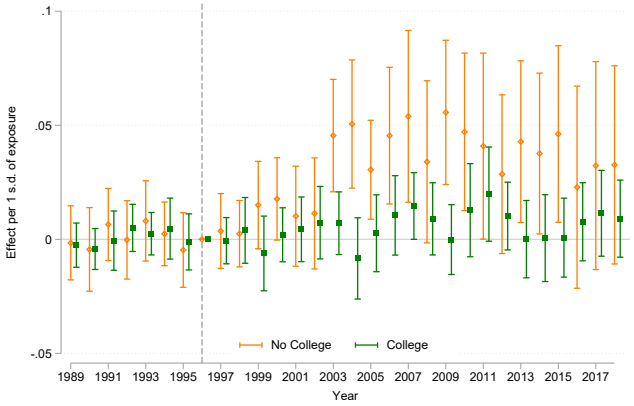
(b) Event-study by Sex



(c) Trends in Drug Induced Mortality by Education

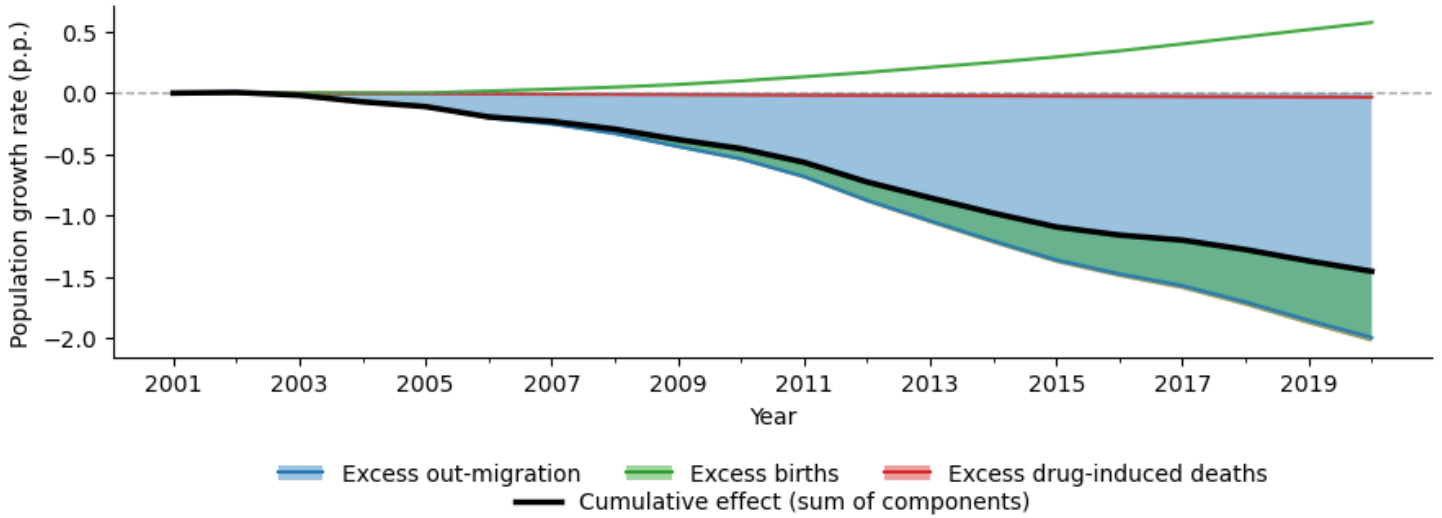


(d) Event-study by Education



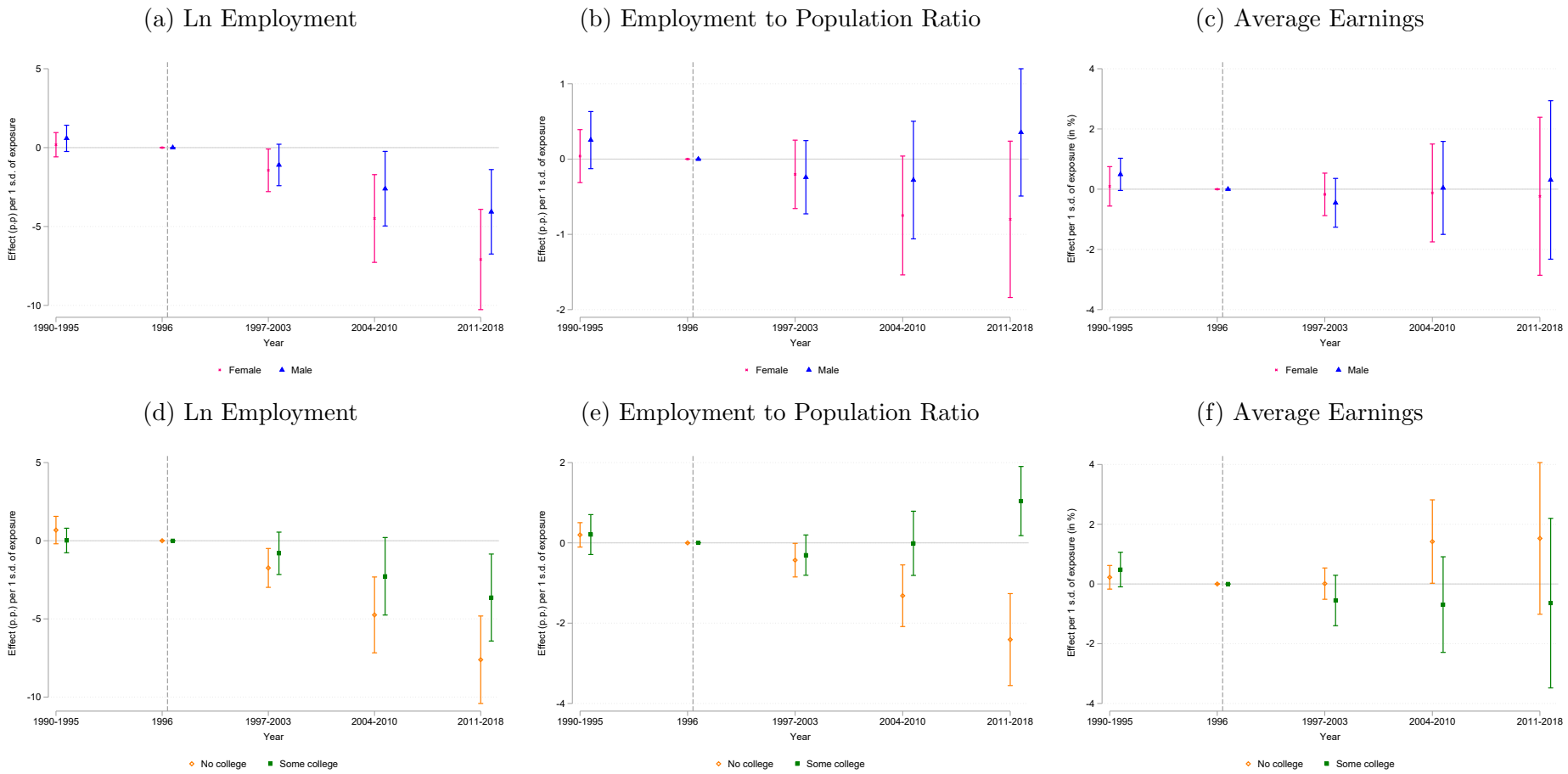
Notes: This figure shows trends in drug induced mortality and the effects of the opioid epidemic on drug induced mortality. Panels (a), (b) and (d) present estimates of the effects of epidemic exposure on drug-induced mortality (per 1,000 people) for the overall population, by sex, and by education. These are estimates of ϕ_τ from Equation (3) multiplied by the standard deviation of the 1996 cancer mortality rate. These estimates exploit continuous variation in cancer mortality in 1996 and control for baseline characteristics and state-by-year fixed effects. Standard errors are clustered at the CZ level. Panel (c) presents the evolution of drug induced mortality by education in CZs in the bottom (dashed lines) and top (solid lines) quartiles of cancer mortality before the launch of OxyContin. This comparison is based on dichotomous high-versus-low categorization of CZs, and the outcome is weighted by population. This figure is referenced in Section VII.c.

Figure 8: Decomposition Exercise: Contribution of Each Margin of Adjustment to Population Growth Rate



Notes: This figure presents our decomposition of the change in population growth attributable to the opioid epidemic into the three channels of demographic adjustment: excess net migration (out-migration), excess births, and excess mortality. For each year, the solid lines show the implied change in population growth when allowing only one margin to operate while holding the others fixed. Shaded areas represent the absolute contribution of each channel to cumulative population growth. The decomposition is constructed using Equation (5), combining demographic rates with the estimated exposure effects on migration, crude birth rates, and drug-induced mortality. The in-migration channel and non-drug-induced mortality are zero, as their estimated effects are statistically indistinguishable from zero. Growth rates are expressed in percentage points relative to the 2000 baseline. This figure is referenced in Section VII.d.

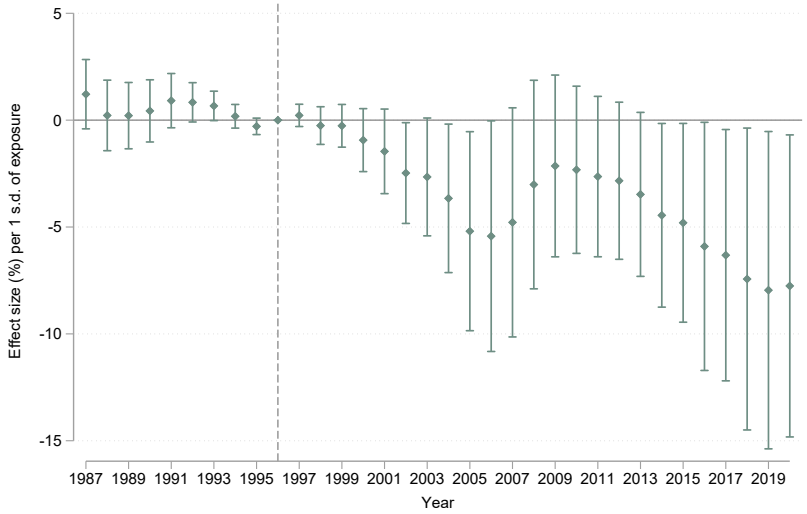
Figure 9: Effects of Exposure to the Opioid Epidemic on Labor Market Outcomes: By Sex and Education



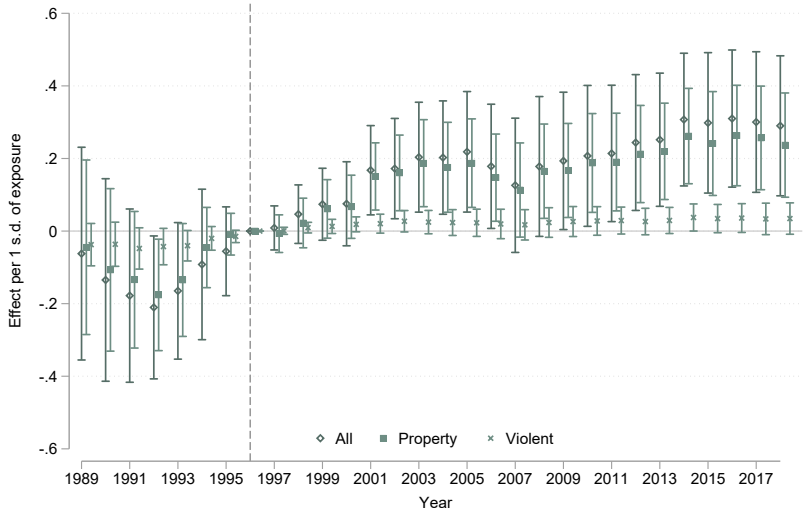
Notes: This figure presents the effects of exposure to the opioid epidemic on labor market outcomes by sex (top panel) and education (bottom panel). Panels (a) and (d) present results on log employment. Panels (b) and (e) present results on the employment to population ratio. These estimates are expressed as percentage point changes in the outcome of interest, scaled by one standard deviation of 1996 cancer mortality. Panels (c) and (f) present results on average earnings, constructed as the ratio of total payroll to employment. These results are reported in percentage terms, per one standard deviation of exposure, i.e., we multiply the estimated coefficients by the standard deviation of 1996 cancer mortality rates and divide by the mean of the outcome variable in 1996. For each panel, we estimate Equation (6), these estimates exploit continuous variation in cancer mortality in 1996 and control for baseline characteristics and state-by-year fixed effects. Standard errors are clustered at the CZ level. This figure is referenced in Section VIII.a

Figure 10: Effects of Exposure to the Opioid Epidemic on House Prices and Crime Rates

(a) House Prices



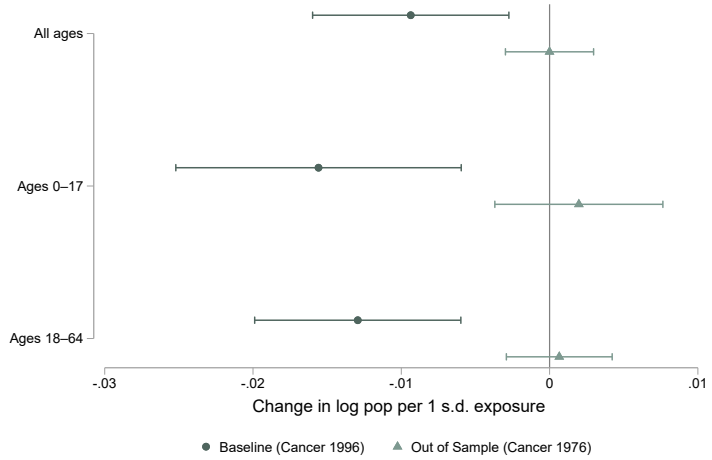
(b) Crime Rate



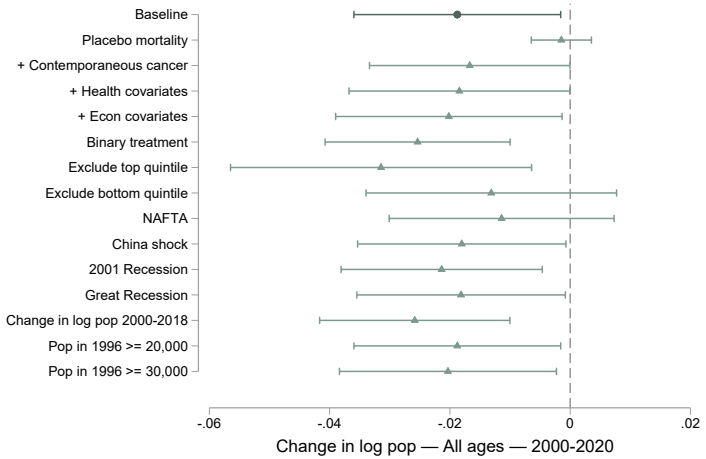
Notes: This figure presents estimates of the effect of exposure to the opioid epidemic on the house price index (left panel) and on crime rates (right panel). The left-hand-side panel presents scaled coefficients from Equation (3). Specifically, we multiply the estimated coefficient by the standard deviation of 1996 cancer mortality rates and divide by the mean of the outcome variable in 1996. The right-hand-side panel shows effects per one standard deviation of 1996 cancer mortality. These estimates exploit continuous variation in cancer mortality in 1996 and control for baseline characteristics and state-by-year fixed effects. Standard errors are clustered at the CZ level. This figure is referenced in Section VIII.b.

Figure 11: Robustness Checks: Population

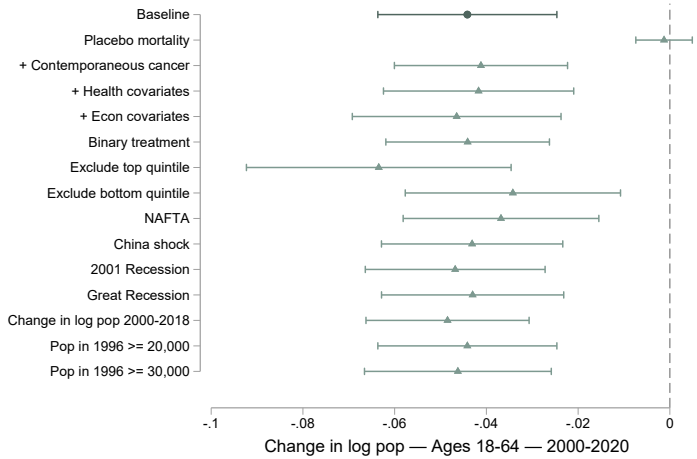
(a) Out-of-sample: 1976 cancer mortality



(b) Total population (2000-2020)

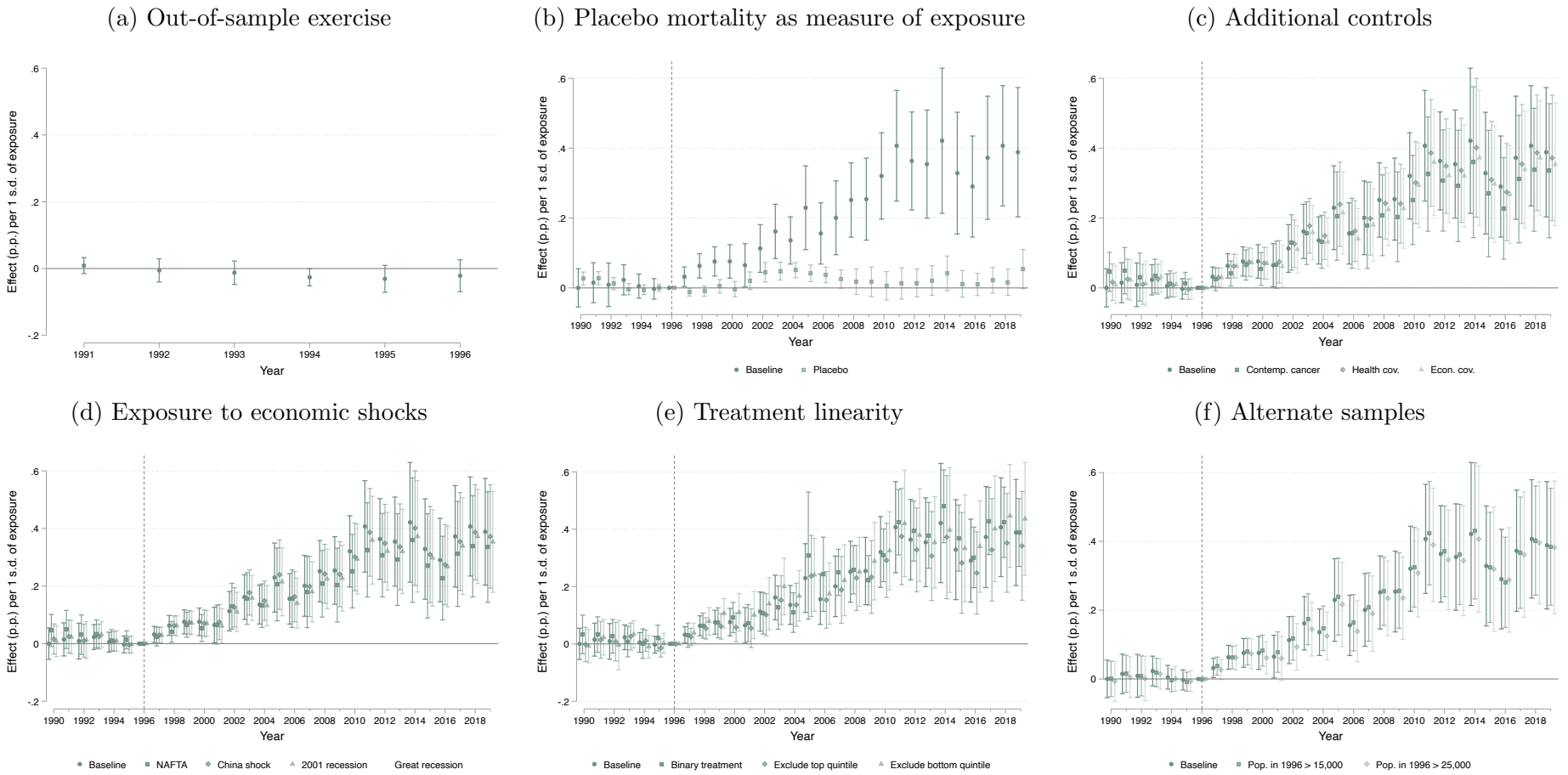


(c) 18-64 year old population (2000-2020)



Notes: Panel (a) presents estimates of the effects of 1976 cancer mortality rates on log population change between 1990 and 2000 (i.e., a 10-year population change). We include the baseline estimates for the 10-year log population change between 2000 and 2010 using 1996 cancer mortality rates for comparison. The effects shown correspond to coefficient ϕ from Equation (3), scaled by the standard deviation of the corresponding cancer mortality. Panels (b) and (c) present additional robustness checks that probe the validity of our empirical strategy. Each estimate corresponds to a separate robustness exercise, as indicated on the horizontal axis (e.g., placebo tests, alternative controls, exposure to economic shocks, and alternative treatment and sample definitions). Each estimate reports the coefficient ϕ from Equation (3) and corresponds to the 20-year log population change for the population of interest. This figure is referenced in Section IX.

Figure 12: Robustness Checks: Out-Migration (IRS)



Notes: This figure presents robustness checks that probe the validity of our empirical strategy. The outcome of interest in each regression is percentage point changes in out-migration rates. Panel (a) shows an out-of-sample exercise where we use 1976 cancer mortality rates as our measure of exposure to the epidemic and estimate effects on migration rates relative to 1993. Panel (b) presents a placebo exercise where we use 1996 mortality from hypertension as the measure of exposure. Panel (c) expands the set of controls to include: contemporaneous cancer mortality; and broad sets of health covariates and economic covariates. Panel (d) adds measures of exposure to various economic shocks. For the regressions in panels (c) and (d), we allow covariates to vary flexibly over time. Panel (e) examines treatment linearity. Panel (f) alters our baseline population restriction of counties, which includes all counties that contribute to our CZ analysis sample and have 1996 populations over 20,000 (93% of our analysis sample population in 1996). All plotted coefficients are $\phi_{o,t}$ from Equation 4, scaled by baseline migration probabilities and by the standard deviation of 1996 cancer mortality, so effects are interpretable as percentage-point changes in migration per one-standard-deviation increase in exposure. Standard errors are two-way clustered by origin and destination. This figure uses IRS migration data which covers inter-county internal migration and provides year-to-year moves. This figure is referenced in Section IX..

XII. Tables

Table 1: Summary Statistics

	Before 1996			After 2010		
	Mean	Median	SD	Mean	Median	SD
	(1)	(2)	(3)	(4)	(5)	(6)
Cancer mortality rate per 1,000	2.5237	2.5246	0.5463	2.5029	2.5155	0.5547
Local population growth rates	*1990 - 2000*			*2000-2020*		
All population	0.0977	0.0917	0.0942	0.0813	0.0618	0.1473
Ages 18-64	0.1206	0.1131	0.0969	0.0601	0.0381	0.1492
Female	0.1071	0.0988	0.0982	0.0420	0.0165	0.1531
Male	0.1338	0.1252	0.1008	0.0774	0.0555	0.1482
Migration						
	1 year rate (1996)			*1 year rate (2010)*		
Out-migration probability (IRS)	0.0470	0.0452	0.0181	0.0422	0.0397	0.0141
	5 year rate (1995)			*1 year rate (2010)*		
Out-migration probability (Census, ACS)	0.1005	0.0936	0.0626	0.0336	0.0304	0.0166
Non-college	0.0739	0.0654	0.0497	0.0288	0.0250	0.0164
College	0.1294	0.1282	0.0764	0.0372	0.0339	0.0191
Fertility Rate (per 1,000)						
Total fertility rate	63.5313	62.2889	9.9684	63.3842	62.5272	9.3884
Non-college	86.7174	84.0333	18.6400	82.8956	83.8296	22.0442
College	51.5383	51.3855	10.7547	58.3841	59.3738	15.8327
Drug-induced mortality (per 1,000)						
All population	0.0332	0.0295	0.0249	0.1780	0.1538	0.1143
Non-college	0.0588	0.0405	0.0739	0.4620	0.3629	0.3840
College	0.0237	0.0000	0.0408	0.1367	0.1181	0.1154

Notes: This table presents summary statistics for the main dependent variables and our measure of exposure to the opioid epidemic for the periods before and after the launch of OxyContin. Data availability varies by outcome, unless otherwise specified, the first three columns compute statistics using yearly data from 1989 to 1996 and the last three columns use yearly data from 2010 to 2018. All statistics are computed at the commuting zone level. This table is referenced in Section III.

Table 2: Effects of Exposure to the Opioid Epidemic on Population Growth Rates

	Change in log population per 1 s.d. exposure			
	All ages	Ages 18-64		
		All	Female	Male
1996 cancer mortality ×	(1)	(2)	(3)	(4)
1990 – 2000	0.0023	0.0042	0.0082	0.0009
	(0.0048)	(0.0055)	(0.0052)	(0.0066)
2000 – 2010	-0.0094***	-0.0129***	-0.0145***	-0.0124***
	(0.0034)	(0.0035)	(0.0034)	(0.0039)
2000 – 2020	-0.0103**	-0.0242***	-0.0226***	-0.0267***
	(0.0048)	(0.0055)	(0.0053)	(0.0078)

Notes: This table presents estimates of the effects of exposure to the opioid epidemic on the change in log population. We consider changes in the total population by sex and age groups. Each cell reports estimates of the coefficient ϕ from Equation (3). All specifications include a set of demographic controls measured in 1990, controls for exposure on connected CZs, and state-level fixed effects. Standard errors are clustered at the CZ level. *p<0.10, **p<0.05, *** p<0.01. This table is referenced in Section VI.

Table 3: Effects of Exposure to the Opioid Epidemic on Population Growth Rates by Education

	Change in log population per 1 s.d. exposure					
			Female		Male	
	No college	College	No college	College	No college	College
1996 cancer mortality ×	(1)	(2)	(3)	(4)	(5)	(6)
1990 – 2000	0.0044	0.0091	0.0096*	0.0141	-0.0003	0.005
	(0.0056)	(0.0097)	(0.0052)	(0.011)	(0.007)	(0.01)
2000 – 2010	-0.0109***	-0.0201***	-0.0141***	-0.0173**	-0.0093**	-0.0228***
	(0.0038)	(0.007)	(0.004)	(0.0072)	(0.0041)	(0.0085)
2000 – 2020	-0.02001***	-0.0378***	-0.0202***	-0.0325***	-0.0209***	-0.0451***
	(0.0053)	(0.0097)	(0.0056)	(0.0096)	(0.0057)	(0.0116)

Notes: This table reports estimates of the effect of exposure to the opioid epidemic on changes in log population. We examine changes in total population by education, sex, and age group for adults aged 18 to 64 years old. College-educated is defined as bachelor's degree or higher; non-college as less than a bachelor's degree. See Appendix Section B.4 for details on construction of the population counts used in this table. Each cell reports the estimate of ϕ from Equation (3). All specifications include demographic controls measured in 1990, controls for exposure on connected CZs, and state fixed effects. The p-value for the test of equality of effects between the no-college and college populations ($H_0 = \phi_{\text{college}} - \phi_{\text{nocollege}}$) is 0.1970 for the 10-year effect and 0.0575 for the 20-year effect. The p-value for these tests for the male population are 0.0961 and 0.0245 for the 10-year and 20-year effects, respectively. Standard errors are clustered at the CZ level. *p<0.10, **p<0.05, *** p<0.01. This table is referenced in Section VI. and Table A3 complements this analysis with alternative educational attainment cuts.

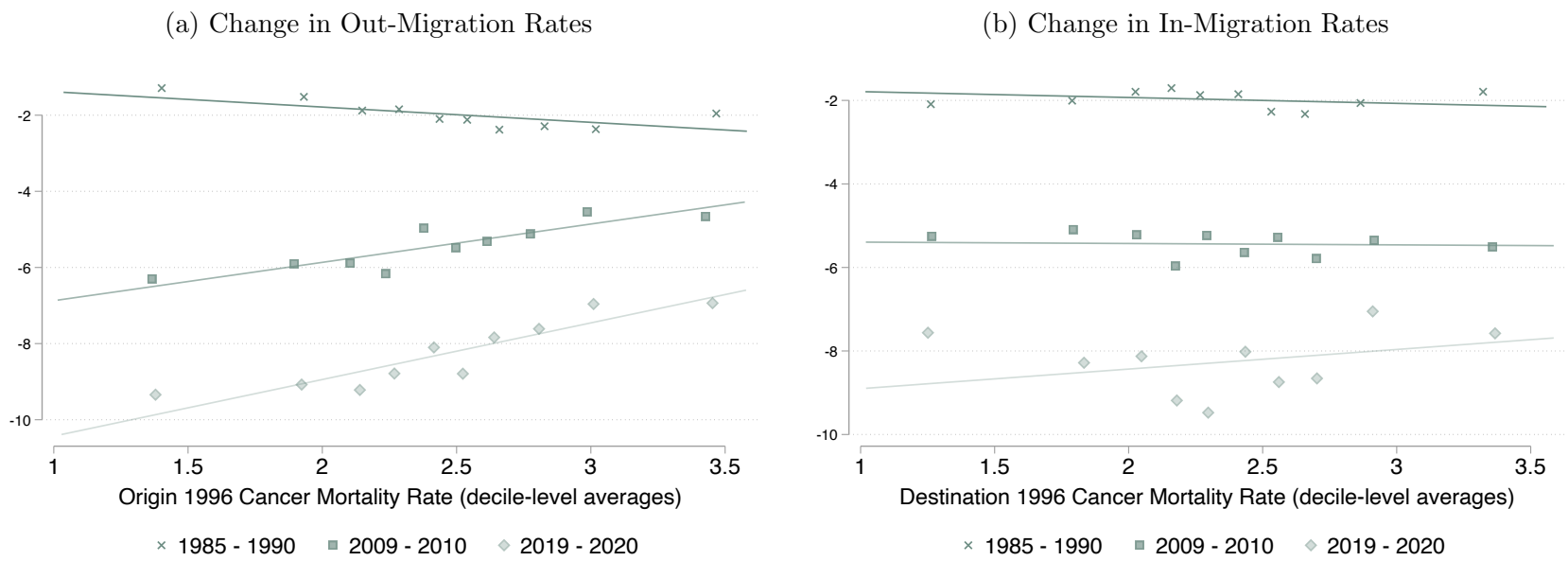
Table 4: Effects of Exposure to the Opioid Epidemic on Rents

Change per 1 unit of exposure	
	Median rent
1996 cancer mortality ×	(1)
1990 – 2000	6.729*
	(3.514)
2000 – 2010	-12.55**
	(5.129)
2000 – 2020	-15.45**
	(6.802)
Observations	8,190
Czones	585

Notes: This table presents estimates of the effects of exposure to the opioid epidemic on median contracted rents computed from the ACS. Standard errors are clustered at the CZ level. *p<0.10, **p<0.05, *** p<0.01. This table is referenced in Section VIII.b.

A. Additional Figures and Tables

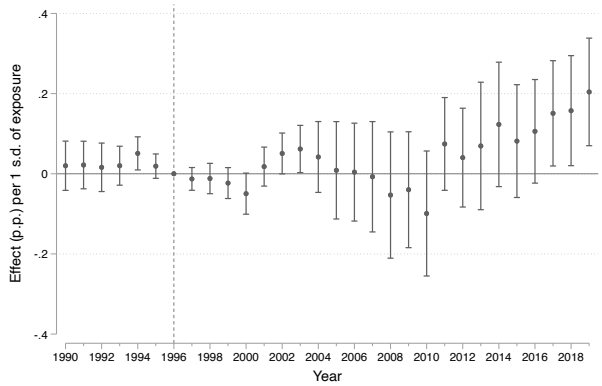
Figure A1: Full Population Effects of the Opioid Epidemic on Out- and In-Migration (Census and ACS)



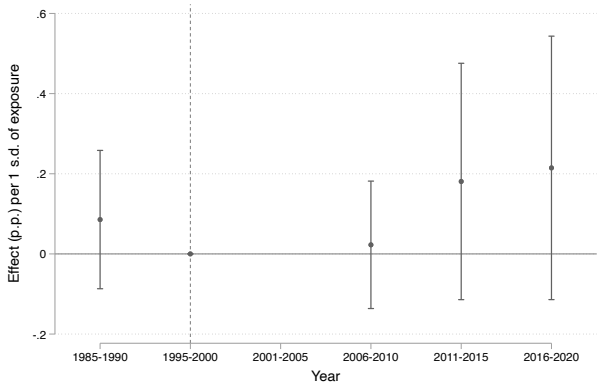
Notes: This figure presents binned scatter plots of percentage point changes in origin-by-destination migration rates, relative to 1996, along the distribution of 1996 cancer mortality rates in origin CZs (panel a) and destination CZs (panel b). The x-axis corresponds to the average 1996 cancer mortality in the origin (destination) CZ among CZ pairs within a given decile of the exposure distribution. We follow the method of Cattaneo et al. (2024) to absorb origin and destination state fixed effects and focus on changes in migration rates across deciles (i.e., slopes). The change in proportional migration rates across bins can be interpreted as semi-parametric estimates of $\phi_{o,t}$ and $\phi_{l,t}$ from Equation 4, multiplied by the average inter-CZ migration rate in 1996 (4.7%). This figure uses Census and ACS data to measure inter-CZ migration. The 1990 and 2000 Censuses report five-year migration, whereas the ACS (2006+) reports one-year migration; this difference contributes to the level shift over time, alongside the secular decline in internal migration. This figure is referenced in Section VII.a and is the CZ-level analogue of Figure 3.

Figure A2: Effects of Exposure to the Opioid Epidemic on Migration

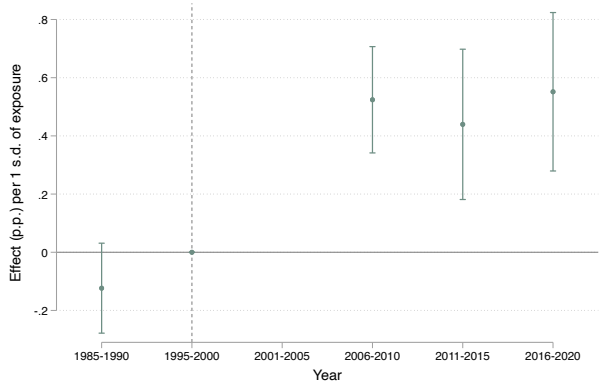
(a) In-migration, overall (IRS)



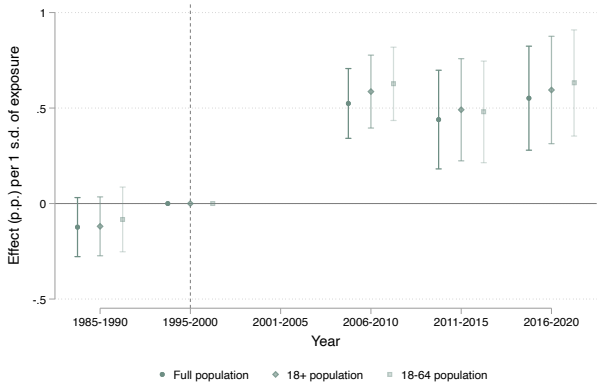
(b) In-migration, overall (Census and ACS)



(c) Out-migration, overall (Census and ACS)



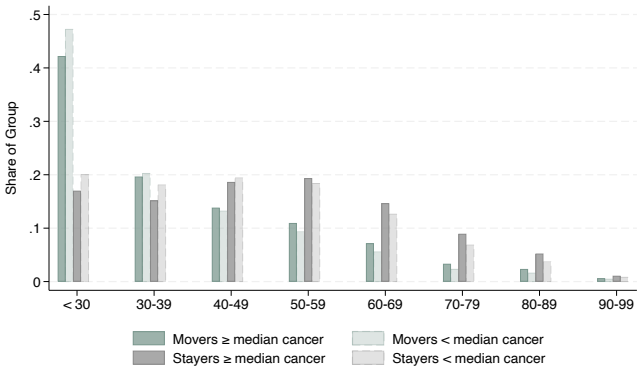
(d) Out-migration, by age (Census and ACS)



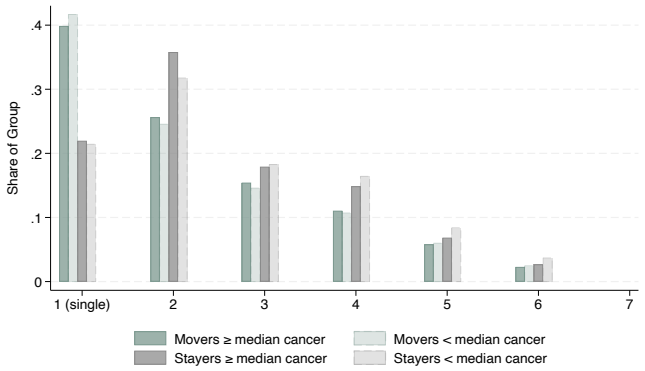
Notes: This figure shows the effects of exposure to the opioid epidemic on migration rates. Panel (a) presents in-migration effects using IRS annual inter-county flows for the full population. Panels (c)–(d) present migration effects using Census/ACS data to construct inter-CZ migration. Panel (c) presents in-migration effects while panels (b) and (d) present out-migration effects. The 1990/2000 Censuses report five-year moves, while the ACS (2006+) reports one-year moves; we pool ACS data into five-year windows for comparability. The plotted coefficients are $\phi_{l,t}$ (panels a and b) and $\phi_{o,t}$ (panels c and d) from Equation 4, scaled by baseline migration probabilities and by the standard deviation of 1996 cancer mortality, so effects are interpretable as percentage-point changes in migration per one-standard-deviation increase in exposure. Standard errors are two-way clustered by origin and destination. This figure is referenced in Section VII.a.

Figure A3: Socioeconomic and Demographic Compositions of Movers and Stayers by Exposure to the Opioid Epidemic

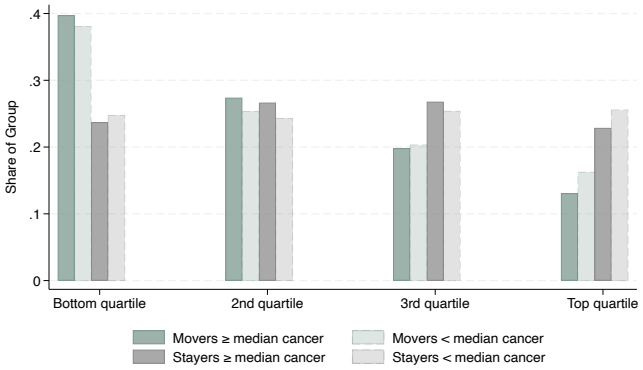
(a) Age (10-year bins)



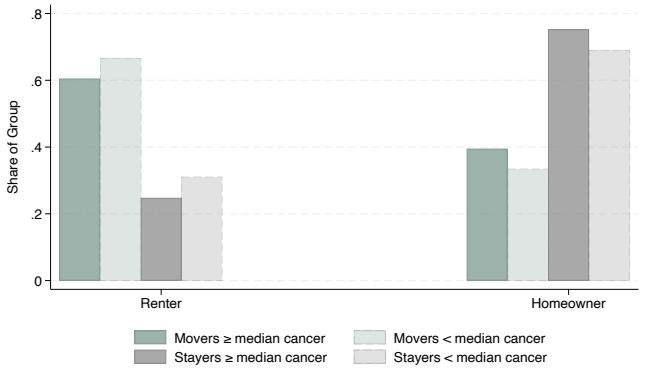
(b) Household size



(c) Income (Quartiles of Population Distribution)



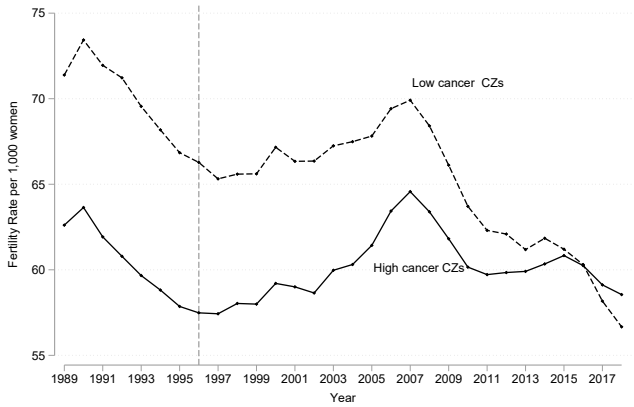
(d) Homeownership



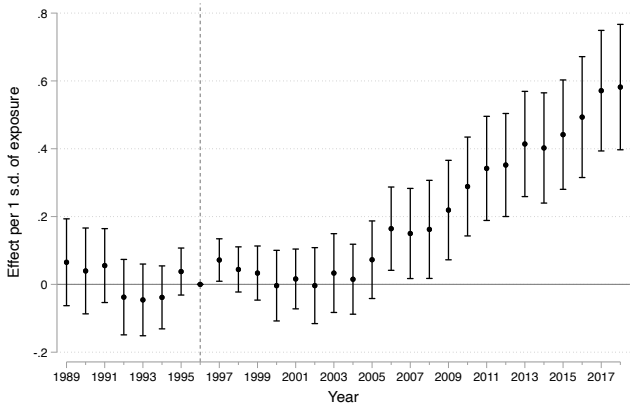
Notes: This figure presents distributions of age (panel a), household size (panel b), income (panel c), and homeownership (panel d) for movers and stayers in 2010, by exposure to the opioid epidemic. The data are from the 2010 ACS, and the sample includes all individuals aged 18+. This figure is referenced in Section VII.a

Figure A4: Exposure to the Opioid Epidemic and Fertility

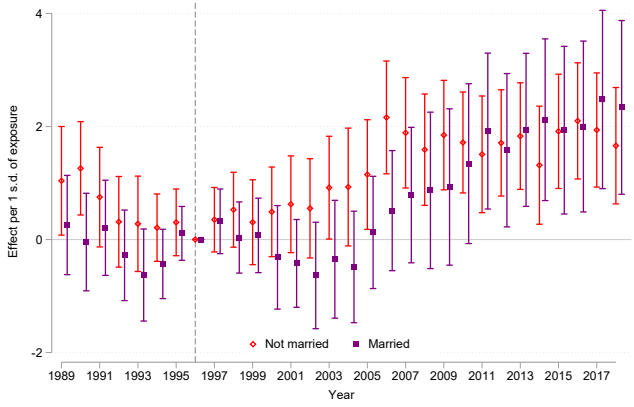
(a) Trends in High- vs. Low-Cancer Mortality CZs (Total Fertility Rate)



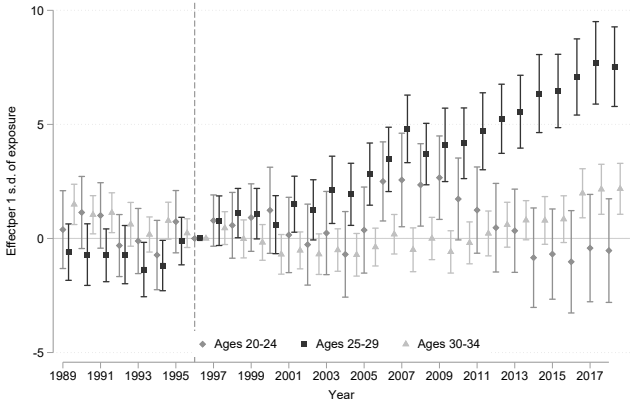
(b) Crude Birth Rate



(c) Marital Status

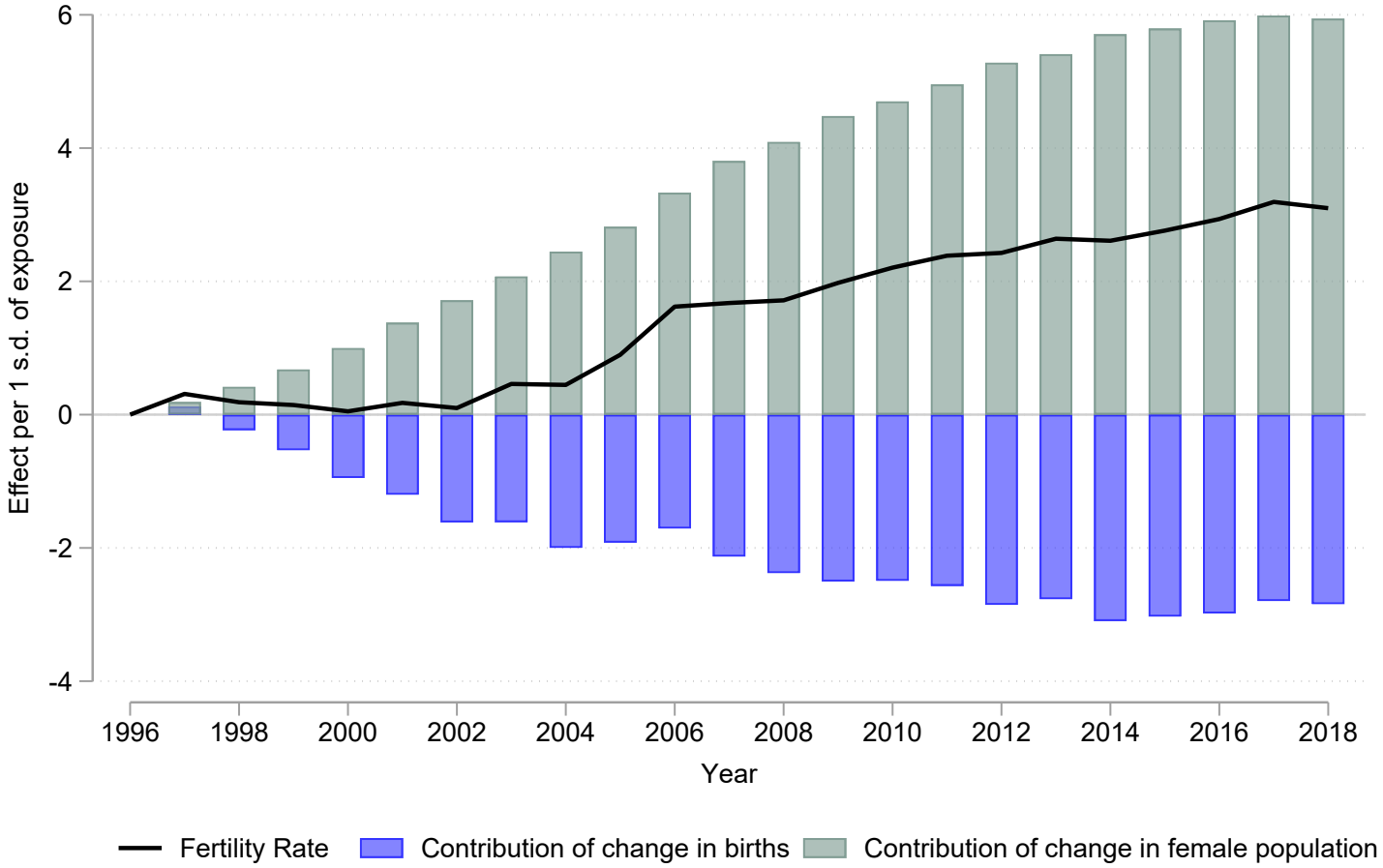


(d) Ages 25-29



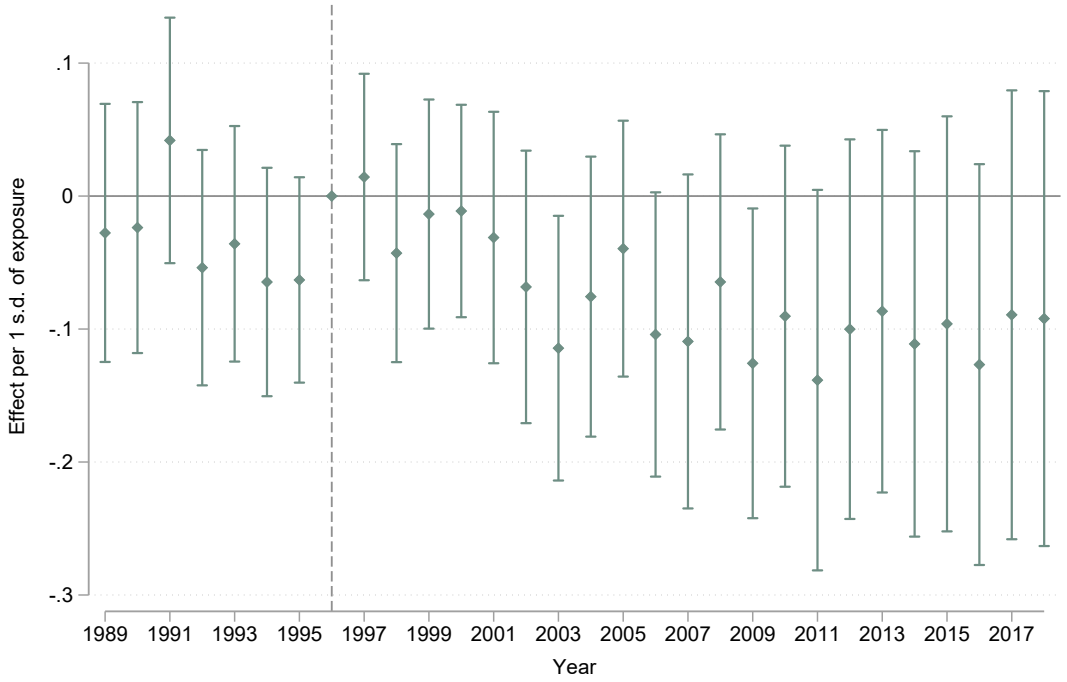
Notes: Panel (a) of this figure presents the evolution of the total fertility rate (per 1,000 women) in CZs in the bottom (dashed lines) and top (solid lines) quartiles of cancer mortality before the launch of OxyContin. This comparison is based on dichotomous high-versus-low categorization of CZs, and the outcome is weighted by population. Panel (b) presents effects on the crude birth rate, i.e., the ratio of births to women aged 15-44 to the total population times 1,000. Panels (c) and (d) show the effects of exposure to the opioid epidemic on fertility rates per 1,000 women by marital status and by age. These are estimates of the ϕ_τ coefficients in Equation (3) multiplied by the standard deviation of the 1996 cancer mortality rate. These estimates exploit continuous variation in cancer mortality in 1996 and control for baseline characteristics and state-by-year fixed effects. Standard errors are clustered at the CZ level. This figure is referenced in Section VII.b and Section VII.d.

Figure A5: Fertility Effect Decomposition



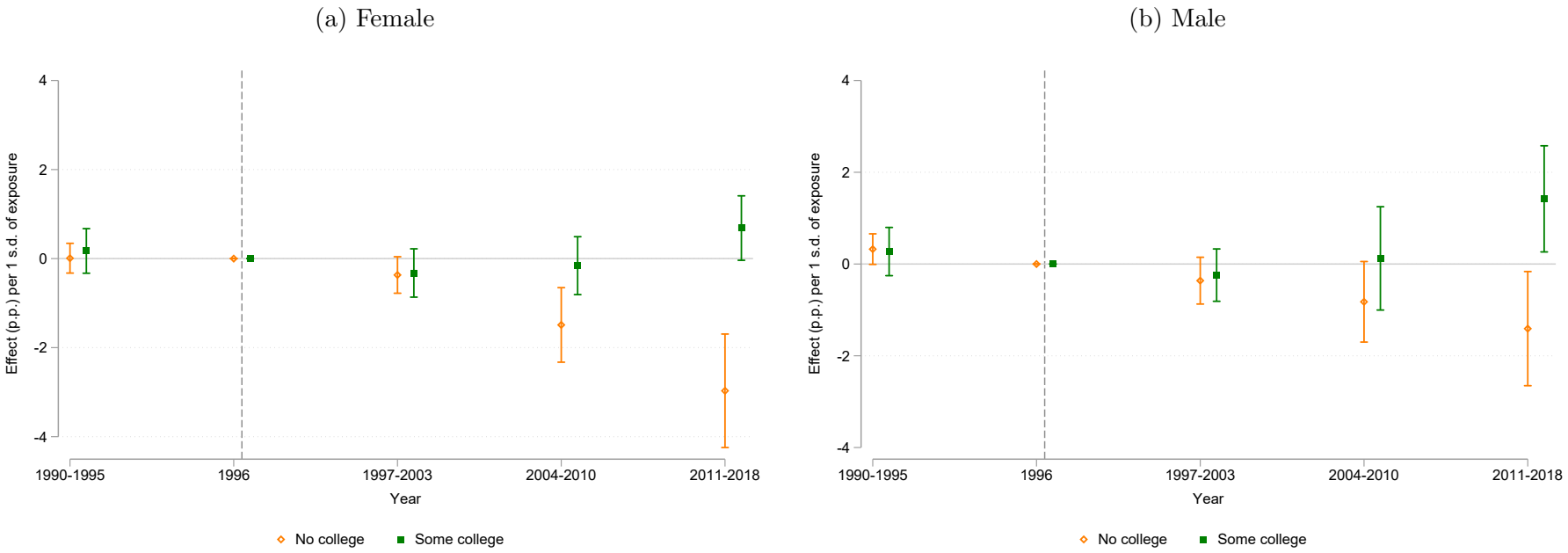
Notes: This figure decomposes the effect of the opioid epidemic on fertility rates (black line) into the changes in the numbers of births, normalized by the female population in 1996, and the difference of the fertility rate, fixing the number of births in t and the population in t and in 1996. This figure is referenced in Section VII.b.

Figure A6: Effect of the Opioid Epidemic on Non-Opioid Mortality



Notes: This figure shows the effects of exposure to the opioid epidemic on non-drug-induced mortality, per 1,000 people, for the overall population. These are estimates of the ϕ_τ coefficients in Equation (3) multiplied by the standard deviation of the 1996 cancer mortality rate. These estimates exploit continuous variation in cancer mortality in 1996 and control for baseline characteristics and state-by-year fixed effects. Standard errors are clustered at the CZ level. This figure is referenced in Appendix E..

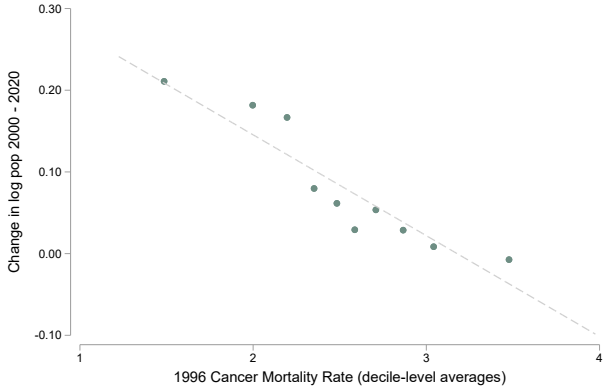
Figure A7: Effects of the Opioid Epidemic on Employment-to-population Ratio: By Sex and Education



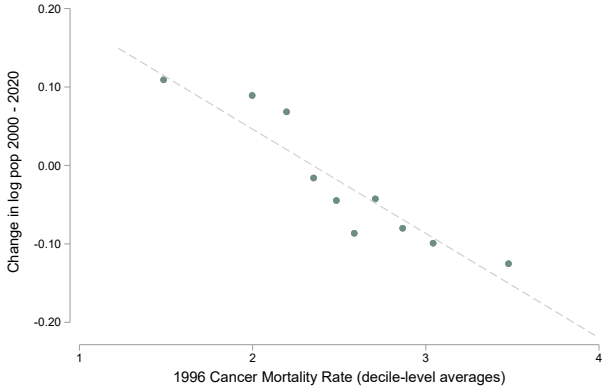
Notes: This figure presents the effects of exposure to the opioid epidemic on the employment to population ratio by sex and education. Panels (a) presents results for women and panel (b) for men. These estimates are expressed as percentage point changes in the outcome of interest, scaled by one standard deviation of 1996 cancer mortality. For each panel, we estimate Equation (6), these estimates exploit continuous variation in cancer mortality in 1996 and control for baseline characteristics and state-by-year fixed effects. Standard errors are clustered at the CZ level. This figure is referenced in Section VIII.a

Figure A8: Binned Scatter Plots: Change in Outcomes by 1996 Cancer Mortality

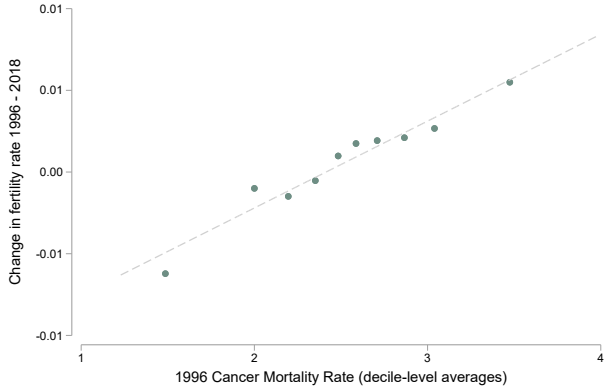
(a) Log Total population



(b) Log Population 18-64

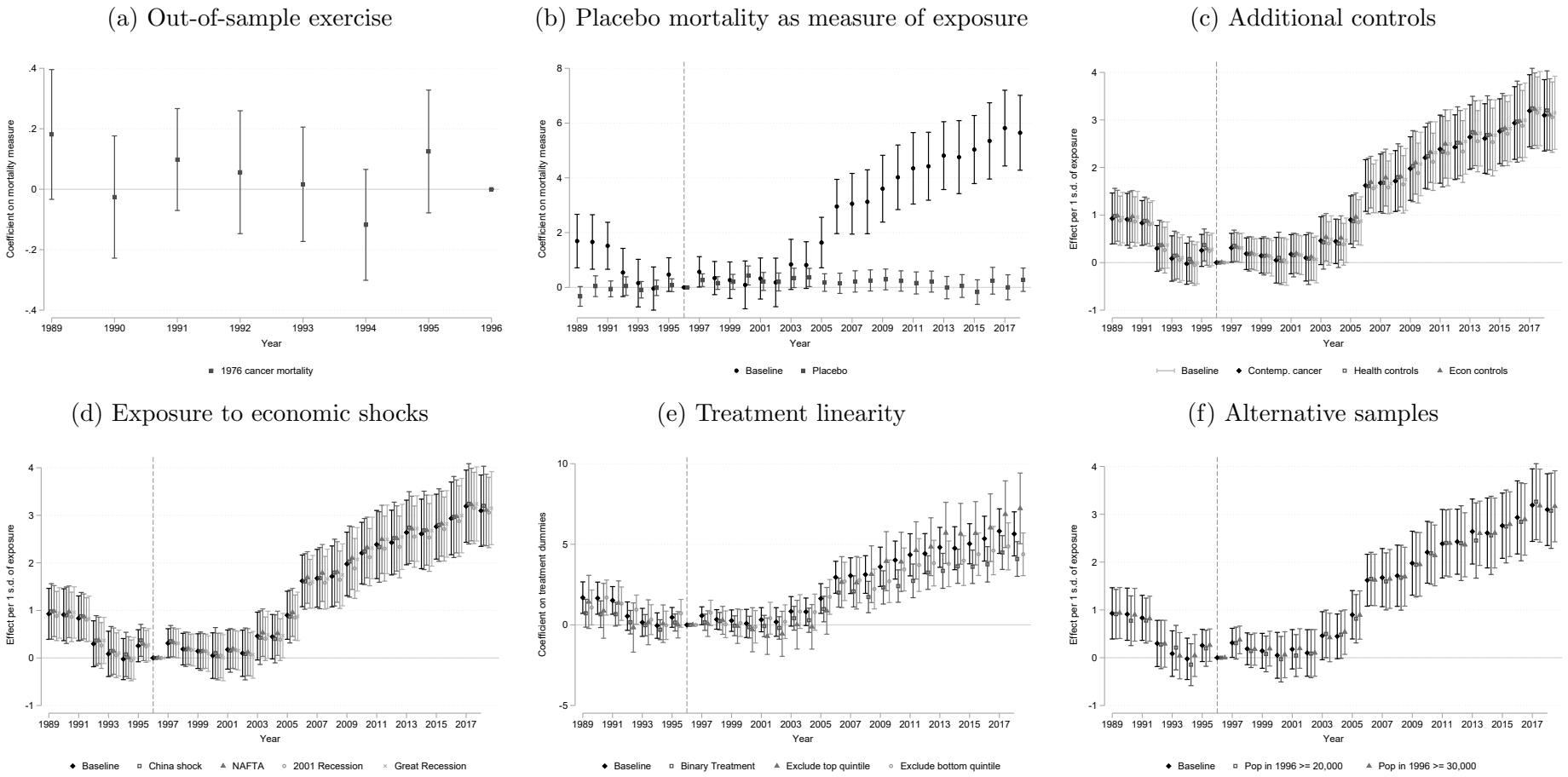


(c) Total Fertility Rate (15 - 44 years old)



Notes: This figure shows the average value of each outcome of interest (y-axis) across the distribution of 1996 cancer mortality (x-axis), our measure of exposure to the opioid epidemic. We split the data into 10 equally sized groups of CZs—either 58 or 59 CZs per group—based on their 1996 cancer mortality. For each group, we compute the average value of the outcome variable of interest. Outcomes on the y-axis are residualized with respect to state fixed effects prior to binning. For example, Panel (a) shows the average log population change between 2000 and 2020 across the support of 1996 cancer mortality. Each panel also includes the regression line corresponding to a linear prediction of the outcome variable on 1996 cancer mortality. This figure is referenced in Section IX.

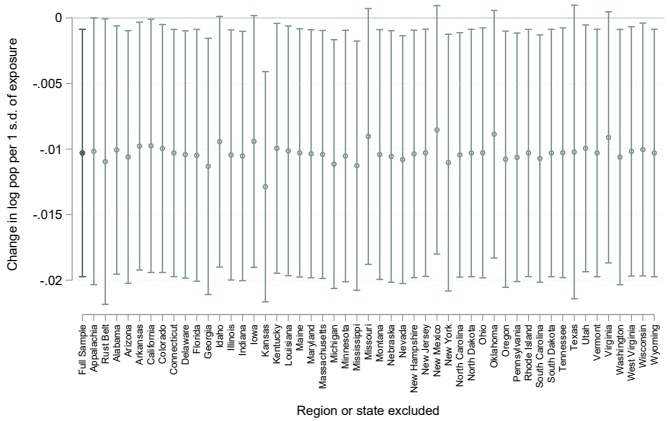
Figure A9: Robustness Checks: Total Fertility Rate (15 - 44 years old)



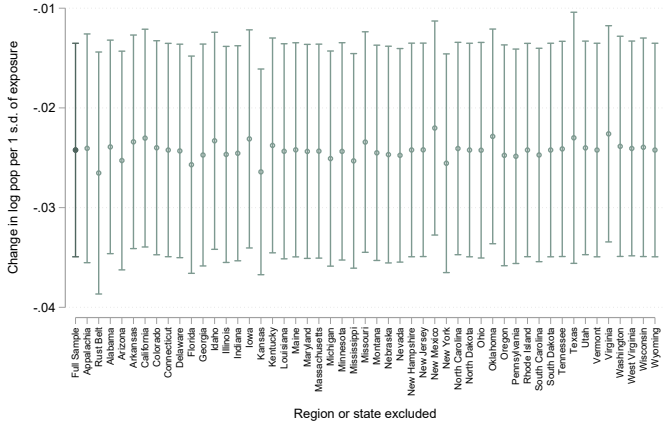
Notes: This figure presents robustness checks that probe the validity of our empirical strategy. The outcome of interest in each regression is the fertility rate per 1,000 women. Panel (a) shows an out-of-sample exercise where we use 1976 cancer mortality rates as our measure of exposure to the epidemic and estimate effects relative to 1989. Panel (b) presents a placebo exercise where we use 1996 mortality from hypertension as the measure of exposure. Panel (c) expands the set of controls to include: contemporaneous cancer mortality; and broad sets of health and economic covariates. Panel (d) adds measures of exposure to various economic shocks. For the regressions in panels (c) and (d), we allow covariates to vary flexibly over time. Panel (e) examines treatment linearity. Panel (f) alters our baseline population restriction. All plotted coefficients are ϕ_τ from Equation 3. In panels (c),(d), and (f) we scale the coefficient by the standard deviation of 1996 cancer mortality. Standard errors are clustered at the CZ level. All regressions include controls for baseline characteristics and state-by-year fixed effects. This figure is referenced in Section IX..

Figure A10: Estimation on Alternative Samples: Leaving out States

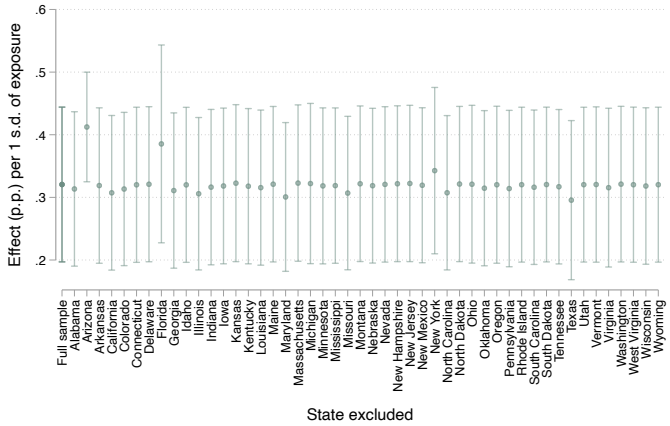
(a) Total Population (2000-2020)



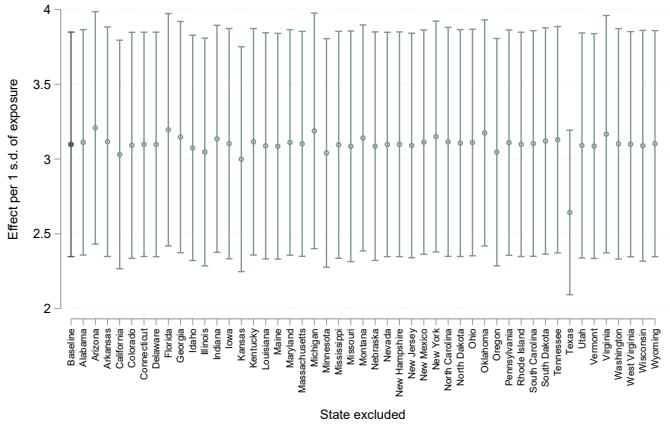
(b) Population 18-64 (2000-2020)



(c) 2010 Out-Migration (IRS)



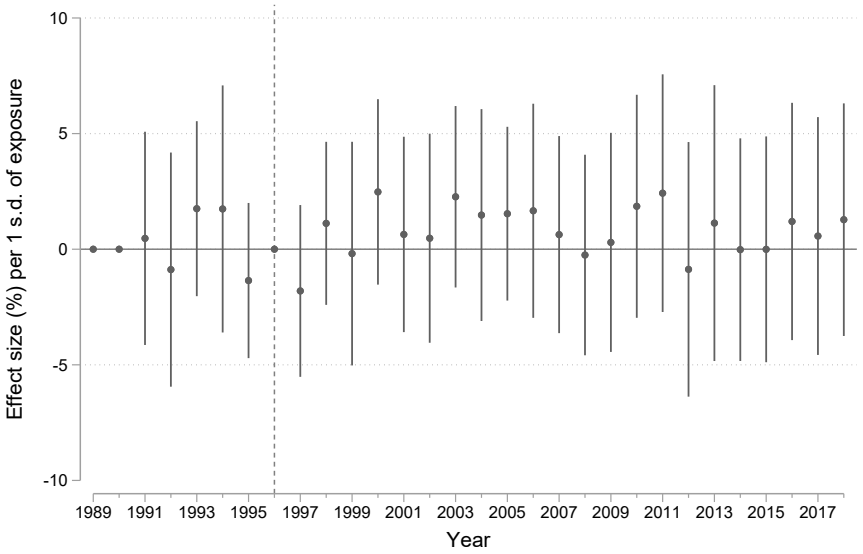
(d) 2018 Fertility Rate



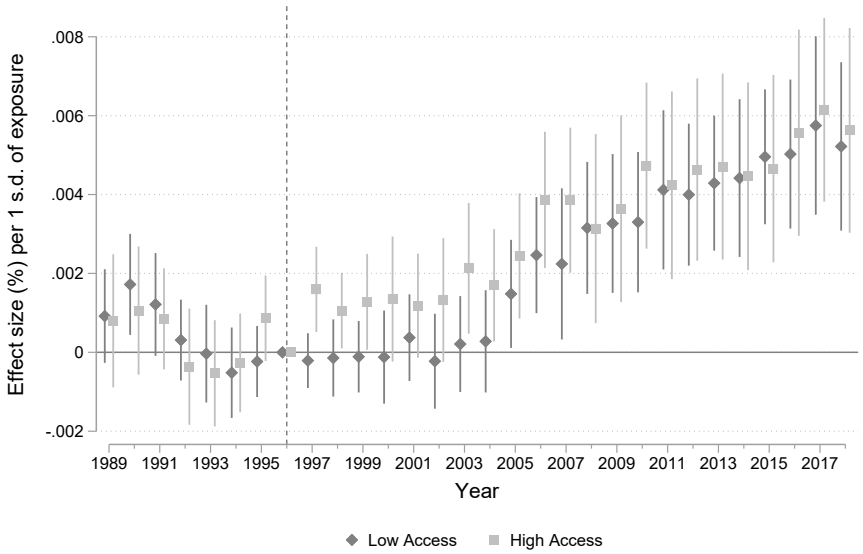
Notes: Panels (a) and (b) present estimates of the effects of exposure to the opioid epidemic on the change in log population on alternative geographic samples, leaving one state out of our analysis sample at a time, and plots estimates of the coefficient ϕ from Equation (3). Panel (d) reproduces this exercise for the effects on total fertility rates in 2018. All specifications include a set of demographic controls measured in 1990, controls for exposure on connected CZs, and state-level fixed effects. Standard errors are clustered at the CZ level. Panel (c) presents the same exercise for out-migration rates constructed from the IRS data. All plotted coefficients are $\phi_{o,2010}$ from Equation 4, scaled by baseline migration probabilities and by the standard deviation of 1996 cancer mortality, so effects are interpretable as percentage-point changes per one-standard-deviation increase in exposure. Standard errors are two-way clustered by origin and destination. This figure uses IRS migration data which covers inter-county internal migration and provides year-to-year moves. This figure is referenced in Section IX..

Figure A11: Effects of the Opioid Epidemic on Abortion Rates and Fertility Heterogeneity

(a) Abortion Rates



(b) Heterogeneity by Abortion Access



Notes: This figure shows the effects of exposure to the opioid epidemic on abortion rates (panel a) and fertility rates by access to abortion (panel b). Access to abortion is defined by above or below median distance to an abortion clinic. These are estimates of the ϕ_τ coefficients in Equation (3) multiplied by the standard deviation of the 1996 cancer mortality rate and divided by the 1996 average of abortion rates (panel a) and fertility rate (panel b). These estimates exploit continuous variation in cancer mortality in 1996 and control for baseline characteristics and state-by-year fixed effects. Standard errors are clustered at the CZ level. This figure is referenced in Section IX.e.

Table A1: Effects of Exposure to the Opioid Epidemic on Population Growth Rates - Extended Sample

	Change in log population per 1 s.d. exposure					
		Ages 18-64				
1996 cancer mortality x	All ages	All	Female	Male	No college	College
	(1)	(2)	(3)	(4)	(5)	(6)
Panel A. State level regressions						
1970 – 1980	-0.0149	-0.0074	-0.0084	-0.0064	0.0076	-0.0099
	(0.0106)	(0.0094)	(0.0079)	(0.011)	(0.0094)	(0.0132)
1980 – 1990	0.0002	-0.0009	-0.0028	0.0009	0.0036	0.0117
	(0.0064)	(0.0063)	(0.0058)	(0.0068)	(0.0054)	(0.0078)
Panel B. CZ level regressions						
1990 – 2000	0.0023	0.0042	0.0082	0.0009	0.0044	0.0091
	(0.0048)	(0.0055)	(0.0052)	(0.0066)	(0.0056)	(0.0097)
2000 – 2010	-0.0094***	-0.0129***	-0.0145***	-0.0124***	-0.0109***	-0.0201***
	(0.0034)	(0.0035)	(0.0034)	(0.0039)	(0.0038)	(0.007)
2000 – 2020	-0.0103**	-0.0242***	-0.0226***	-0.0267***	-0.02***	-0.0378***
	(0.0048)	(0.0055)	(0.0053)	(0.0078)	(0.0053)	(0.0097)

Notes: This table presents estimates of the effects of exposure to the opioid epidemic on the change in log population. Panel A uses state-level data to construct population counts. Columns (1) to (4) leverage data from the 1960, 1970, 1980, and 1990 Censuses. Columns (5) and (6) leverage data from the 1950, 1970, 1980, and 1990 Census to construct population counts by years of schooling for adults aged 25 years and older. Educational level data are not available from the 1960 Census. See Appendix Section B.3 for details on construction of the population counts used in this table. These regressions include a vector of demographic controls measure in 1990 and 1980 to account for state baseline characteristics. Standard errors are clustered at the state level. Panel B reproduces the results presented in Tables 2 and 3. *$p<0.10$, **$p<0.05$, *** $p<0.01$. This table is referenced in Section VI.

Table A2: Effects of Exposure to the Opioid Epidemic on Population Growth Rates - Additional age groups

	Change in log population per 1 s.d. exposure			
1996 cancer mortality ×	All ages (1)	Ages 0-17 (2)	Ages 18-64 (3)	Ages 65 plus (4)
1990 – 2000	0.0023	0.0046	0.0042	-0.0034
	(0.0048)	(0.0065)	(0.0055)	(0.0043)
2000 – 2010	-0.0094***	-0.0156***	-0.0129***	-0.0011
	(0.0034)	(0.0049)	(0.0035)	(0.0035)
2000 – 2020	-0.0103**	-0.0138**	-0.0242***	-0.0094
	(0.0048)	(0.0065)	(0.0055)	(0.0076)

Notes: This table presents estimates of the effects of exposure to the opioid epidemic on the change in log population. We consider changes in the total population by age groups. Each cell reports estimates of the coefficient ϕ from Equation (3) multiplied by the standard deviation of cancer mortality in 1996. All specifications include a set of demographic controls measured in 1990, controls for exposure on connected CZs, and state-level fixed effects. Standard errors are clustered at the CZ level. *p<0.10, **p<0.05, *** p<0.01. This table is referenced in Section VI.

Table A3: Effects of Exposure to the Opioid Epidemic on Population Growth Rates by Education - Alternative Definitions

	Change in log population per 1 s.d. exposure					
			Female		Male	
	No college	College	No college	College	No college	College
1996 cancer mortality ×	(1)	(2)	(3)	(4)	(5)	(6)
Panel A. College defined as BA or higher						
1990 – 2000	0.0044	0.0091	0.0096*	0.0141	-0.0003	0.005
	(0.0056)	(0.0097)	(0.0052)	(0.011)	(0.007)	(0.01)
Panel B. College defined as any post-secondary education						
2000 – 2010	-0.0084*	-0.0232***	-0.0115**	-0.0256***	-0.0073	-0.0201***
	(0.0047)	(0.0058)	(0.0052)	(0.0058)	(0.005)	(0.0068)
2000 – 2020	-0.0273***	-0.0333***	-0.0343***	-0.0304***	-0.0231***	-0.0376***
	(0.0067)	(0.0079)	(0.0076)	(0.0069)	(0.007)	(0.0095)

Notes: This table reports estimates of the effect of exposure to the opioid epidemic on changes in log population. We examine changes in total population by education, sex, and age group. Each cell reports the estimate of ϕ from Equation (3). All specifications include demographic controls measured in 1990, controls for exposure on connected CZs, and state fixed effects. Panel A reproduces the estimates presented in Table 3 to ease comparison. See Appendix Section B.4 for details on construction of the population counts used in this table. Standard errors are clustered at the CZ level. *p<0.10, **p<0.05, *** p<0.01. This table is referenced in Section VI.

Table A4: Effects of Exposure to the Opioid Epidemic on Fertility by Marital Status and Education

1996 cancer mortality ×	Unmarried	Married	No college	Some college
	(1)	(2)	(3)	(4)
1989 - 1995	0.5934*	-0.1161	-0.4279	0.3651
	(0.3285)	(0.3079)	(0.3124)	(0.2552)
1997 - 2003	0.5382	-0.1848	0.1939	-0.1593
	(0.3502)	(0.3608)	(0.3622)	(0.2552)
2004 - 2010	1.612***	0.5828	2.2971***	0.5927*
	(0.4372)	(0.555)	(0.5345)	(0.3289)
2011 - 2018	1.746***	2.0366***	3.8721***	1.8205***
	(0.4663)	(0.6977)	(0.6156)	(0.4052)
Mean of dep variable in 1996	47.93	75.14	82.95	53.10
Number of CZs	579	579	579	579
Observations	17,340	17,340	17,370	17,370

Notes: This table shows the effects of the opioid epidemic on fertility rates (per 1,000 women) by marital status and by education for the period 1989 to 2018. Effects are estimated following Equation (6) where years are grouped as listed in the left column of the table. We report changes in the outcome variable multiplied by the standard deviation of the 1996 cancer mortality rate. These estimates exploit continuous variation in cancer mortality in 1996 and control for baseline characteristics and state-by-year fixed effects. Standard errors are clustered at the CZ level. This figure is referenced in Section VII.c.

Table A5: Effects of Exposure to the Opioid Epidemic on Drug Induced Mortality by Sex and Education

1996 cancer mortality x	Female	Male	No college	Some college
	(1)	(2)	(3)	(4)
1989 - 1995	0.0021	0.002	0.0009	0.0005
	(0.0061)	(0.0059)	(0.0071)	(0.0044)
1997 - 2003	0.0129**	0.0093	0.0151**	0.0025
	(0.0063)	(0.0078)	(0.0077)	(0.0051)
2004 - 2010	0.0238***	0.0338***	0.0453***	0.0059
	(0.0074)	(0.0098)	(0.0115)	(0.0056)
2011 - 2018	0.0241***	0.0234**	0.0355**	0.0074
	(0.0074)	(0.0112)	(0.0146)	(0.0056)
Mean of dep variable in 1996	0.0413	0.0821	0.0767	0.0263
Number of CZs	587	587	586	586
Observations	17,608	17,608	17,578	17,578

Notes: This table shows the effects of the opioid epidemic on drug-induced mortality rates (per 1,000) by sex and by education for the period 1989 to 2018. Effects are estimated following Equation (6) where years are grouped as listed in the left column of the table. We report changes in the outcome variable multiplied by the standard deviation of the 1996 cancer mortality rate. These estimates exploit continuous variation in cancer mortality in 1996 and control for baseline characteristics and state-by-year fixed effects. Standard errors are clustered at the CZ level. This figure is referenced in Section VII.c.

B. Data Appendix

B.1 Mortality Data

We use restricted-use data from the Detailed Multiple Cause of Death (DMCD) files from 1989 to 2018. The 1989–1998 data use ICD-9 codes to classify causes of death, while the 1999–2018 data use ICD-10 codes. We analyze drug-related deaths separately for women and men, and also leverage educational attainment data included in death certificates to document effects by education level—specifically, for individuals with some college or more, and those without any college education.[39]

B.2 SEER Population Data and County Adjustments

We construct commuting zone (CZ) level population counts by aggregating county-level population data from SEER to 1990 CZs using the crosswalk from Autor and Dorn (2013). For decennial census years (e.g., 2000), SEER uses population counts directly from the U.S. Census Bureau. For intercensal years, SEER interpolates population counts. Due to a combination of data availability (for SEER) and boundary changes of counties over time (e.g., mergers, splits, renamings), we make several adjustments to the county-level data before aggregating to CZs which we describe below. Also discussed below are certain cases where boundary changes occurred but were pre-processed by SEER and therefore did not require any adjustments. Further documentation is available at the following links: SEER county boundary documentation; David Dorn's county changes documentation.

Arizona:

- 1983: La Paz county (04012) was created from Yuma county (04027). As death records for the two counties were not reported separately until 1994 SEER data provides a combined county (04910) until 1993 (La Paz and Yuma are reported separately thereafter). Since La Paz and Yuma counties map to different CZs, we drop both CZs (38100 and 38300) from the analysis.

Colorado:

- 2001: Broomfield county (08014) was created out of parts of Adams (08001), Boulder (08013), Jefferson (08059) and Weld (08123) counties. Mortality data was not available in Broomfield until 2003 so SEER created retroactive versions of those

[39]The 2018 data were the first for which educational attainment was consistently reported using the 2003 revision of the death certificate across all deaths (unless missing entirely). In prior years, some deaths still used the 1989 revision's categorization. This change prevents us from constructing more granular education categories. The sub-section on fertility data discusses a related challenge and provides more detail on these definitions.

counties prior to 2003. Since: (i) all excepting Weld county map to CZ 28900; and (ii) Weld was the smallest contributor (the population loss for Weld was only 69 people as compared to 39,108 between the other counties) we proceed by mapping Broomfield (08014) to CZ 28900 as soon as it is available in SEER data (2003) and map retroactive versions of Adams, Boulder, Jefferson and Weld counties according to the the current CZ mapping for those counties.

Florida:

- 1997: Dade county (FIPS 12025) was renamed to Miami-Dade county (FIPS 12086). SEER retroactively uses the new FIPS code from 1980 to 2020. We replace all instances of 12086 with 12025 to align with Autor and Dorn (2013).

Montana:

- 1997: Yellowstone National Park Territory (30113) was merged into Gallatin (30031) and Park (30067) counties. In SEER data, Yellowstone National Park Territory is always included in Gallatin county so no adjustment is required.

New Mexico:

- 1981: Cibola county (35061) was created out of parts of Valencia county (35006). We combine these back into one county which maps to the same CZ for all years.

South Dakota:

- 1983: Washabaugh county (46071) was merged into Jackson county (46071). Consistent with the Census Bureau making this adjustment effective 1979, SEER only provides Jackson county. There is never a discontinuous jump in Jackson county population in 1983 so no adjustment is required.
- 2015: Shannon county (46113) was renamed to Oglala Lakota county (46102). SEER data never renames Shannon county so no adjustment is required.

Virginia:

- 1982: James City (51095), York (51119), Poquoson City (51735) and Williamsburg City (51830) counties are not available until 1982 separately in SEER data and are therefore grouped under FIPS code 51911 in 1980 and 1981. All counties map to to CZ 2500 so no aggregate adjustment is required.

- 1982: Prince William (51153), Manassas City (51683) and Manassas Park City (51685) counties are not available until 1982 separately in SEER data and are grouped under FIPS code 51910 in 1980 and 1981. All counties map to CZ 11304, so no aggregate adjustment is required.

- 1995: South Boston City (51780) merged into Halifax County (51083). SEER documentation notes that South Boston City is included directly in Halifax County. Consistent with this, we never observe South Boston City in the data, and Halifax County population does not show a discontinuous jump in 1995 when South Boston City was merged into it. No adjustment is required.

- 2001: Clifton Forge (51560) merged into Alleghany County (51005). In the SEER data, Clifton Forge is always directly included directly in Alleghany County (51005) so no adjustment is required.

- 2013: Bedford (51515) is merged into Bedford county (51019), however, neither county ever shows up separately in SEER data, instead, they show up jointly as 51917. Since both counties merge to the same CZ in Autor and Dorn (2013) crosswalk (2300) we replace all instances of 51917 with 51515.

B.3 Population Counts for State-Level Analysis

Constructing population counts prior to 1980 requires several compromises due to data limitations. For 1960, the most granular geographic unit available is the Public Use Microdata Area (PUMA), which does not nest within commuting zones, and no comparable education data are available for this year. For 1970, data are reported at the county group level, which is likewise less granular than commuting zones. Given these constraints, we use state-level population counts by sex and age from NHGIS for 1960 and 1970, and SEER data for 1980 and 1990. For education counts, we draw on NHGIS state-level data for 1950, 1970, 1980, and 1990, which provide information on years of schooling completed by sex.

B.4 Population Counts by Education

Data on educational attainment by sex and age come from the NHGIS B89 nominal time series table, which links comparable county-level statistics across the 1980, 1990, and 2000 decennial censuses and all available ACS 5-year estimates from 2006–2010 through 2020–2024. For decennial years, the data originate from the long-form census questionnaire administered to a sample of approximately one-in-six households; ACS estimates pool five years of continuous survey data. The NHGIS B89 table provides three education categories—less than 9th grade, 9th grade through some college or associate's degree, and

bachelor's degree or higher—which we collapse into two groups: college-educated (bachelor's degree or higher) and non-college (less than a bachelor's degree). Because the NHGIS B89 table does not provide a separate some-college category in any year, grouping some college with non-college is the only consistently available binary split across the full sample period.

For all other outcomes, we define college-educated as any post-secondary education (some college, associate's, bachelor's, or graduate degree) and non-college as high school graduate or less. While we cannot construct these categories using county-level data in 1980, we can since 1990 using the NHGIS B90 nominal time series table, which provides six education categories spanning the 1990 decennial census through the 2020–2024 ACS.

B.5 IRS SOI Migration Data

B.5.1 County Adjustments

Due to boundary changes of counties over time (e.g., mergers, splits, renamings), we make several adjustments to the IRS SOI county-level migration data. Further documentation is available at: David Dorn's county changes documentation.

- 1995: The independent city of South Boston (FIPS 51780) was merged into into Halifax county (FIPS 50183). We therefore combine South Boston into Halifax county for all years.
- 2000:
  - Dade county (FIPS 12025) was renamed to Miami-Dade county (FIPS 12086). We replace all instances of 12086 with 12025 for all years.
  - The independent city of Clifton Forge (FIPS 51560) was merged into Alleghany county (FIPS 51005). We combine Clifton Forge into Alleghany county for all years.
- 2002: Broomfield county (FIPS 08014) was created out of parts of Adams (FIPS 08001), Boulder (FIPS 08013), Jefferson (FIPS 08059) and Weld (FIPS 08123) counties. Due to related challenges arising from SEER data (see Appendix B.2), we drop Broomfield county from our county-level migration analysis.
- 2012: The independent city of Bedford (FIPS 51515) was merged into Bedford county (FIPS 51019). We combine Bedford into Bedford county for all years.
- 2015: Shannon county (FIPS 46113) was renamed to Oglala Lakota county (FIPS 46102). We replace all instances of 46113 with 46102 for all years.

B.5.2 Gravity Imputation of Suppressed County-County Migrant Flows

The IRS SOI county-to-county migration data suppress small (< 10 or 20 migrants, depending on the year) flows for confidentiality. Since suppression applies symmetrically to inflows and outflows, we solely discuss outflows. In each year, the IRS reports: (i) origin–destination flows whenever the threshold number of migrants (exemptions) move from an origin o to a destination d; (ii) total outflows from o; (iii) total outflows from o to U.S. destinations; (iv) total outflows from o to foreign destinations; and, in many cases, (v) aggregate *within-state* suppressed outflows and aggregate *out-of-state* suppressed outflows.

To construct CZ-level outflows and inflows, we must remove intra-CZ county–county moves from the county-level flows. We proceed as follows:

1. **Remove observed within-CZ flows.** We remove observed county–county flows where origin and destination belong to the same CZ.

2. **Treat out-of-state suppressed flows as between-CZ moves.** We assume that aggregate suppressed outflows from origin o to *out-of-state* destinations solely refelct inter-CZ flows.

3. **Impute within-state suppressed flows using a gravity model.** For aggregate *within-state* suppressed outflows from origin o, we use gravity based imputation to allocate these flows across destination counties. This involves the following steps:

   - Let $\mathcal{D}_o$ denote the set of candidate destination counties that (i) are in the same state as o; (ii) have ever received a non-suppressed flow from o in any year-pair; and (iii) are not destinations for which we already observe a flow from o in the current year-pair (and hence cannot be part of the suppressed set).
   - For each $d \in \mathcal{D}_o$, define

     $$\pi_{od} = \frac{\text{Pop}_d / \text{Dist}_{od}^2}{\sum_{d' \in \mathcal{D}_o} \text{Pop}_{d'} / \text{Dist}_{od'}^2},$$

     where Pop_d is the population of county d and Dist_{od} is the distance between counties o and d.
   - We then allocate the aggregate within-state suppressed outflow from o across destinations $d \in \mathcal{D}_o$ in proportion to π_{od}.

4. **Residual suppression.** In the rare cases where within-state and out-of-state suppressed totals are themselves censored, we repeat step 3 using as the candidate set all U.S. counties except those for which we observe a positive flow from o in the current year-pair.

B.6 Fertility

We further disaggregate fertility rates by educational attainment.[40] [41] To compute fertility rates by educational attainment, we classify mothers into two groups: those with some college or more, and those without any college education. The NCHS data include information on years of schooling, but we reclassify education levels to account for changes in how this information is reported across time and states. We define "some college or more" as having completed more than 13 years of education, any number of years of college without a degree, or any higher degree (e.g., a bachelor's or master's degree). If education is reported but does not meet this definition, we classify the individual as having "no college education." The denominator is constructed using Census and ACS data. Table 1 reports summary statistics for fertility rates overall and by education. Fertility rates are higher among those without any college education (86.7 births per 1,000 in 1996 vs. 51.5 for the college group) and this gap persists through 2018.

B.7 Economic outcomes.

We collect data from the Longitudinal Employer-Household Dynamics (LEHD) program, which provides detailed information on employment and earnings at the county-level and by age, race, sex and education. Specifically, we use the Quarterly Workforce Indicators (QWI) employment counts and average monthly earnings. We construct education-specific employment counts and employment-to-population ratios relying on the number of stable jobs divided and counts for the working age population. We also construct a measure of average earnings as the ratio between earnings across all permanent jobs to the total number of permanent jobs.

B.8 Amenities measures.

The FHFA House Price Index (HPI) is a broad measure of changes in single-family home values, published by the Federal Housing Finance Agency. It is constructed using a weighted repeat-sales methodology, which tracks price changes on the same properties over time by exploiting multiple mortgage transactions on the same home. This approach controls for compositional changes in the housing stock, making it a reliable measure of price appreciation at the local level. Median contracted rents are drawn from the American Community Survey (ACS) and measure the median monthly rent agreed upon

[40] We also disaggregate fertility rates by marital status. For the analysis by marital status, we define the married (unmarried) fertility rate as the number of births to married (unmarried) individuals in a given age group divided by the population of married (unmarried) women in that age group. The numerator is obtained directly from the NCHS Files; the denominator is constructed using data from the U.S. Census and the American Community Survey (ACS).

[41] The Natality Detail Files include information obtained from each U.S. birth certificate. There is some variation across states and over time in the availability of specific variables. In some cases, we exclude states from specific analyses due to data limitations; we note these exclusions when relevant.

in the lease contract for renter-occupied housing units paying cash rent. Contracted rent reflects the price tenants are obligated to pay regardless of whether utilities or other services are included, and is therefore distinct from gross rent, which adds the cost of utilities. Units where no cash rent is paid — such as those provided rent-free or in exchange for services — are excluded from the universe.

Crime rates are computed using data from the FBI Uniform Crime Reporting System (UCRS) and are defined as the number of crimes in a given category divided by the population of the commuting zone. The UCRS contains information on "Index Crimes" (also referred to as Part I crimes) reported by local law enforcement agencies. Index crimes are divided into two categories: violent crimes — including murder, rape, robbery, and aggravated assault — and property crimes — including burglary, theft, and motor vehicle theft. To ensure consistency over time, we restrict the sample to agencies that report complete data in every month of every year in the sample period, yielding 4,391 agencies. Crime counts are then aggregated to the commuting zone level and normalized by population to construct crime rates for each category.

C. Model

This section presents all derivations for the model in Section IV.. For ease of reference, we restate all elements of the model described in the main text.

C.1 Setup

Consider a small open economy with multiple sectors $n \in \mathcal{N}$ produced across locations $l \in \mathcal{L}$. Goods are differentiated by location of production, product markets are frictionless, and production uses labor as the only input with sector-location productivity φ_{ln}. Output and labor markets are perfectly competitive. Each location is characterized by exogenous amenities A_l and an inelastic housing supply $\bar{H}_l$ which introduces a local congestion force in equilibrium.

There are two types of workers indexed by $h \in \{c, nc\}$, representing college- and non-college-educated workers. They differ in their willingness to pay for local amenities, ζ^h; their sector-location-specific productivity, φ^h_{ln}; and their migration elasticity, θ^h. The exogenous initial distribution of type-h workers across locations is given by L_o^{0h}. Workers choose consumption, housing, and location of employment subject to migration frictions. Each worker supplies one unit of labor inelastically in their chosen location and earns wage rate w_l^h. Changes in employment are equivalent to changes in population.

C.2 Workers Utility

Utility from consumption is Cobb-Douglas across sectors and CES across location-specific varieties within a sector. Worker type h in location d derives utility from consumption goods and housing as follows:

$$U_d^h = A_d^{\zeta^h} \left(\prod_n \left(\frac{Q_n}{\alpha \eta_n} \right)^{\alpha \eta_n} \right) \left(\frac{x_d}{1-\alpha} \right)^{1-\alpha}, \quad \text{where} \quad Q_n \equiv \left(\sum_{l \in \mathcal{L}_w} q_{ln}^{\frac{\sigma-1}{\sigma}} \right)^{\frac{\sigma}{\sigma-1}},$$

where η_n is the share of expenditure on sector-n within the consumption bundle, such that $\sum_n \eta_n = 1$. Q_n aggregates over location-specific varieties q_{ln} produced around the world, including those within the country of interest $\mathcal{L} \subset \mathcal{L}_w$. α is the share of expenditure on consumption goods, (1-α) is the share of expenditure on consumption of local housing, represented by x_d. Normalizing world aggregate expenditure (on consumption goods) to one, the aggregate optimal consumption bundle satisfies:

$$q_{ln} = p_{ln}^{-\sigma} P_n^{\sigma-1} \eta_n, \tag{C.1}$$

where $P_n \equiv \left(\sum_l p_{ln}^{1-\sigma}\right)^{\frac{1}{1-\sigma}}$ is the CES exact price index for sector n and p_{ln} is the price of a sector-n good produced in location l. P_n is set on the world market, exogenous to our country of interest. Given wages w_l^h, a worker of type h in location l spends $\alpha\eta_n$ share on sector-n. Optimal demand for the sector-n CES aggregate is $Q_n = \alpha\eta_n w_l^h / P_n$, so the consumption component of log-utility is:

$$\sum_n \alpha\eta_n \ln\left(\frac{Q_n}{\alpha\eta_n}\right) = \alpha \ln w_l^h - \alpha \sum_n \eta_n \ln P_n = \alpha \ln\left(\frac{w_l^h}{P}\right).$$

$P \equiv \prod_n P_n^{\eta_n}$ is the Cobb-Douglas exact price index.

The market clearing condition for housing is $\bar{H}_l = x_l^c L_l^c + x_l^{nc} L_l^{nc}$, where x_l^h is the consumption of local housing for worker-type h in location l. Landlords are absentee. The local rental rate clears the housing market such that:

$$r_l = (1-\alpha)\frac{w_l^c L_l^c + w_l^{nc} L_l^{nc}}{\bar{H}_l} = (1-\alpha)\frac{W_l}{\bar{H}_l} \tag{C.2}$$

where W_l is the total wage bill in location l. The housing component of log-utility is:

$$(1-\alpha)\ln\left(\frac{x_l^h}{1-\alpha}\right) = (1-\alpha)\ln\left(\frac{w_l^h \bar{H}_l}{(1-\alpha)W_l}\right) = (1-\alpha)\ln\left(\frac{w_l^h \bar{H}_l}{W_l}\right) + (1-\alpha)\ln\left(\frac{1}{1-\alpha}\right),$$

where the last term is an additive constant common across locations and its dropped from the indirect utility.

Combining these components and bilateral migration costs τ_{ol} ($\tau_{oo} = 1$), which generate a network structure of migration, the indirect utility of a worker i of type h migrating from o to l is:

$$V_{iol}^h = \zeta^h \ln A_l + \alpha \ln\left(\frac{w_l^h}{P}\right) + (1-\alpha)\ln\left(\frac{w_l^h \bar{H}_l}{W_l}\right) - \ln \tau_{ol} + \frac{1}{\theta^h}\epsilon_{il}^h. \tag{C.3}$$

$\bar{V}_{ol}^h$ is the deterministic component of indirect utility. ϵ_{il}^h is an i.i.d. taste shock following the standard Gumbel distribution across individuals and locations.

C.3 Local Labor Supply

Based on the assumptions on Equation C.3, the probability of a type h worker from o moving to l is:

$$\pi_{ol}^h = \frac{\exp(\theta^h \bar{V}_{ol}^h)}{\sum_d \exp(\theta^h \bar{V}_{od}^h)},$$

where θ^h is the migration elasticity, capturing how strongly workers respond to differences in location attractiveness, influenced by wages, amenities, and housing congestion. The resulting labor supply of workers type h in location l is:

$$L_l^h = \sum_o \pi_{ol}^h L_o^{0h}.$$

Migration probability and local labor supply responses to an amenity shock. Consider a small amenity shock across locations. Let hats represent proportional changes relative to the no-change counterfactual, so $\hat{x} = \frac{dx}{x} = d\ln x$. The proportional change in local labor supply is given by:

$$\hat{L}_l^h = \sum_o \gamma_{ol}^h \hat{\pi}_{ol}^h.$$

$\gamma_{ol}^h \equiv \pi_{ol}^h L_o^{0h}/L_l^h$ is the share of type-h residents in location l who originated from location o, which can be understood as "in-migration shares". The change in the migration probability when the deterministic location utility solely reflects an amenity shock is given by:

$$\hat{\pi}_{ol}^h = \theta^h \zeta^h \left(\hat{A}_l - \pi_{oo}^h \hat{A}_o - \sum_{d \neq o} \pi_{od}^h \hat{A}_d \right). \tag{C.4}$$

Substituting into $\hat{L}_l^h = \sum_o \gamma_{ol}^h \hat{\pi}_{ol}^h$ yields:

$$\hat{L}_l^h = \theta^h \zeta^h \left[\hat{A}_l - \sum_o \gamma_{ol}^h \sum_d \pi_{od}^h \hat{A}_d \right],$$

and can be written in matrix notation:

$$\hat{\mathbf{L}}^h = \theta^h \zeta^h \left(\mathbf{I} - \mathbf{\Gamma}^h \mathbf{\Pi}^h \right) \hat{\mathbf{A}}. \tag{C.5}$$

$\mathbf{I}$ is the identity matrix, $\mathbf{\Gamma}^h$ is the matrix of in-migration shares γ_{ol}^h, $\mathbf{\Pi}^h$ is the matrix of location choice probabilities π_{od}^h, and $\hat{\mathbf{A}}$ is the vector of amenity shocks.

C.4 Local Labor Demand

We model production with a CES aggregator over college and non-college labor.[42] Each sector n in location l employs L_{ln}^h workers of type h and combines them using a CES technology. The production function for sector n in location l is:

$$Y_{ln} = \left[\beta_{ln}^{\frac{1}{\rho}} (\varphi_{ln}^c L_{ln}^c)^{\frac{\rho-1}{\rho}} + (1-\beta_{ln})^{\frac{1}{\rho}} (\varphi_{ln}^{nc} L_{ln}^{nc})^{\frac{\rho-1}{\rho}} \right]^{\frac{\rho}{\rho-1}}.$$

[42] The use of a CES aggregator over education groups follows a large literature, including Katz and Murphy (1992); Card and Lemieux (2001). Embedding that structure in the Armington (1969)-style labor-demand framework of Borusyak et al. (2022) follows Claassen (2025).

Here, β_{ln} is the share parameter for college labor in sector n and location l, φ_{ln}^h is the productivity of type-h workers in sector-location (l,n), and ρ is the elasticity of substitution between college and non-college labor. Let the productivity-adjusted price of labor type h be $\tilde{w}_{ln}^h \equiv w_l^h/\varphi_{ln}^h$. Cost minimization implies:

$$p_{ln} = \left[\beta_{ln}(\tilde{w}_{ln}^c)^{1-\rho} + (1-\beta_{ln})(\tilde{w}_{ln}^{nc})^{1-\rho}\right]^{\frac{1}{1-\rho}}. \tag{C.6}$$

The cost shares ω_{ln}^h are determined endogenously by relative wages and the substitution elasticity ρ. By Shephard's lemma:

$$\omega_{ln}^c = \beta_{ln}\left(\frac{\tilde{w}_{ln}^c}{p_{ln}}\right)^{1-\rho}, \quad \omega_{ln}^{nc} = (1-\beta_{ln})\left(\frac{\tilde{w}_{ln}^{nc}}{p_{ln}}\right)^{1-\rho}, \quad \omega_{ln}^c + \omega_{ln}^{nc} = 1. \tag{C.7}$$

Under perfect competition, total revenue equals total cost: $p_{ln}q_{ln} = w_l^c L_{ln}^c + w_l^{nc} L_{ln}^{nc}$. Combined with the cost shares, the wage bill of type h in sector-location (l,n) is $w_l^h L_{ln}^h = \omega_{ln}^h p_{ln} q_{ln}$. Substituting $q_{ln} = p_{ln}^{-\sigma} P_n^{\sigma-1}\eta_n$ from Equation C.1 and solving for L_{ln}^h yields:

$$L_{ln}^h = \omega_{ln}^h p_{ln}^{1-\sigma} P_n^{\sigma-1}\eta_n (w_l^h)^{-1}.$$

Substituting the cost shares from Equation C.7 for ω_{ln}^h yields sector-location labor demand:

$$L_{ln}^h = b_{ln}^h (\varphi_{ln}^h)^{\rho-1} p_{ln}^{\rho-\sigma} P_n^{\sigma-1}\eta_n (w_l^h)^{-\rho}, \tag{C.8}$$

where $b_{ln}^c \equiv \beta_{ln}$ and $b_{ln}^{nc} \equiv 1-\beta_{ln}$ are the CES share parameters for each worker type. The sector-level labor demand has wage elasticity $-\rho$, reflecting substitution between worker types within the CES nest. The term $p_{ln}^{\rho-\sigma}$ combines two effects of the local product price: a $p_{ln}^{-\sigma}$ Armington scale effect (a higher price reduces output demand) and a $p_{ln}^{\rho-1}$ CES cost-share effect (a higher price shifts labor's revenue share responses to the output price). The net exponent $\rho-\sigma$ determines the overall price sensitivity of labor demand. Aggregating over all sectors $n \in \mathcal{N}$ yields total labor demand for worker type h in l:

$$L_l^h = D_l^h (w_l^h)^{-\rho}, \quad \text{where} \quad D_l^h \equiv \sum_{n\in\mathcal{N}} b_{ln}^h (\varphi_{ln}^h)^{\rho-1} p_{ln}^{\rho-\sigma} P_n^{\sigma-1}\eta_n. \tag{C.9}$$

Recall that P_n is the sector-level CES price index, set on the world market and exogenous to any single location. D_l^h is a composite demand shifter that depends on local sector composition, sector-level prices, and world demand conditions. Conditional on D_l^h, location-level labor demand is isoelastic in the wage with elasticity $-\rho$. Inverting this relationship, $w_l^h \propto (L_l^h)^{-1/\rho}$, so ρ also governs the equilibrium wage response to local labor supply shifts: a higher ρ (easier substitution between types) implies wages are less sensitive to population changes. Importantly, labor demands for both worker types are linked through p_{ln}: since the unit cost p_{ln} depends on both w_l^c and w_l^{nc} via Equation C.6,

a change in one worker type's wage shifts p_{ln} and thereby affects demand for the other type. This cross-type interdependence is what gives rise to the 2×2 wage system in equilibrium.

Local labor demand responses to an amenity shock. Consider again a shock to amenities in location l, totally log-differentiating Equation C.6 yields:

$$\hat{p}_{ln} = \omega_{ln}^{c} \left(\hat{w}_{l}^{c} - \hat{\varphi}_{ln}^{c} \right) + \omega_{ln}^{nc} \left(\hat{w}_{l}^{nc} - \hat{\varphi}_{ln}^{nc} \right). \tag{C.10}$$

Equation C.10 says that the log-change in the local product price is a cost-share-weighted average of the productivity-adjusted wage changes across worker types. A location becomes cheaper to produce in when wages fall or productivity rises.

The log-change in sector-location labor demand follows from log-differentiating C.8:

$$\hat{L}_{ln}^{h} = \hat{D}_{ln}^{h} - \rho \hat{w}_{l}^{h} + (\rho - \sigma) \hat{p}_{ln}, \tag{C.11}$$

It has three components: $\hat{D}_{ln}^{h}$ collects exogenous shifters (productivity, world prices, sector demand)[43]; $\rho \hat{w}_{l}^{h}$ is the own-wage substitution effect; and $(\rho - \sigma)\hat{p}_{ln}$ is the price-of-output effect, capturing how changes in local product prices affect the scale of output and thus demand for labor. Substituting Equation C.10 into Equation C.11 while holding productivities fixed, allow us to characterize labor demand purely in terms of the local wage vector:

$$\hat{L}_{ln}^{h} = \hat{D}_{ln}^{h} - \rho \hat{w}_{l}^{h} + (\rho - \sigma) \left(\omega_{ln}^{c} \hat{w}_{l}^{c} + \omega_{ln}^{nc} \hat{w}_{l}^{nc} \right).$$

The result shows that both types' labor demands depend on both wages. Collecting wage terms separately for each type:

$$\hat{L}_{ln}^{c} = \hat{D}_{ln}^{c} - \left[\rho - (\rho - \sigma) \omega_{ln}^{c} \right] \hat{w}_{l}^{c} + (\rho - \sigma) \omega_{ln}^{nc} \hat{w}_{l}^{nc},$$

and for non-college labor:

$$\hat{L}_{ln}^{nc} = \hat{D}_{ln}^{nc} + (\rho - \sigma) \omega_{ln}^{c} \hat{w}_{l}^{c} - \left[\rho - (\rho - \sigma) \omega_{ln}^{nc} \right] \hat{w}_{l}^{nc}.$$

Each type's sector-level demand has an own-wage term $-[\rho - (\rho - \sigma)\omega_{ln}^{h}]$ and a cross-wage term $(\rho - \sigma)\omega_{ln}^{-h}$. The own-wage term combines the direct substitution elasticity ρ with the indirect scale channel through p_{ln}. The cross-wage term operates only through the scale channel: a change in the other type's wage shifts p_{ln}, which in turn shifts output demand and hence demand for both types.

Moving to aggregation over sectors, let $\lambda_{ln}^{h} \equiv L_{ln}^{h} / L_{l}^{h}$ be the employment share of sector n in location l for type-h. The effective own- and cross-wage elasticities at the

[43] Specifically, $\hat{D}_{ln}^{h} = (\rho - 1)\hat{\varphi}_{ln}^{h} + (\sigma - 1)\hat{P}_{n} + \hat{\eta}_{n}$.

location level are:

$$a_l^{cc} \equiv \sum_n \lambda_{ln}^c \left[\rho - (\rho - \sigma)\omega_{ln}^c\right], \quad a_l^{c,nc} \equiv \sum_n \lambda_{ln}^c (\rho - \sigma)\omega_{ln}^{nc},$$

a_l^{cc} is the own-wage elasticity of college labor demand at the location level, aggregated across sectors using employment weights λ_{ln}^c. $a_l^{c,nc}$ is the cross-wage elasticity: how college labor demand responds to non-college wages through the shared output price. The non-college analogs $a_l^{nc,nc}$ and $a_l^{nc,c}$ have the same form but use employment weights λ_{ln}^{nc}. Let $\mathbf{a}^{hh'}$ denote diagonal matrices with entries $a_l^{hh'}$, and stack $\hat{\mathbf{L}} \equiv [\hat{\mathbf{L}}^c; \hat{\mathbf{L}}^{nc}]$ and $\hat{\mathbf{w}} \equiv [\hat{\mathbf{w}}^c; \hat{\mathbf{w}}^{nc}]$. The location-level demand system is:

$$\hat{\mathbf{L}} = \hat{\mathbf{D}} - \mathbf{a}\hat{\mathbf{w}}, \quad \text{where} \quad \mathbf{a} \equiv \begin{bmatrix} \mathbf{a}^{cc} & -\mathbf{a}^{c,nc} \\ -\mathbf{a}^{nc,c} & \mathbf{a}^{nc,nc} \end{bmatrix}. \tag{C.12}$$

Amenities do not enter the production function, so a pure amenity shock leaves sectoral productivities unchanged. World prices P_n and demand shifters η_n are exogenous in the small open economy. Therefore $\hat{D}_{ln}^h = 0$ for all h, l, n, and the demand system reduces to a mapping from population changes to wage changes:

$$\hat{\mathbf{w}} = -\mathbf{a}^{-1}\hat{\mathbf{L}}. \tag{C.13}$$

C.5 Equilibrium Responses to an Amenity Shock

Building on the previous derivations, in this section we characterize the three equilibrium responses in sequence: first population, then wages and rents, and lastly migration flows.

C.5.1 Local population changes

The equilibrium population response to an amenity shock $\hat{\mathbf{A}}$ is the solution to a system of equations: labor supply, labor demand, and housing market clearing. These equations are coupled: housing clearing pins down rents as a function of the local wage bill; labor supply then links population changes to wages and rents through workers' location choices; and labor demand closes the loop by linking wages back to population. We derive each component in turn before solving the system.

Housing market clearing. The local housing stock $\bar{H}_l$ is inelastic. With Cobb-Douglas preferences, each worker spends the share $(1-\alpha)$ of income on housing, so housing market clearing pins down the local rent as shown in Equation C.2. Changes in the rental rate are proportional to changes in the total local wage bill: $\hat{r}_l = \hat{W}_l$.

Log-differentiating the total local wage bill and expressing it in matrix form:

$$\hat{\mathbf{W}} = \mathbf{R}(\hat{\mathbf{w}} + \hat{\mathbf{L}}), \quad \mathbf{R} \equiv \begin{bmatrix} \mathbf{s}^c & \mathbf{s}^{nc} \end{bmatrix}, \tag{C.14}$$

where $\mathbf{s}^h$ is the diagonal matrix with l-th entry $s_l^h \equiv w_l^h L_l^h / W_l$, the share of the total wage bill corresponding to skill-group h.

Labor supply. Totally differentiating the deterministic component of indirect utility from the indirect utility function (Equation C.3) gives:

$$d\bar{V}_l^h = \zeta^h \hat{A}_l + \hat{w}_l^h - (1-\alpha)\hat{W}_l.$$

The three terms are, respectively: the direct amenity gain, the wage change from labor demand Equation C.13, and the housing congestion from Equation C.14. Similar to the derivation of Equation C.5, and stacking both worker types in the type-specific migration response $\hat{\mathbf{L}}^h = \theta^h(\mathbf{I} - \mathbf{\Gamma}^h\mathbf{\Pi}^h)d\bar{\mathbf{V}}^h$ we get the labor supply equation:

$$\hat{\mathbf{L}} = \mathbf{G}\left(\hat{\mathbf{w}} - (1-\alpha)\mathbf{J}\hat{\mathbf{W}} + \boldsymbol{\zeta}\hat{\mathbf{A}}\right), \tag{C.15}$$

where

$$\mathbf{G} \equiv \begin{bmatrix} \theta^c\left(\mathbf{I} - \mathbf{\Gamma}^c\mathbf{\Pi}^c\right) & \mathbf{0} \\ \mathbf{0} & \theta^{nc}\left(\mathbf{I} - \mathbf{\Gamma}^{nc}\mathbf{\Pi}^{nc}\right) \end{bmatrix}, \quad \mathbf{J} \equiv \begin{bmatrix} \mathbf{I} \\ \mathbf{I} \end{bmatrix}, \quad \boldsymbol{\zeta} \equiv \begin{bmatrix} \zeta^c\mathbf{I} \\ \zeta^{nc}\mathbf{I} \end{bmatrix}.$$

The block-diagonal structure of $\mathbf{G}$ reflects the fact that each worker type responds to its own utility changes, with no direct cross-type migration interaction. The matrix $\mathbf{J}$ ($2L \times L$) broadcasts the L-dimensional location-level wage-bill change $\hat{\mathbf{W}}$ to both skill groups, since housing costs depend on the total local wage bill rather than on type-specific wages. The diagonal matrices $\boldsymbol{\zeta}$ allow the amenity valuation to differ between college and non-college workers.

Equilibrium population response. Equations C.13, C.14, and C.15 jointly determine $\hat{\mathbf{L}}$, $\hat{\mathbf{w}}$, and $\hat{\mathbf{W}}$ given $\hat{\mathbf{A}}$. In general, this system can be reduced to a single linear equation in $\hat{\mathbf{L}}$, but the resulting matrix inverse mixes migration network structure, labor demand elasticities, and housing cost shares in a way that obscures economic interpretation. Instead, we follow Borusyak et al. (2022) and study the general equilibrium response under the low-mobility approximation, which yields a transparent closed form.

The low-mobility approximation imposes: $\mathbf{\Pi}^h \approx \mathbf{I}$, so that most workers remain at their origin in the baseline, i.e., the effects of indirect connections become unimportant. This has two implications. First, $(\mathbf{I} - \mathbf{\Gamma}^h\mathbf{\Pi}^h)$ is first-order small in the off-diagonal elements of $\mathbf{\Pi}^h$, so $\hat{\mathbf{L}}$ is first-order small. Second, since $\hat{\mathbf{w}} = -\mathbf{a}^{-1}\hat{\mathbf{L}}$ and $\hat{\mathbf{W}} = \mathbf{R}(\hat{\mathbf{w}} + \hat{\mathbf{L}})$ are both proportional to $\hat{\mathbf{L}}$, they are also first-order small. The feedback terms $\mathbf{G}(\hat{\mathbf{w}} - (1-\alpha)\mathbf{J}\hat{\mathbf{W}})$ then involve $\mathbf{G}$ — which itself contains $(\mathbf{I} - \mathbf{\Gamma}^h\mathbf{\Pi}^h)$ — multiplied by a first-order small vector, making them second-order. Dropping these terms yields:

$$\hat{\mathbf{L}}^c \approx \theta^c \zeta^c \left(\mathbf{I} - \mathbf{\Gamma}^c \mathbf{\Pi}^c\right) \hat{\mathbf{A}}, \tag{C.16}$$

$$\hat{\mathbf{L}}^{nc} \approx \theta^{nc} \zeta^{nc} \left(\mathbf{I} - \mathbf{\Gamma}^{nc} \mathbf{\Pi}^{nc}\right) \hat{\mathbf{A}}. \tag{C.17}$$

Under this approximation, the population response is proportional to the amenity shock: each type's population change depends linearly on the local amenity gain, scaled by the type-specific migration elasticity θ^h and amenity valuation ζ^h, and transmitted through the migration network structure $(\mathbf{I} - \mathbf{\Gamma}^h \mathbf{\Pi}^h)$.

It is useful to express these equations in scalar form to understand the role of migration linkages. Expanding the l-th element of $\left(\mathbf{I} - \mathbf{\Gamma}^h \mathbf{\Pi}^h\right) \hat{\mathbf{A}}$ and applying $\mathbf{\Pi}^h \approx \mathbf{I}$ (so $\sum_d \pi^h_{od} \hat{A}_d \approx \hat{A}_o$) consistently to both the inner and outer sums gives:

$$\hat{L}^h_l \approx \theta^h \zeta^h \left[(1 - \pi^h_{ll}) \hat{A}_l - \sum_{o \neq l} \gamma^h_{ol} \hat{A}_o \right]. \tag{C.18}$$

This corresponds to Equation 1. Amenity shocks change populations for both worker types, with larger changes for those with higher amenity valuations ζ^h, higher migration elasticities θ^h, and/or higher baseline out-migration rates $(1 - \pi^h_{ll})$. If college workers place greater value on local amenities (Diamond, 2016), are more responsive to differences in location attractiveness (e.g., Bound and Holzer, 2000), and/or have higher baseline mobility (e.g., Molloy et al., 2011), then a negative amenity shock leads to a larger equilibrium population decline for college workers than for non-college workers:

$$\theta^c \zeta^c (1 - \pi^c_{ll}) > \theta^{nc} \zeta^{nc} (1 - \pi^{nc}_{ll}) \implies \left|\hat{L}^c\right| > \left|\hat{L}^{nc}\right|.$$

Which entails the first prediction of the model.

C.5.2 Local wage changes

To characterize the equilibrium wage effects following an amenity shock, we start from Equation C.13 which we reproduce below:

$$\hat{\mathbf{w}} = -\mathbf{a}^{-1} \hat{\mathbf{L}}$$

Inverting location-by-location gives:[44]

$$\hat{w}^c_l = \frac{-a^{nc,nc}_l \hat{L}^c_l - a^{c,nc}_l \hat{L}^{nc}_l}{\det \mathbf{a}_l}, \qquad \hat{w}^{nc}_l = \frac{-a^{cc}_l \hat{L}^{nc}_l - a^{nc,c}_l \hat{L}^c_l}{\det \mathbf{a}_l}, \tag{C.19}$$

[44] Note that $\mathbf{a}$ is block-diagonal with $L \times L$ location-specific blocks, we can work location by location.

where $\det \mathbf{a}_l = a_l^{cc} a_l^{nc,nc} - a_l^{c,nc} a_l^{nc,c} > 0$, $\hat{L}_l^c < 0$, and $\hat{L}_l^{nc} < 0$ following a negative amenity shock.[45]

Each of these expressions contain two forces operating in opposite directions. The first term is the *scarcity effect*: the exit of type-h workers contracts their own local supply, pushing wages up (since $a_l^{h,h} > 0$). The second term is the *scale and complementarity effect*: the exit of workers with complementary skills (-h type workers) shrinks the aggregate local scale of production, pulling wages down under the assumption that $\sigma > \rho$.[46] Thus, the net effect on wages for both types is theoretically ambiguous.

Remark 1 Comparison to standard Rosen (1979); Roback (1982). *Unlike in the standard Rosen-Roback framework, where a local amenity decline unambiguously raises wages, the wage response here is ambiguous due to complementarity between worker types. The source of ambiguity is the sign of* $a_l^{c,nc} = \sum_n \lambda_{ln}^c (\rho - \sigma) \omega_{ln}^{nc}$*: when* $\sigma > \rho$*, cross-wage terms are negative, so the exit of non-college workers depresses college wages via the scale channel. When* $\rho > \sigma$*, this sign flips, the scale effect no longer offsets scarcity, and the unambiguous Rosen-Roback result is restored. The same logic applies to* $a_l^{nc,c}$*, the exit of college workers depresses non-college wages via the scale channel when* $\sigma > \rho$*.*

C.5.3 Local rent changes

To determine the equilibrium effect on local housing prices, we rely on the housing market clearing condition. As discussed before, with an inelastic local housing supply $\bar{H}_l$ and a constant expenditure share $(1-\alpha)$ on housing derived from the Cobb-Douglas utility structure, the log-change in the local rental rate $\hat{r}_l$ is exactly equal to the log-change in the total local wage bill $\hat{r}_l = \hat{W}_l$.

Under CRS and perfect competition, the total wage bill equals total local revenue: $W_l = \sum_n p_{ln} Y_{ln}$. Log-differentiating gives $\hat{W}_l = \sum_n \chi_{ln} (\hat{p}_{ln} + \hat{Y}_{ln})$, where $\chi_{ln} \equiv p_{ln} Y_{ln} / W_l$ is the revenue share of sector n. In the small open economy, the sector-level price index P_n and demand shifter η_n are exogenous, so Armington demand implies $\hat{Y}_{ln} = -\sigma \hat{p}_{ln}$, giving $\hat{p}_{ln} + \hat{Y}_{ln} = (1-\sigma)\hat{p}_{ln}$. Applying the CES unit cost relation $\hat{p}_{ln} = \sum_h \omega_{ln}^h \hat{w}_l^h$ yields $\hat{W}_l = (1-\sigma) \sum_h \bar{\omega}_l^h \hat{w}_l^h$, where $\bar{\omega}_l^h \equiv \sum_n \chi_{ln} \omega_{ln}^h$. Under CRS and perfect competition, $\bar{\omega}_l^h = s_l^h \equiv w_l^h L_l^h / W_l$ exactly: since w_l^h carries no sector subscript (wages equalize across sectors within a location), $\chi_{ln} \omega_{ln}^h = w_l^h L_{ln}^h / W_l$, so $\sum_n \chi_{ln} \omega_{ln}^h = w_l^h L_l^h / W_l = s_l^h$. Equating this revenue-route expression $(1-\sigma) \sum_h s_l^h \hat{w}_l^h$ with the wage bill identity $\sum_h s_l^h (\hat{w}_l^h + \hat{L}_l^h)$

[45] Under the additional assumption that the employment-share-weighted cost shares equal the wage-bill shares at each location (which holds exactly in the single-sector case and approximately when within-location sectoral heterogeneity in cost shares is second-order), $-\mathbf{a}^{-1}$ admits a closed-form decomposition: $\hat{w}_l^h \approx -\frac{1}{\rho} \hat{L}_l^h + \left(\frac{1}{\rho} - \frac{1}{\sigma} \right) \sum_{h \in \{c,nc\}} s_l^h \hat{L}_l^h$, with a scarcity term and a scale-and-complementarity term.

[46] There is empirical evidence that σ is meaningfully larger than ρ. For example, Broda and Weinstein (2006) and Feenstra et al. (2018) find $\sigma \approx 4$ (as noted by Borusyak et al. (2022)) while $\rho \approx 2$ (e.g. Katz and Murphy, 1992; Card and Lemieux, 2001).

and solving gives:

$$\hat{r}_l = \hat{W}_l = \frac{\sigma - 1}{\sigma} \sum_h s_l^h \hat{L}_l^h. \tag{C.20}$$

This prediction is unambiguously negative when $\sigma > 1$ and both groups exit ($\hat{L}_l^h < 0$). The magnitude of this housing price decline is disproportionately driven by college workers. Because they have higher out-migration rates ($|\hat{L}^c| > |\hat{L}^{nc}|$) and capture a larger share of the local wage bill due to their higher productivity ($s_l^c > s_l^{nc}$), their exit exerts the dominant downward pressure on local real estate values.

C.5.4 Migration Responses to an Amenity Shock

Next, we derive the bilateral flow equation under the low-mobility approximation which we use to study the effects of an amenity shock on migration flows between pairs of locations. The log-change in the probability of a type-h worker from o moving to l is:

$$\hat{\pi}_{ol}^h = \theta^h \left(d\bar{V}_l^h - \sum_d \pi_{od}^h d\bar{V}_d^h \right).$$

The change in the deterministic component of utility is given by: $d\bar{V}_l^h = \zeta^h \hat{A}_l + \hat{w}_l^h - (1-\alpha)\hat{W}_l$. Under the low-mobility approximation wages adjust only through population changes, and are therefore first order small, and indirect migrant connections are unimportant. This simplifies the expression for the equilbrium migration response to an amenity shock to:

$$\hat{\pi}_{ol}^h \approx \theta^h \zeta^h \left(\hat{A}_l - \hat{A}_o \right). \tag{C.21}$$

This corresponds to Equation 2.

D. The size of the cancer pain market in 1996 and the unfolding of the opioid epidemic

Our identification strategy follows Arteaga and Barone (2026), who collect evidence from unsealed internal Purdue materials showing that OxyContin's early rollout explicitly targeted the cancer pain market. In repeated statements from internal meetings the company stated that *"OxyContin tablets will be targeted at the cancer pain market"* (OxyContin Team Meeting, April 1994), *"OxyContin primary market positioning will be for cancer pain"* (OxyContin Team Meeting, March 1995), and *"At the time of launch, OxyContin will be marketed for cancer pain"* (OxyContin Launch Plan, September 1995). These documents also make clear that this cancer focus was an entry strategy to expand prescribing into the larger chronic/noncancer pain market. *"The use of OxyContin in cancer patients, initiated by their oncologists and then referred back to FPs/GPs/IMs, will result in a comfort that will enable the expansion of use in chronic nonmalignant pain patients also seen by the family practice specialists."* (OxyContin Launch Plan, September 1995) As a result, because Purdue's initial rollout relied on the pre-existing cancer pain market, locations with larger cancer pain markets at baseline experienced systematically higher initial marketing intensity and earlier adoption of OxyContin, and later, greater cumulative exposure as the epidemic unfolded.

Motivated by the above marketing pathway, we measure baseline differential exposure using local cancer mortality in 1996, aggregated to the commuting-zone (CZ) level. A first test of this identification strategy, is to study the evolutions of opioids prescription as a function of baseline cancer mortaltiy rates. In Panel (a) of Figure D1, we divide CZs into quartiles by their level of cancer mortality before the launch of OxyContin and trace the evolution of prescriptions opioids. The figure shows that high-cancer communities (solid lines) experienced a substantially larger increase in opioid prescriptions than low-cancer communities (dashed lines), despite their starting from comparable baseline levels. Between 1997 and 2010, CZs in the highest quartile of cancer mortality saw a 1,800% increase in grams of oxycodone prescribed per capita, while those in the lowest quartile experienced less than half that growth—even though cancer incidence varied similarly across both groups. Panel (b) of Figure D1, shows an analogous graph for drug induced mortality. The data show that high and low cancer CZs experienced similar trends in drug induced mortality up to the mid-nineties, but soon after that higher cancer places substantial excess mortality from this cause of death. Arteaga and Barone (2026) show that this excess mortality is from younger adults, rather than from those suffering from cancer.

D.1 What Explains the Variation in Cancer Mortality?

The key identifying assumption is that, in the absence of the opioid epidemic, population and economic outcomes of areas with higher cancer mortality would have followed the same *trends* as those of areas with lower cancer mortality (Goldsmith-Pinkham et al., 2020, Callaway et al., 2024). Importantly, the validity of our identification strategy does not rely on cancer mortality being randomly assigned. Indeed, variation in 1996 cancer mortality reflects underlying demographic, environmental, and socioeconomic factors. In Table D1, we show that cancer mortality is strongly correlated with the share of the population over age 65, negatively associated with the share of the Hispanic population, and positively associated with mortality from other causes. Nonetheless, we show that augmenting our baseline specification to control for these determinants yields virtually identical results (see Figures 11 and 12).

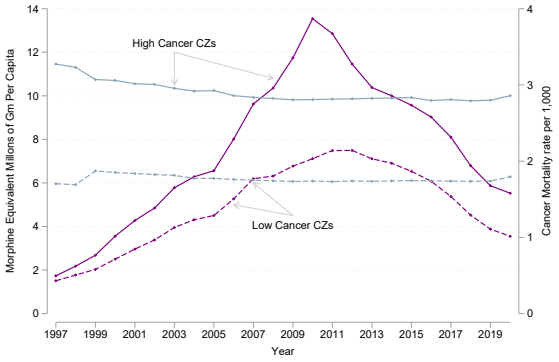
D.2 Additional Evidence on the Validity of the Identification Strategy

Following the exercises in IX.a we perform an out-of-sample dynamic reduced-form analysis to test whether lagged cancer mortality predicts future opioid mortality, employment in the mining and manufacturing sectors and the unemployment rate prior to the onset of the opioid epidemic. That is we run our main specification over a sample of CZs for the years 1982 (or the first available year) to 1995 and estimate whether cancer mortality in 1976 predicts any of these outcomes in the next fourteen years. We present the results of this analysis in Figure D2. These results demonstrate that before the introduction of OxyContin, there was no relationship between our outcome measures or additional economic outcomes and lagged cancer mortality—the estimated coefficients are statistically indistinguishable from zero, and there is no evidence of a pattern.

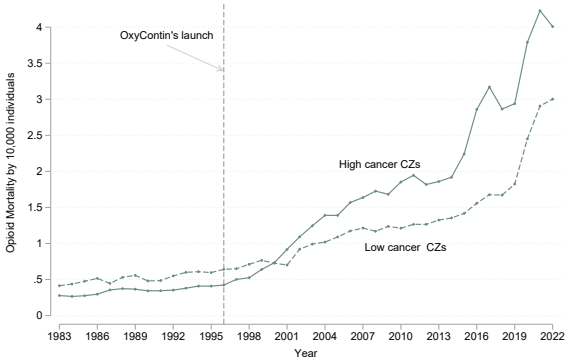
Finally, we complement our analysis on the potential threats of health behaviors and health trends by providing direct evidence that there is no systemic relationship between mid-nineties cancer mortality and overall health trends or despair. In Figure D3, we study the relationship between 1996 cancer mortality and smoking rates, suicides and overall mortality excluding cancer (for adults 75 years old and older and 20 years old and older). We find no evidence of pretrends or effects after the introduction of OxyContin.

Figure D1: The Cancer Pain Market and the Unfolding of the Epidemic

(a) Prescription Opioids



(b) Drug Mortality



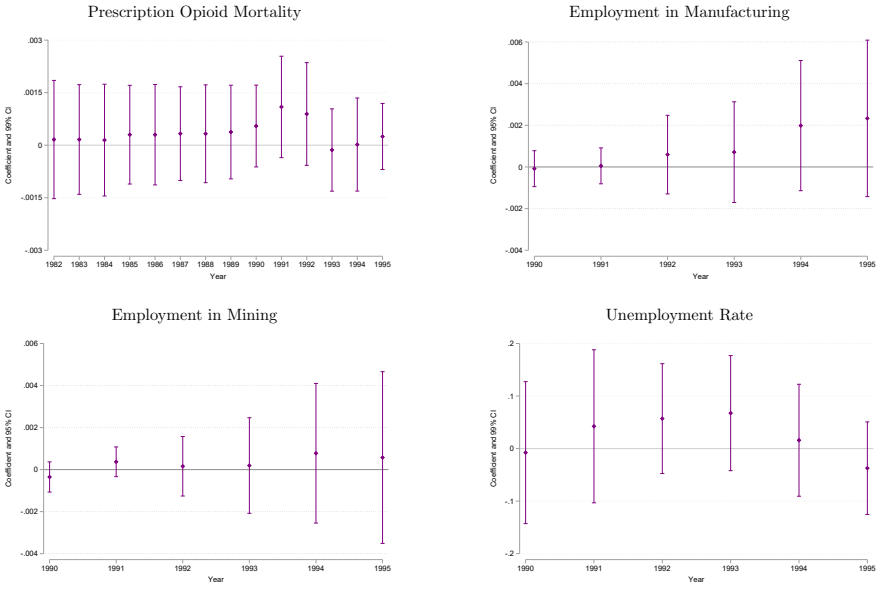
Notes: Panel (a) shows the evolution of the distribution of prescription opioids in the bottom (dashed lines) and top (solid lines) quartiles of cancer mortality before the launch of OxyContin. This comparison is based on dichotomous high-versus-low categorization of CZs, and the outcome is weighted by population. Prescription drugs corresponds to the sum of oxycodone, codeine, morphine, fentanyl, hydrocodone, hydromorphone, and meperidine in morphine-equivalent kg per capita. This panel uses data from ARCOS which are available only from 1997 on. Panel (b) shows the evolution of drug induced mortality for the same partition. Drug-induced deaths include poisonings and other drug-related conditions involving legal or illegal substances, including prescription opioids, heroin, and synthetic opioids (e.g., fentanyl).

Table D1: Baseline Determinants of Cancer Mortality

Dependent variable: Cancer mortality 1996	(1)		(2)
Sh. of population 50 - 64	4.505***	Sh. HS diploma or less	0.60
	[1.697]		[0.394]
Sh. of population over 66	10.08***	Sh. empl in manufacture	-0.06
	[1.271]		[0.169]
Sh. White	-0.34	Ln. income	-0.05
	[0.218]		[0.226]
Sh. Hispanic	-1.179***	Employment rate	-1.89
	[0.197]		[1.385]
Sh. Female	-0.11	Labor force participation	-0.45
	[1.816]		[0.528]
Opioid mortality	3.642*	Adult non-cancer mortality	39.50**
	[1.956]		[17.29]
Rurality in 1993	-0.0207*	Republican vote share 1996	-0.107
	[0.0121]		[0.179]

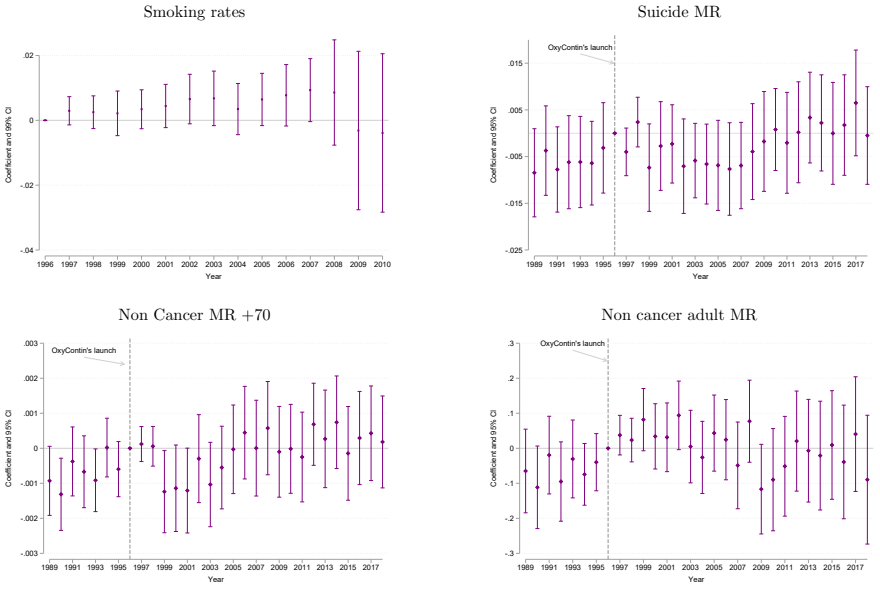
Notes: This table presents estimated coefficients from a cross-sectional regression of cancer mortality rate in 1996 on demographic and economic characteristics and health outcomes at the c-zone level. Standard errors are robust to heteroskedasticity. *$p<0.10$, **$p<0.05$, *** $p<0.01$.

Figure D2: Out-of-sample: Cancer Mortality and Health and Economic Outcomes



Notes: This figure presents event-study results from an out-of-sample exercise. We regress cancer mortality in 1976 interacted with year dummies on mortality and economic outcomes. That is, $y_{ct} = \sum_{\tau=0}^{T} \phi_\tau \; CancerMR_{c,1976} \mathbf{1}(Year = \tau) + \alpha X_{ct} + \delta_c + \delta_{st} + \upsilon_{ct}$. The sample period for each outcome varies depending on data availability. We omit the coefficient corresponding to the first year of available data.

Figure D3: Cancer Mortality in 1996 and Health Trends



Notes: This figure shows event-study estimates of the effects of the opioids epidemic on additional health-related outcomes: smoking rates (Panel (a)), suicides (Panel (b)), noncancer mortality of adults 75 years old and older (Panel (c)), and noncancer mortality for adults aged 20 years old and older (Panel (d)). These estimates use continuous variation in 1996 cancer mortality and include time-varying controls and CZ and state–year fixed effects. Standard errors are clustered at the CZ level. This

E. Decomposition Exercise

This section provides the details of the population decomposition presented in Equation 5 in Section VII.d.

Excess migration $\tilde{\phi}_t^{\text{out-mig}}$ is constructed as Out-mig. $\text{rate}_t \times \phi_t^{\text{out-mig}}$, where $\phi_t^{\text{out-mig}}$ is the semi-elasticity of out-migration in year t from Equation 4, converted to percentage points by multiplying by the average out-migration rate in t. We scale semi-elasticities using contemporaneous migration rates to account for the well documented decline in migration rates over time (e.g., Molloy et al., 2011). In Section VII.a, we present evidence that migratory responses to the opioid epidemic are driven solely by out-migration from areas with higher exposure. Thus, in this decomposition exercise, we set in-migration channel to be zero. Formally, the excess net-migration term includes both out-migration and in-migration flows and can be written as: Excess net-migration_t = Out-Mig. $\text{rate}_t \times \phi_t^{\text{out-mig}}$ + In-Mig. $\text{rate}_t \times \phi_t^{\text{in-mig}}$. Setting $\phi^{\text{in-mig}} = 0$ yields the term in Equation 5.

Excess births are computed as the estimated effect of exposure on the crude birth rate from Equation 3.[47] The use of the crude birth rate, rather than the fertility rate, is natural in this context since our goal is to compute changes in total population growth. Panel (b) of Figure A4 presents yearly estimates for this outcome, i.e., estimates of ϕ^{birth}. Excess mortality is calculated as the estimated effect of exposure on drug-induced mortality from Equation 3. We include only the effects of exposure on drug-induced mortality, since the effects on non-drug-induced mortality are statistically indistinguishable from zero. Figure A6 presents estimates for non-drug-induced mortality rates. We do not reject the null hypothesis that the post-1997 coefficients are jointly equal to zero; the p-value of this test is 0.4041. The logic here is similar to the net-migration component. One can decompose excess mortality as Excess $\text{mortality}_t = \phi_t^{\text{Non DI mort}} + \phi_t^{\text{DI mort}}$. Setting $\phi_t^{\text{Non DI mort}} = 0$ yields the expression in Equation 5.

[47] The crude birth rate (CBR) is defined as the ratio of total births to women aged 15-44 to the total population.